

SEISMIC LOSS ASSESSMENT OF SEQUENTIAL RUPTURE OF  
NEW MADRID SEISMIC ZONE ON THE CENTRAL US

BY

ANISA COMO

THESIS

Submitted in partial fulfillment of the requirements  
for the degree of Master of Science in Civil Engineering  
in the Graduate College of the  
University of Illinois at Urbana-Champaign, 2009

Urbana, Illinois

Adviser:

Professor Amr S. Elnashai

## **ABSTRACT**

The New Madrid Seismic Zone (NMSZ) is described as a low probability high risk event. In case of a repetition of the 1811-1812 earthquake series, the expected consequences will cause catastrophic impacts to directly affected areas and beyond. An accurate earthquake impact assessment of the NMSZ is essential to generate an efficient response from FEMA and its associates and to educate and prepare the general population.

The objective of this project is to provide scientifically defensible earthquake impact assessments with the most improved hazard, inventory, and fragility data to save lives and protect property. The study region encompasses eight states: Alabama, Arkansas, Illinois, Indiana, Kentucky, Mississippi, Missouri, and Tennessee. The implemented scenario aspires to recreate the events of 1811-1812 as accurately as possible within modeling constraints. The resulting scenario is a 7.7 magnitude earthquake event with sequential rupture of all three segments of the NMSZ simultaneously.

Hazard improvements include complete liquefaction and shaking maps, while multiple inventory datasets are incorporated and added to the existing default assets. An advanced methodology for fragility derivation is applied and improved fragility functions are included for buildings and bridges, based on inelastic response. Additionally, secondary effects of flooding due to dam failure are analyzed. The analytical analysis is executed in HAZUS-MH MR3 developed by FEMA.

Several damage criteria were developed to determine the most critically impacted counties. The results of the impact assessment are staggering, with 140 impacted counties and over 700,000 damaged buildings. Essential facilities such as schools and hospitals incur severe damage. Transportation and utility lifelines experience serious functionality impairments. Catastrophic consequences result in nearly 86,000 casualties and approximately \$300 billion in direct economic losses. Finally, essential components of future research work are identified. The employed approaches and lesson learned in this project are applicable for worldwide earthquake impact assessments.

# TABLE OF CONTENTS

LIST OF FIGURES .....	VI
LIST OF TABLES .....	IX
CHAPTER 1: INTRODUCTION .....	1
1.1 Foreword .....	1
1.2 Objectives and Overview .....	2
CHAPTER 2: REVIEW OF PREVIOUS LOSS ASSESSMENT STUDIES .....	4
2.1 Evolution of Seismic Loss Assessment .....	4
2.2 Previous Loss Assessment Studies .....	6
CHAPTER 3: IMPACT ASSESSMENT FOR THE CENTRAL USA.....	9
3.1 Definition of Regional Hazard.....	9
3.1.1 Regional Seismicity Overview .....	9
3.1.2 Earthquake Scenario .....	12
3.1.3 Default Model for Hazard.....	13
3.1.3.1 Definition of Ground Shaking in HAZUS .....	13
3.1.3.2 Liquefaction.....	17
3.1.4 Hazard Improvements.....	23
3.1.4.1 Soil Site Class Maps.....	23
3.1.4.2 Liquefaction Susceptibility Map .....	25
3.1.4.3 Soil Response Map.....	26
3.2 Assets .....	31
3.2.1 Definition and Categorization.....	31
3.2.2 Inventory Capture Methods .....	32
3.2.3 Overview of HAZUS Inventory Classification.....	34
3.2.3.1 General Buildings.....	35
3.2.3.2 Essential Facilities .....	41
3.2.3.3 High Potential Loss Facilities.....	42
3.2.3.4 Transportation Systems .....	43
3.2.3.5 Utilities Lifelines .....	44

3.2.4 Inventory Additions .....	46
3.2.4.1 Buildings .....	47
3.2.4.2 Transportation Systems .....	51
3.2.4.3 Utility Systems .....	56
3.2.4.4 High Potential Loss Facilities.....	59
3.2.4.5 Regional Overview of Inventory Improvements .....	59
3.3 Vulnerability Functions .....	61
3.3.1 Definition .....	61
3.3.2 HAZUS Building Fragility Relationships.....	62
3.3.3 Building Fragility Improvements.....	68
3.3.4 Threshold Limit States .....	72
3.4 Additional Modeling – Flood Risk Analysis .....	74
CHAPTER 4: ASSESSMENT RESULTS AND DISCUSSION .....	78
4.1 General Buildings .....	81
4.2 Essential Facilities .....	85
4.3 Transportation Systems.....	87
4.4 Utility Lifelines .....	89
4.5 High Potential Loss Facilities .....	92
4.6 Induced Damage, Casualties, and Economic Losses .....	93
4.7 Flood Potential .....	95
CHAPTER 5: CONCLUDING REMARKS .....	100
5.1 Summary .....	100
5.2 Future Research and Development Needs .....	102
5.2.1 Roadway Fragilities .....	102
5.2.2 Fragility Relationships for Dams and Levees .....	102
5.2.3 Utilities Network Interdependencies.....	103
5.2.4 Uncertainty Modeling .....	103
5.2.5 Cumulative Damage Fragilities .....	104
5.2.6 Fire Following Earthquakes .....	104
CHAPTER 6: REFERENCES .....	106
CHAPTER 7: APPENDICES .....	112

Appendix 1. Hazard .....	112
Appendix 2. Inventory .....	115
Appendix 3. Detailed Damage Results .....	120
Appendix 4. Flood Risk Modeling.....	140

## List of Figures

Figure 1. Topographical Effects of 1811-1812 Earthquake Series .....	10
Figure 2. Perception Extent of Similar Earthquakes in NMSZ and California .....	11
Figure 3. WUS and CEUS Regions .....	15
Figure 4. Source-to-Site Distances for (a) Vertical and (b) Dipping Faults .....	16
Figure 5. Liquefaction Process due to Seismic Shaking .....	17
Figure 6. Conditional Liquefaction Probability Relationships .....	21
Figure 7. Soil Site Class Map .....	25
Figure 8. Liquefaction Susceptibility Map for NMSZ Scenario Event .....	26
Figure 9. Soil Response Map (Cramer, 2006; Toro and Silva, 2001) .....	27
Figure 10. NMSZ Fault Segments .....	28
Figure 11. PGA for NMSZ Scenario Event .....	29
Figure 12. PGV for NMSZ Scenario Event .....	30
Figure 13. Short-Period (0.3 sec) Spectral Acceleration for NMSZ Scenario Event .....	30
Figure 14. Long-Period (1.0 sec) Spectral Acceleration for NMSZ Scenario Event .....	31
Figure 15. Remote Sensing Methodologies (Yamazaki, 2001) .....	33
Figure 16. Conventional Fragility Curves (MAEC, 2007) .....	62
Figure 17: Characteristic Fragility Relationships (FEMA, 2008) .....	63
Figure 18: Derivation of HAZUS Fragilities (FEMA, 2008) .....	66
Figure 19: Soil Profiles for the Upper Mississippi Embayment .....	70
Figure 20: Improved Fragility Relationships (Gencturk et al., 2008) .....	72
Figure 21. Simulated Illustration of Flood Risk Analysis Methodology .....	77
Figure 22. Impacted Counties for the Eight-State NMSZ Region .....	81
Figure 23. General Building Damage for NMSZ Region .....	84
Figure 24. Hospital Damage for Eight-State Study Region .....	86
Figure 25. Major River Crossing Damage for Eight-State Study Region .....	89
Figure 26. Electric Power Outages at Day 1 for Impacted Region .....	92
Figure 27. Total Casualties for 2:00 AM Event in Study Region .....	94
Figure 28. New Madrid Seismic Zone Flood Risk .....	96

Figure 29. Illinois Essential Facilities Flood Potential .....	97
Figure 30. Hospitals Regional Impact .....	120
Figure 31. Fire Stations Regional Impact .....	121
Figure 32. Police Stations Regional Impact.....	122
Figure 33. Schools Regional Impact.....	123
Figure 34. Airports Regional Impact .....	124
Figure 35. Highway Bridges Regional Impact .....	125
Figure 36. Railway Bridges Regional Impact.....	126
Figure 37. Communication Facilities Regional Impact .....	127
Figure 38. Electric Power Facilities Regional Impact .....	128
Figure 39. Natural Gas Facilities Regional Impact.....	129
Figure 40. Oil Facilities Regional Impact.....	130
Figure 41. Waste Water Facilities Regional Impact .....	131
Figure 42. Potable Water Facilities Regional Impact .....	132
Figure 43. Potable Water Regional Outages.....	133
Figure 44. Dam Regional Damage.....	134
Figure 45. Levee Regional Damage.....	135
Figure 46. Hazardous Material Facilities Regional Damage .....	136
Figure 47. Regional Casualties at 2:00 AM.....	137
Figure 48. Regional Total Debris (in thousand tons).....	138
Figure 49. Building Regional Damage Percentage.....	139
Figure 50. Danger Reach Length Determination .....	140
Figure 51. Flood Risk of Arkansas Essential Facilities .....	142
Figure 52. Flood Risk of Arkansas Transportation Systems .....	143
Figure 53. Flood Risk of Arkansas Utility Systems .....	144
Figure 54. Flood Risk of Illinois Essential Facilities.....	146
Figure 55. Flood Risk of Illinois Transportation Systems.....	147
Figure 56. Flood Risk of Illinois Utility Systems .....	148
Figure 57. Flood Risk of Kentucky Essential Facilites.....	150
Figure 58. Flood Risk of Kentucky Transportation Systems.....	151
Figure 59. Flood Risk of Kentucky Utility Systems.....	152

Figure 60. Flood Risk of Missouri Essential Facilities .....	154
Figure 61. Flood Risk of Missouri Transportation Systems .....	155
Figure 62. Flood Risk of Missouri Utility Systems .....	156
Figure 63. Flood Risk of Tennessee Essential Facilities .....	158
Figure 64. Flood Risk of Tennessee Transportation Systems.....	159
Figure 65. Flood Risk of Tennessee Utility Systems.....	160



## List of Tables

Table 1. CEUS Attenuation Relationships.....	15
Table 2: Liquefaction Susceptibility of Sedimentary Deposits .....	19
Table 3. Proportion of Map Unit Susceptible to Liquefaction.....	20
Table 4. Ground Settlement Amplitudes for Liquefaction Susceptibility Categories .....	23
Table 5. HAZUS Building Classification by Occupancy Type .....	37
Table 6. Building Model Types .....	38
Table 7. Mapping of Occupancy-Model Type for Low-rise Buildings in Mid-west US .	40
Table 8. Classification of Essential Facilities .....	41
Table 9. Classification of High Potential Loss Facilities.....	42
Table 10. Classification of Electric Power Systems .....	45
Table 11. Classification of Communication Systems .....	45
Table 12. Hospital Replacement Cost.....	48
Table 13. Fire Station Replacement Cost .....	49
Table 14. Police Station Replacement Cost.....	50
Table 15. Schools Replacement Cost.....	50
Table 16. EOC Replacement Cost .....	51
Table 17. Replacement Cost of Highway Bridges.....	52
Table 18. Railway Bridge Replacement Cost .....	52
Table 19. Light Rail Facility Replacement Cost.....	53
Table 20. Bus Facility Replacement Cost.....	54
Table 21. Port Facility Replacement Cost .....	54
Table 22. Ferry Replacement Cost.....	55
Table 23. Airport Facility Replacement Cost .....	55
Table 24. Communication Facilities Replacement Cost.....	56
Table 25. Electric Power Facilities Replacement Cost.....	57
Table 26. Waste Water Facilities Replacement Cost.....	57
Table 27. Oil Facilities Replacement Cost .....	58
Table 28. Natural Gas Facilities Replacement Cost .....	58

Table 29. Regional Inventory Improvements Summary .....	60
Table 30: Single Value Representations of Earthquake Record Sets .....	70
Table 31: Threshold Values .....	74
Table 32: Building Damage Distribution by State.....	82
Table 33: Building Damage by Occupancy Type.....	82
Table 34: Building Damage by Building Type.....	83
Table 35. Building Damage Distribution by State for Wood and URM .....	84
Table 36: Regional Essential Facilities Damage .....	85
Table 37: Regional Transportation Systems Damage.....	88
Table 38: Regional Utility Facilities Damage .....	90
Table 39: Utility Pipeline Damage for Study Region .....	90
Table 40: Service Outages at Day 1 for Eight-State Study Region .....	91
Table 41: Other Critical Facilities Damage for Eight-State Study Region.....	93
Table 42: Regional Total Debris Generation .....	93
Table 43: Casualties at 2:00AM for Eight-State Study Region.....	94
Table 44: Direct Economic Loss for Eight-State Study Region (\$ millions) .....	95
Table 45. List of Counties with Flood Potential .....	96
Table 46. Regional Summary of Flood Risk Results.....	99
Table 47. Atkinson and Boore Regression Coefficients .....	112
Table 48. Attenuation Coefficients of Toro, Abrahamson, and Schneider.....	113
Table 49. Coefficients of Campbell Attenuation Equation.....	113
Table 50. Attenuation Coefficients of Somerville et al. ....	114
Table 51. HAZUS Classification of Highway Systems.....	116
Table 52. HAZUS Classification of Railway Systems .....	117
Table 53. HAZUS Light Rail Systems Classification .....	118
Table 54. HAZUS Bus Facility Classification.....	118
Table 55. HAZUS Port Facility Classification .....	119
Table 56. HAZUS Ferry Facility Classification .....	119
Table 57. HAZUS Airport Facility Classification .....	119
Table 58. Arkansas Flood Risk Assessment Results .....	141
Table 59. Illinois Flood Risk Assessment Results.....	145

Table 60. Kentucky Flood Risk Assessment Results.....	149
Table 61. Missouri Flood Risk Assessment Results .....	153
Table 62. Tennessee Flood Risk Assessment Results .....	157

# **CHAPTER 1: Introduction**

## **1.1 Foreword**

As one of the most dangerous natural hazards, earthquakes have always caused disastrous impacts on infrastructure, human life, and economic prosperity. Moreover, catastrophic impacts have increased exponentially with the rapid expansion of world population and density of urban development. The total economic losses experienced during the Kobe earthquake in 1995 are the second highest losses in the history of natural disasters, only preceded by losses resulting from hurricane Katrina. The Mid-America Earthquake (MAE) Center, under the initiative of the Federal Emergency Management Agency (FEMA) for catastrophic planning of a New Madrid Seismic Zone (NMSZ) event, has conducted an earthquake impact assessment for the region. The obtained results from the impact assessment are suitable for use by agencies, local and federal government, private businesses, and emergency planners to identify gaps in resources and prioritize possible pre-event measures such as retrofit and general public education. Furthermore, the results can be used to articulate emergency response strategies for short term and long term post-event requirements.

Loss assessment requires the collaboration of many technical fields and the process that studies numerous consequences such as structural damage, casualties, and socio-economical losses due to a specific event. Specifically, seismic loss assessment corresponds to the determination of the impact extent of an earthquake to regional assets in a region of interest. In this impact assessment, the most current available models for the Central US are implemented to produce the most accurate data possible at this time. The software tool of choice to conduct the seismic loss assessment is HAZUS, which is an analytical impact assessment software that can estimate impact of infrastructural damage and socio-economic losses and consequences. There are three main components that comprise loss assessment: hazard, inventory, and fragility relationships.

Hazard depicts the intensity of ground motion due to ground shaking and permanent ground deformation. Inventory consists of all assets and their physical values in the region of study. Inventory can be separated into two main categories: population

and infrastructure. Population describes regional demographics characteristics such as ethnicity, age, and economic income. Infrastructure encompasses all physical assets ranging from buildings to transportation lifelines, utility lifelines, and other critical structures such as dams and levees. Fragility relationships relate the hazard to the inventory by quantifying the probability that a limit state is exceeded for different levels of incurred damage to assets exposed to a certain hazard event.

Direct damage results from the model are obtained and utilized to perform additional post-processing analyses such as secondary effects due to floods caused by dam damage. Additional studies were performed on social impact, uncertainty quantification, and advanced transportation and utility systems for specific regions, though these additional studies are not explicitly described in this thesis, with the exception of flood risk analysis. The implementation of the most current models and new methodologies to account for post-earthquake effects (floods) generates the most comprehensive and accurate impact assessment results available for the Central US. Additionally, this is by far the most comprehensive loss assessment in the US in terms of its region size.

Obtained results from the analysis can be applied by regional and national emergency agencies in collaboration with other agencies and businesses to implement strategic plans in order to minimize the impact of a catastrophic event and to minimize cascading effects. Additionally, results from a comprehensive and accurate loss assessment can be employed to identify critical infrastructure at risk such as major highway bridges or hospitals, and have the ability to retrofit or take other measures to prevent life loss or system impairment during an actual event.

## **1.2 Objectives and Overview**

The intent of this study is to present the most advanced and comprehensive available tools to assess the regional seismic impact of the New Madrid Seismic Zone. The result of this assessment can support planning strategies to minimize impact to infrastructure, life loss, and socio-economic components in the case of a similar earthquake as the implemented scenario in this study. A NMSZ event would directly

impact central states: Alabama, Arkansas, Illinois, Indiana, Kentucky, Mississippi, Missouri, and Tennessee. Within the eight states, a critical region is identified. A variety of criteria is taken in consideration to determine critical counties that, in turn, comprise the critical region.

Initially, the thesis includes a brief outline of the history of seismic risk assessment and some milestone loss assessment studies utilizing software packages. In the following chapter, detailed descriptions for each of the components are included. The general process starts with default definition for each component and concludes with respective improvements to each component. The methodology of estimating flood due to dam damage is also explained. Following the definition of each component, the results obtained by analytical analysis conducted in HAZUS are shown for the eight-state region. The presented results include structural damage and relevant interruptions to general buildings, essential facilities, transportation systems, utility lifelines, and high potential loss facilities. Additional results concerning the cascading effects of floods following earthquakes are reported. In conclusion, results are summarized and general remarks are stated. Finally, gaps in methodology are defined and recommended research avenues for future research are illustrated.

## **CHAPTER 2: Review of Previous Loss Assessment Studies**

This chapter centers on the history of seismic loss assessment; its beginnings and the relatively rapid evolution of earthquake engineering. Firstly, a brief review highlights a few crucial points in the advancement of the field. Subsequently, a list of previous comprehensive loss assessments is discussed, and the chapter is concluded with the identification of some significant challenges in loss assessment and steps on how to overcome the challenges and/or how to obtain the most accurate solutions with the available resources.

### **2.1 Evolution of Seismic Loss Assessment**

The first attempts of seismic loss assessments commenced in the second part of the 17<sup>th</sup> century with the lectures of Robert Hook, titled “Lectures and Discourse in Earthquakes and Subterranean Eruptions”, given to the Royal Society in 1667 and 1668 (Elnashai, 2008). His steps were followed by the work of Robert Mallet, which presented a catalogue of global seismicity (Scawthorn, 2008). Significant developments were accomplished in terms of scale measurements and instrumentation by followers such as Rossi, Forel, and Mercalli (Scawthorn, 2008).

The 1908 earthquake in Messina, Italy with a death toll estimated in the range of 72,000 to 110,000 (USGS, 2009) was a pivotal development in loss assessment since it instigated one of the first initiatives for the drafting and implementation of seismic provisions. The methodology of these provisions consisted of assigning a fraction of the structure’s gravity load in the design of the building to achieve lateral resistance. The recommendation was supplied by Professor Modesto Panetti from the Polytechnic of Turin, who suggested that seismic loads equal to  $1/8^{\text{th}}$  of the structure’s weight should be applied to the first floor, and then reducing to the  $1/12^{\text{th}}$  of the weight for the above floors (second and third) (Elnashai, 2008). This methodology represents the origin of what is recognized as the equivalent static approach still used in seismic design worldwide.

The first official seismic code provisions, however, originated in Japan, in 1924, after the disastrous aftermath of the Kanto earthquake in 1923; the Urban Building Law was revised to incorporate seismic design requirements, including the application of a

seismic coefficient of 0.1 (Kuramoto, 2006). Japan can also be accredited with the creation of the first seismological society. Following the earthquake of Yokohama, Milne, a British seismologist, created the Seismological Society of Japan in spring 1880 (Dewey and Byerly, 1969). This society went on to be dissolved in 1892 and re-established in 1929.

Another monumental earthquake such as the 1906 San Francisco earthquake event instigated the formation of the Seismological Society of America. The occurrence of San Francisco earthquake had major importance also in terms of bringing to focus secondary or cascading events that follow earthquakes such as fires. The human losses resulting from the earthquake are estimated to 3,000 people; while the economic losses possibly amount to \$500,000,000 (Hansen, 1996). Most importantly, it is estimated that up to 80% of sustained damages during the event were caused by fire. Another historical earthquake is the 1933 Long Beach Earthquake in California. Though the damage incurred was not massive (death toll of 115), the educational significance of this earthquake stands in the pattern of damage (Stover and Coffman, 1993).

A considerably large number of school buildings were severely damaged and the relatively low death toll was attributed to the occurrence time of the earthquake which was later in the day. If the earthquake would have occurred while the schools were in session, significantly larger impact would have been expected. Based on the observed damage to schools, came the concept of essential facilities, which are structures that have critical effect on the functionality of normal life operations. After the Long Beach earthquake, the Field and Riley Acts were instated in California which required the ability of schools and government structures to withstand seismic loading.

A monumental development in the field of seismic risk assessment was the formation of the Earthquake Engineering Research Institute (EERI) in 1949, which further supported research in the subject matter. In the beginning of the second half of the 20<sup>th</sup> century seismic probabilistic maps were being developed and seismic zones were identified, like for Japan and California. Furthermore, influential geotechnical effects such as liquefiable soils were observed since the beginning of seismic studies, where only now being seriously considered and studied. The term liquefaction was first used by Mogami and Kubo (1953) and later extensively discussed by Housner. The most



impressive observed liquefaction effects were witnessed during the 1964 Nigata earthquake in Japan.

In the later years, with the parallel evolvement of structural dynamics, mapping technologies, and computational tools, the aptitude to accurately conduct loss assessment studies has increased exponentially. A considerable improvement has been the collection of seismic data. Valuable data in terms of quantity and quality has been collected during earthquakes for the past few decades. Major earthquakes during this time period can include events such as Loma Prieta in 1989, Northridge in 1994, Kobe (Japan) in 1995, Chi-Chi (Taiwan) in 1999, Izmit (Turkey) in 1999, Kashmir (Pakistan) in 2005, and lastly the event of 2008 in Sichuan, China. Several loss assessment tools have been developed and implemented to analyze and predict losses due to earthquake events.

The most comprehensive tool for the US is the HAZUS software developed by FEMA in collaboration with National Institute for Building Sciences (NIBS). The inclusiveness and capability of analyzing large regions confirmed HAZUS as the software of choice for the project. An analogous software package SELENA was developed by the International Centre for Geohazards, a Norwegian research institute. HAZUS and SELENA share the same core methodology, but differ in terms of Geographic Information System usage. The combination of loss assessment tools advancement and implementation of multi-disciplinary approach has allowed the capability of additional estimates other than structural damage, such as secondary effects (floods and fires following earthquakes) and socio-economical effects.

## **2.2 Previous Loss Assessment Studies**

Seismic loss assessment studies have significantly evolved in the last few decades. One of the first significant loss assessments was conducted by Davis et al. (1982) and it concerned the Earthquake Planning Scenario for a Magnitude 8.3 on the San Andreas Fault in the San Francisco Bay area. The study aimed to provide evidence of significant differences between the northern and southern San Andrea fault segments which corresponded to locations near San Francisco and Los Angeles. Two different scenarios were implemented which were adapted from the real events of 1906 San Francisco

earthquake and the 1857 earthquake in southern California. Loss assessment results monitored the performance of critical infrastructure categories such as ground transportation, communications, water supply, waste water treatment, electricity, and oil and natural gas pipeline systems.

Several loss assessment studies have been conducted for the Hayward fault in the San Francisco Bay Area, starting with the loss assessment by Steinbrugge et al. (1987), which implemented a 7.5 magnitude earthquake scenario and estimated fatalities ranging in 1,400- 1,500 at any time of the day. EERI (1996) utilized a 7.0 earthquake scenario and estimated losses up to \$4 billion. Several other assessments and different scenarios have been considered and implemented for an event originating at the Hayward fault.

Between the late 1990s and early 2000s, HAZUS became the preferred choice among analytical tools to estimate losses. Several seismic studies were conducted throughout US in different levels and details. Some examples include seismic loss assessment of Memphis, Tennessee by Shinozuka et al. (1997). The project studied the loss assessment of buildings, and the Memphis light, gas, and water division (MLGW) damage, and specifically implements improvements to existing methodologies.

A study conducted for Oregon by Wang (1999) represented the first seismic study at the state level using HAZUS. Two earthquake scenarios were utilized to obtain impacts of building damage and social and economic losses. One of the scenarios included an event originating from the Cascadia subduction zone off the coast of Oregon, while the other scenario involved statewide probabilistic ground motions for a 10% probability of exceedance in 50 years.

A comprehensive earthquake loss assessment was conducted for the state of South Carolina using HAZUS and four different earthquake scenarios. Three of the selected scenarios were derived from Charleston seismic events, with the greatest magnitude of 7.3, to adopt the scenario of the 1886 Charleston earthquake. The fourth scenario was obtained from an earthquake in Columbia. The implemented models accounted for comprehensive hazard and inventory characterizations through considering regionally specific seismic parameters such as seismic source, path, and site effects, and ground motion numerical modeling. Significant inventory additions were implemented along

with an enhancement in resolution by utilizing a 2 km by 2 km grid size rather than the default HAZUS census tracks (Wong et al., 2005).

HAZUS was also implemented in the estimation of seismic impact of the Seattle Fault (2005). The earthquake scenario has a magnitude of 6.7 and its estimated damages result in more than 25,500 casualties and economic losses of about \$33 billion.

Kircher et al. (2006) also utilized HAZUS to evaluate loss assessments to San Francisco area with a scenario event obtained by the 1906 San Francisco Earthquake. The study area includes 24,000 square miles with a population of 10 million people and inventory assets of \$1.5 trillion. The estimated impacts resulted in a range of 800 to 3,400 fatalities (depending on time of the day) and total direct economic losses of \$90 to \$120 billion.

Previous studies were also conducted by the MAE Center regarding seismic loss assessment of New Madrid Seismic Zone (Cleveland, 2006). The study considered a total of eight states and damage to general buildings, essential facilities, utilities, and transportation and the analysis was performed in two levels: Level I with no user improvements, and Level II where hazard and inventory improvements were included.

Throughout the years, loss assessment methodologies and computational tools have evolved exponentially and model advancements as well as easily implemented post-processing methodologies allow for more accurate and intricate levels of direct and indirect losses, along with secondary and cascading effects.

## **CHAPTER 3: Impact Assessment for the Central USA**

This chapter aims to describe the three main components of earthquake impact assessment: hazard, inventory, and fragility relationships. Specifically, the relevance of each component with respect to the project will be discussed and detailed information will be provided regarding the improvements to baseline components. The chapter chronology for each of the three components initiates with the description of default methodology (HAZUS definition for each components) and then is followed by the respective improvements.

### **3.1 Definition of Regional Hazard**

#### **3.1.1 Regional Seismicity Overview**

The Central United States is not perceived as a seismic zone by the general public; however, scientific evidence as well as testimonies of previous earthquakes have proved that this is a highly seismic region. The seismicity of the region is mainly due to the existence of the New Madrid Seismic Zone (NMSZ), as well the Wabash Valley Seismic Zone and so on. The NMSZ is composed of three segments: northeast, central, and southwest segments, and it extends through northeast Arkansas to southern Illinois, passing through Missouri, western Tennessee, and western Kentucky. The NMSZ is considered to be a low-probability high-consequence event, indicating high uncertainties of accurate occurrence predictions and catastrophic consequences. The period of occurrence is directly related to the earthquake magnitude, thus, the magnitude of an earthquake tends to be greater if the time period between events is longer.

The strongest evidence of earthquake occurrence in the region by far is the series of earthquakes in 1811-1812. This series of events ranks as one of the largest earthquake events in the seismic history of the United States, with three main events with estimated moment magnitudes ranging from 7.2 to 8.1 and several hundreds of earthquake aftershocks (USGS, 2009). The extent of strong shaking perception during these events is estimated to be 2-3 times larger than the 1964 Alaska earthquake and about 10 times larger than the 1906 San Francisco earthquake. Human testimonials at the time confirm

the perception of shaking as far as New York and Washington, DC. Evidence other than the direct damage to man-made buildings is supplied in the form of geotechnical phenomena and significant changes to topography such as liquefaction (sand blows and soil collapses), creation and destruction of fissures, landslides, uplifting of trees, and creation of several lakes, as shown in Figure 1.

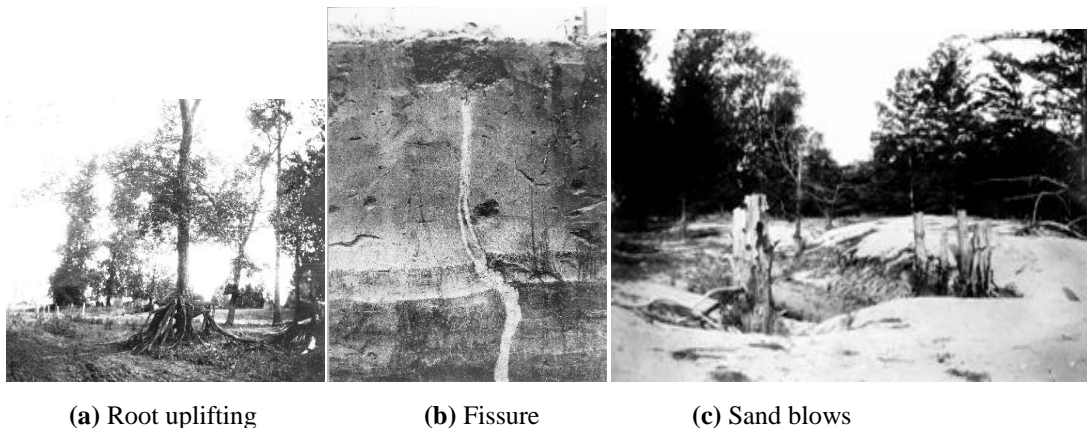


**Figure 1. Topographical Effects of 1811-1812 Earthquake Series**

Furthermore, scientific evidence shows seismic activity in the New Madrid prior to the 1811-112 earthquake events. Geologic evidence of prehistoric earthquakes has been increasing since the late 1970s. In addition to geological features, archeological evidence such as the evidence obtained by Tuttle and Schweig (1995) verifies the occurrence of prehistoric earthquakes in the NMSZ from liquefaction feature studies such as sand blows. A series of major earthquakes with moment magnitude equal to or greater than 7 (including the 1811-1812 series) is presumed to have occurred through a period of approximately 2400 years, resulting in a return period range of 400 to 1200 years (USGS, 2007).

Wabash Valley Seismic Zone is another significant fault zone in the central US, located between southeastern Illinois and Indiana. Geological evidence shows seismic activity of more than 20,000 years. Though the magnitudes of these events are not in the same amplitudes as the NMSZ, the damage potential of an event from this fault is still quite high; the magnitudes of previous events could have reached up to 7.0. A recent

proof of the seismicity of the region is the 2008 Mt. Carmel earthquake which originated from the WVSZ.

During the 1811-1812 NMSZ earthquake series, little structural damage was observed and human life loss was not catastrophic, even with estimated event magnitudes as high as 8.2. The most significant effects that were commented and documented were the topological changes and ground deformation that took place, such as landslides, liquefaction, ground uplift and collapse, and sand blows. The main reason for “low” damage was the low inhabitation density of the region at that time period. Other than Saint Louis, most of the region had sparse population, thus the non-catastrophic losses in terms of structural damage and human life. However, if a similar event were to take place in the region today, the consequences would be much more significant and damage levels would be much higher in terms of life losses, structural damage, and economic and social factors.

In order to understand the potential of the damage magnitude and extent due to such an event and the significant differences between seismic regions, a comparison of two events with similar magnitudes is presented in Figure 2, where one event epicenter is in California (widely recognized area of high seismicity) and the other one originates in the NMSZ (USGS, 2003).

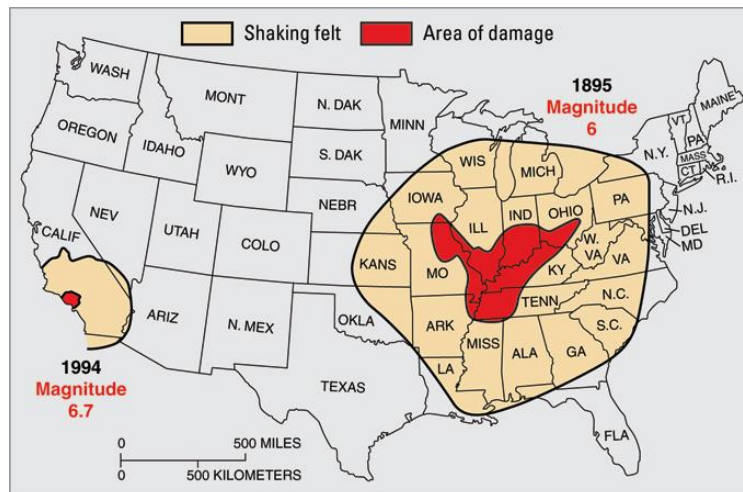


**Figure 2. Perception Extent of Similar Earthquakes in NMSZ and California**

According to USGS (2007), 150 to 200 earthquakes are recorded every year in the NMSZ region. Today, the Central US is densely populated in terms of people, critical structures, and infrastructure. Damage to certain facilities such as the Memphis airport, which hosts the largest FedEx hub, would cause service interruption and, consequentially, would negatively affect the regional, country, and global economy. Additionally, disastrous consequences would result from the interruption of damaged oil and gas pipelines. Most of oil and natural gas follow a flow direction of southwest-northeast. Interruption of power or supply of oil and natural gas would not only affect the immediate eight-state region, but would significantly influence supply of the northwestern states such as Michigan and Ohio, resulting in much graver consequences than possibly predicted, especially if an event occurred during the winter when heat would be most essential for shelter and medical requirements. The overall result due to a similar event would be catastrophic; therefore, the model accuracy and intricacies are crucial in providing the best available and useful loss assessment results that could be utilized to aid the preparedness of officials, agencies, and general public in the case of such an event.

### **3.1.2 Earthquake Scenario**

The scenario used in this thesis was based on the series of the 1811 – 1812 earthquakes. The event is considered as low probability high consequence event, similar to the referred earthquake event. The shaking event is assumed to have a moment magnitude  $M_w = 7.7$ , while the latest major earthquake series had possible moment magnitudes in the range of 7.0 to 8.2. The NMSZ has three segments; northeast, central, and southwest segment. During major earthquakes, especially during the 1811-12 series, the seismic shaking caused the rupture of all three fault segments. Therefore, during this impact assessment model, it is assumed that all three faults are ruptured to address a worst-case scenario.

The scenario event it designed to represent a nationally-catastrophic earthquake event in the Central US. Historically, earthquakes on the New Madrid Seismic Zone occur in groups of three where each of the three segments of the fault ruptures over a period of several months. The implemented scenario involves the sequential rupture of all

three faults simultaneously. Realistically, the faults would not fracture subsequently, but rather break over a longer period of time. However, in order to account for this event, modeling should be able to capture the effects of cumulative damage. Currently, modeling constraints do not provide the ability to account for the cumulative effects, thus the assumption of subsequent rupture of all three segments is implemented which represents the next best solution under current conditions. Based on the aforementioned modeling assumptions, soil type and liquefaction susceptibility maps were developed by CUSEC for an accurate hazard definition.

### **3.1.3 Default Model for Hazard**

Hazard is defined as any earthquake-related physical phenomenon that has the potential or does impact human life and normal activities. Seismic hazard involves ground shaking and ground deformation which causes ground failure, surface faulting, and landslides, and so on. While there are numerous ways and different levels of hazard definition, the minimum level of definition involves the quantification of ground motion through peak ground motion parameters or peak spectral values. Attenuation functions are then utilized to propagate the level of shaking. The following sections will focus on a detailed explanation of the default definition of hazard in HAZUS and its shortcomings, and further continue with comprehensive measures that were undertaken to improve the accuracy of ground shaking regarding soil and liquefaction susceptibility maps.

#### **3.1.3.1 Definition of Ground Shaking in HAZUS**

In HAZUS Technical Manual (FEMA, 2008), ground motion is characterized by spectral response (based on a standard spectrum shape), peak ground acceleration, and peak ground velocity. There are three available methodologies to define ground motion in HAZUS:

- Deterministic ground motion analysis
- USGS probabilistic ground motion maps
- User-supplied probabilistic or deterministic ground motion maps



Three levels of analysis are available in HAZUS, Levels I through III, with gradual increase in terms of user interference and analysis details. Level I analysis offers little room for improvements and the analysis is based generally on default parameters. Level II analysis allows the user to improve several parameters such as soil maps, liquefaction susceptibility maps, fragility relationships, and so on. Level III analysis is by far the most advanced modeling level; however it requires high degrees of expert input as well as significant detailed improvements in terms of hazard, inventory, and fragilities, thus resulting in considerable amounts of time and financial resources. Such level of analysis would be unfeasible in regions of substantial size. As a result, for this project, advanced Level II analysis is employed by implementing state-of-the art modeling for all three seismic loss assessment components: hazard, inventory, and fragility relationships.

To assess the ground shaking demand, HAZUS requires the input of the following parameters: scenario, attenuation relationships, and soil maps. Prior to determining the scenario itself, the user is required to decide the basis for determining ground shaking demand from one of three alternative methodologies: a deterministic calculation, probabilistic maps which are supplied with the program, or user-supplied maps. For a deterministic calculation of ground shaking, the user specifies a scenario earthquake magnitude and location. In some cases, the user may also need to specify certain source attributes required by the attenuation relationships supplied with the methodology.

Attenuation relationships are analytical expressions that illustrate the propagation of ground shaking from the source of the event to the local site of interest. A series of attenuation relationships are supplied with the default program. In the case of a deterministic event, the user can select several attenuation relationships among the provided list. The provided attenuations are separated into two general groups depending on geographical location of the event. The two identified regions are distinct in various significant parameters such as earthquake mechanisms, soil type and response, and type of earthquakes (intra-plate versus inter-plate), and they are divided into the Western United States (WUS) and Central and Eastern United States (CEUS). Figure 3 shows the regional separation of WUS and CEUS locations as defined by USGS in the development of the National Seismic Hazard Maps.

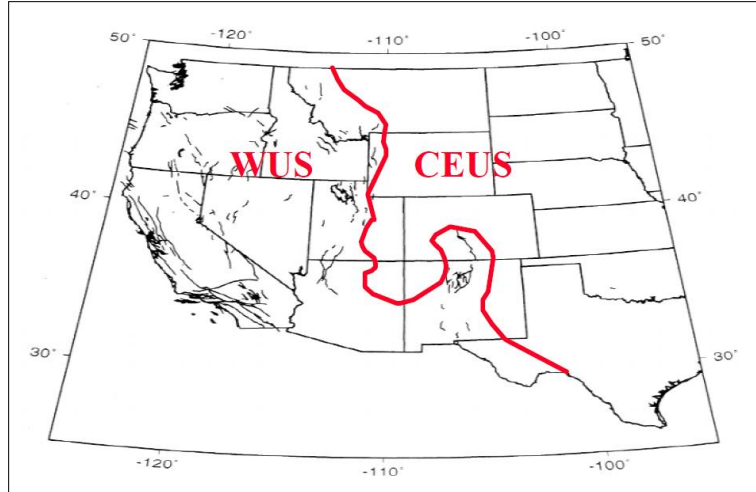


**Figure 3. WUS and CEUS Regions**

As previously mentioned, attenuation relationships illustrate the progression of ground shaking by correlating source parameters to local site conditions. Several parameters are considered in attenuation relationships, but there are three primary parameters generally used to attenuate ground shaking: magnitude, distance from source (typically, the epicenter), and site soil conditions. HAZUS provides default attenuation functions pertinent to the two US regions, WUS and CEUS. The relevant attenuation relationships for NMSZ (part of CEUS) are outlined in Table 1, where the distance column represents the type of source-to-site distance used.

**Table 1. CEUS Attenuation Relationships**

<b>CEUS Attenuation Functions</b>	<b>Distance</b>
Atkinson and Boore (1995)	$r_{\text{hypo}}$
Toro, Abrahamson and Schneider (1997)	$r_{\text{jb}}$
Frankel, Mueller, Barnhard, Perkins, Leyendecker, Dickman, Hooper (1996)	$r_{\text{hypo}}$
Campbell (2002)	$r_{\text{rup}}$
Somerville, Collins, Abrahamson, Braves, and Saikia (2002)	$r_{\text{jb}}$

$r_{\text{hypo}}$  = Distance from hypocenter to site

$r_{\text{jb}}$  = Distance from site to the vertical projection of the fault rupture plane

$r_{rup}$  = Distance from the site to the fault rupture plane

The different site-to-source distances used in the above attenuation relationships are graphically illustrated in Figure 4, while further details about the implemented attenuation functions is included in Appendix 1.

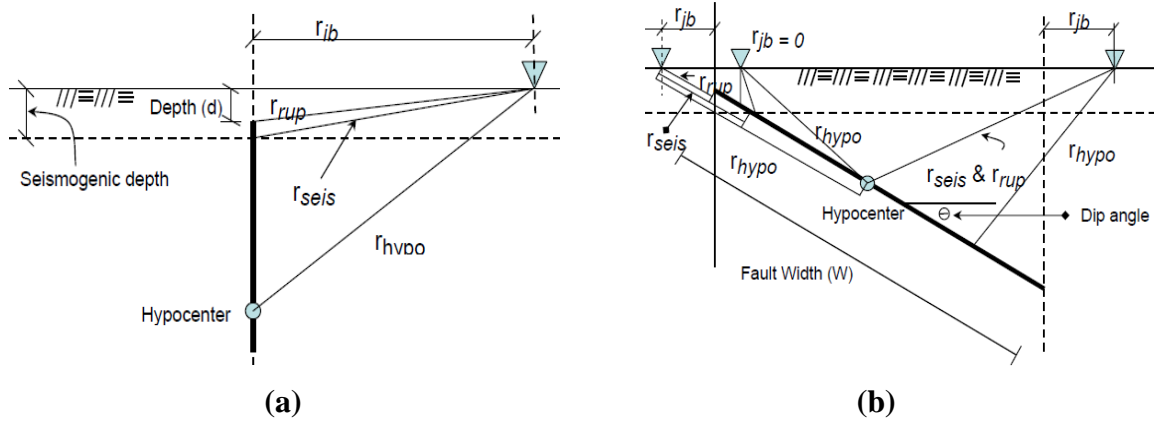


**Figure 4. Source-to-Site Distances for (a) Vertical and (b) Dipping Faults**

Soil maps may and are recommended to be user-supplied, in order to account for local site conditions and increase the accuracy of model and predictions. The supplied maps need to identify soil types classification based on the site class definitions specified in the 1997 NEHRP Provisions. In the case where no soil maps are available, the ground motion will be amplified by default assuming Site Class D Soil throughout the study region. If the default approach is implemented, the user has the option to change the overall Soil Site Class from D to A, B, C, or E.

For a deterministic event, the user specifies the location and magnitude of the scenario event. Three options are available to determine the source (typically, the epicenter) of an event; specify an event from a database of WUS faults, choose an historical earthquake event, or use an arbitrary epicenter location. To define hazard, the user must supply peak ground acceleration (PGA), peak ground velocity (PGV), and spectral acceleration contour maps at 0.3 ( $S_{a03}$ ) and 1.0 ( $S_{a10}$ ) seconds. This option permits the development of a scenario event from various source models not available in HAZUS. Contrary to default options, soil amplification maps are not applied to any user-

supplied maps; therefore, soil amplification should be taken in consideration during the process of soil map development to account for local site effects.

Hazard definition is obtained by defining ground motion, as discussed above, and ground deformation. Ground deformation constitutes three types of ground failure: liquefaction, landslides, and surface fault rupture. Each of these types of ground failure is quantified by permanent ground deformation (PGD). The subsequent section will focus on liquefaction and its definition.

### 3.1.3.2 Liquefaction

Liquefaction refers to the response of loose soils (typically sand) subjected to ground shaking, which terminates in a complete loss of strength and cohesion, and enters a liquefied state. If a saturated loose soil is subjected to ground motion, it tends to compact and decrease in volume; if the soil cannot drain rapidly enough, the decrease in volume results in an increase in pore pressure (Hunt, 2005). When the pore pressure increases until it equals the overburden confining pressure, the effective stress between soil particles becomes zero, the soil loses its shear strength, and enters a liquefied state. The liquefaction phenomenon is illustrated in Figure 5 (Newton Consultants, 2007) where the soil state is presented before and after a seismic event.

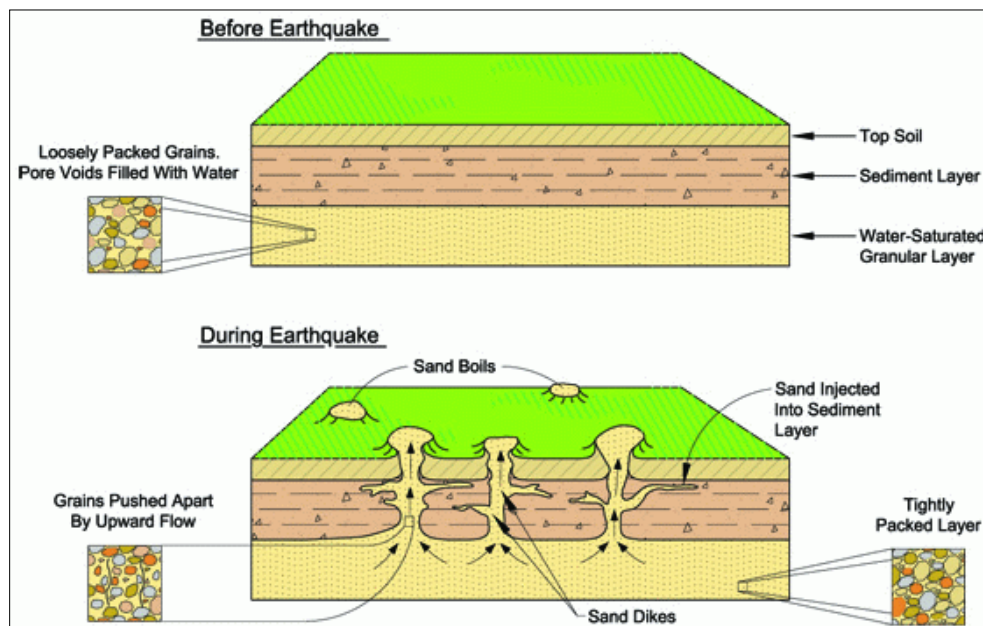


**Figure 5. Liquefaction Process due to Seismic Shaking**

Liquefaction susceptibility expresses the relation between soil and ground motion and it is dependent on numerous parameters such as soil type, soil gradation, relative density of soil particles, soil stratigraphy, boundary drainage conditions, period of motion, and especially duration and magnitude of ground motion (Hunt, 2005). Consideration of liquefaction susceptibility is a critical component in hazard definition, since liquefaction causes permanent ground deformations such as lateral spreading and vertical settlement, both of which increase the likelihood of damage to infrastructure located on these vulnerable soils.

The development of liquefaction susceptibility maps based on regional conditions was accomplished by Youd and Perkins (1978). The study addressed the susceptibility of various types of soil deposits by assigning a qualitative susceptibility rating based upon the general depositional environment and geologic age of deposits. Table 2 (Youd and Perkins, 1978) shows the predicted levels of liquefaction susceptibility of several liquefiable soils, based on geographical position as well as age of deposits and depositional environment. These levels of liquefaction susceptibility are utilized by HAZUS in order to evaluate ground deformation which includes lateral spreading and permanent ground settlement.

**Table 2: Liquefaction Susceptibility of Sedimentary Deposits**

Type of Deposit	General Distribution of Cohesionless Sediments in Deposits	Likelihood that Cohesionless Sediments when Saturated would be Susceptible to Liquefaction (by Age of Deposit)			
		< 500 yr Modern	Holocene < 11 ka	Pleistocene 11 ka-2 Ma	Pre-Pleistocene > 2 Ma
(a) Continental Deposits					
River channel	Locally variable	Very High	High	Low	Very Low
Flood plain	Locally variable	High	Moderate	Low	Very Low
Alluvial fan and plain	Widespread	Moderate	Low	Low	Very Low
Marine terraces and plains	Widespread	--	Low	Very Low	Very Low
Delta and fan-delta	Widespread	High	Moderate	Low	Very Low
Lacustrine and playa	Variable	High	Moderate	Low	Very Low
Colluvium	Variable	High	Moderate	Low	Very Low
Talus	Widespread	Low	Low	Very Low	Very Low
Dunes	Widespread	High	Moderate	Low	Very Low
Loess	Variable	High	High	High	Very Low
Glacial till	Variable	Low	Low	Very Low	Very Low
Tuff	Rare	Low	Low	Very Low	Very Low
Tephra	Widespread	High	High	?	?
Residual soils	Rare	Low	Low	Very Low	Very Low
Sebka	Locally variable	High	Moderate	Low	Very Low
(b) Coastal Zone					
Delta	Widespread	Very High	High	Low	Very Low
Estuarine	Locally variable	High	Moderate	Low	Very Low
Beach					
High wave energy	Widespread	Moderate	Low	Very Low	Very Low
Low wave energy	Widespread	High	Moderate	Low	Very Low
Lagoonal	Locally variable	High	Moderate	Low	Very Low
Fore shore	Locally variable	High	Moderate	Low	Very Low
(c) Artificial					
Uncompacted Fill	Variable	Very High			
Compacted Fill	Variable	Low			

Liquefaction susceptibility is primarily influenced by earthquake magnitude, duration of ground shaking, and depth of water table. It is also highly dependent on grain size distribution and relative density of soil particles. As a result, portions of soil can exist that are not likely to liquefy. In other words, in a zone of high liquefaction susceptibility it cannot be assumed that the whole surface area will have the same likelihood of liquefaction. In order to account for this occurrence, HAZUS implements a default relationship between relative susceptibility and proportion of map unit, shown in Table 3. The relationship between relative susceptibility and the proportion of map unit was developed based on judgments resulting from soil properties examination data sets for several regional liquefaction studies (FEMA, 2008). As such, it is a very generic relationship, and, when available, the user is encouraged to utilize specific regional data to improve the strength and accuracy of this correlation.

**Table 3. Proportion of Map Unit Susceptible to Liquefaction**

<b>Mapped Relative Susceptibility</b>	<b>Proportion of Map Unit</b>
Very High	0.25
High	0.20
Moderate	0.10
Low	0.05
Very Low	0.02
None	0.00

The likelihood of liquefaction is related to magnitude, duration, liquefaction susceptibility, and water table depth. Based on the level of susceptibility, relationships are derived that correlate the probability of liquefaction to the peak ground acceleration considering the dependency to the aforementioned parameters. Figure 6 illustrates the conditional liquefaction probability for the five liquefaction susceptibility categories: very high, high, moderate, low, and very low.

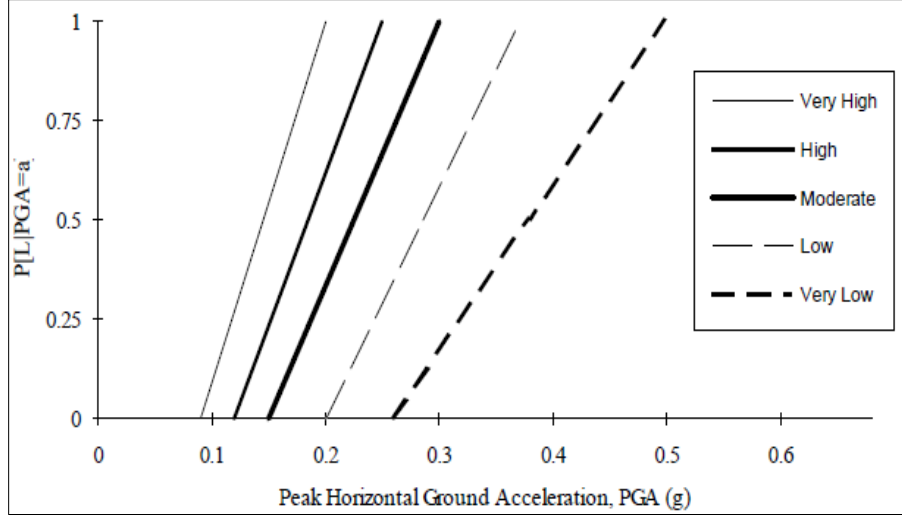


**Figure 6. Conditional Liquefaction Probability Relationships**

The relationship was derived assuming an earthquake moment magnitude,  $M$ , equal to 7.5 and water depth of 5 ft., and it is determined through the following relationship (FEMA, 2008):

$$P[Liquefaction_{SC}] = \frac{P[Liquefaction_{SC}|PGA=a]}{K_M \cdot K_W} \cdot P_{ml} \quad (1)$$

where

$P[Liquefaction_{SC}]$  = the conditional liquefaction probability for a given susceptibility category at a specified level of peak ground acceleration

$K_M$  = Moment magnitude correction factor

$K_W$  = Ground water correction factor

$P_{ml}$  = Proportion of map unit susceptible to liquefaction

The correction factors  $K_M$  and  $K_W$  account for  $M$  other than 7.5 and water depth other than 5 ft, respectively, and they are defined through the equations below:

$$K_M = 0.0027M^3 - 0.0267M^2 - 0.2055M + 2.9188 \quad (2)$$



$$K_W = 0.022d_W + 0.93 \quad (3)$$

where

$M$  = moment magnitude

$d_W$  = depth of ground water in feet

An additional relationship is used in HAZUS to estimate the effects of lateral spreading, the second component of permanent ground deformation caused by earthquake-induced liquefaction. This relationship is derived from combining the Liquefaction Severity Index (LSI) by Youd and Perkins with the attenuation relationships developed by Sadigh, et. al. (FEMA, 2008)

$$E[PGD_{SC}] = K_{\Delta} \cdot E[PGD|(PGA/PL_{SC}) = a] \quad (4)$$

where

$E[PGD|(PGA/PL_{SC}) = a]$  = the expected permanent ground displacement  
for a given susceptibility category under a specified ground  
shaking ( $PGA/PGA(t)$ )

$PGA(t)$  = Threshold value of PGA required to induce liquefaction

$K_{\Delta}$  = Displacement correction factor for magnitudes other than 7.5

$$= 0.0086M^3 - 0.0914M^2 + 0.4698M - 0.9835$$

$M$  = moment magnitude

Additionally, permanent ground settlement (vertical deformation) default values are assumed for different liquefaction susceptibility categories. As expected, liquefaction susceptibility and permanent ground deformation are directly related.

**Table 4. Ground Settlement Amplitudes for Liquefaction Susceptibility Categories**

<b>Relative Susceptibility</b>	<b>Settlement (in.)</b>
Very High	12
High	6
Moderate	2
Low	1
Very Low	0
None	0

The hazard modeling corresponds to an advanced Level II analysis. Significant improvements of ground motion include both improvements to ground shaking and ground deformation (closely related to liquefaction). User specified maps for the eight-state region pertaining to soil type, liquefaction susceptibility, and soil response were utilized in hazard definition. All the improved maps were developed by the Central United States Earthquake Consortium (CUSEC) State Geologists. The maps of soil classification and liquefaction susceptibility derived by the CUSEC State Geologists were combined to form the regional hazard maps used in the impact assessment.

### **3.1.4 Hazard Improvements**

#### **3.1.4.1 Soil Site Class Maps**

The Soil Site Class Maps were developed by CUSEC State Geologists by following the procedures outlined in the NEHRP provisions (Building Seismic Safety Council, 2004) and the 2003 International Building Codes (International Code Council, 2002). Preliminarily, soils were categorized into liquefiable soils, thick soft clay, or thin (or no) soil areas.

*Liquefiable Soils (Soil Site Class F):* Liquefiable soils classification was accomplished through identification of any of the four categories of Site Class F. If site soil profile characteristics corresponded to any of these categories, the site was classified as Site Class F.

The four categories of soil profile consist of:

- Soils vulnerable to potential failure or collapse under seismic loading such as liquefiable soils, quick and highly sensitive clays, or collapsible weakly cemented soils.
- Peats and/or highly organic clays ( $H > 10$  feet of peat and/or highly organic clays where  $H$  = thickness of soil)
- Very high plasticity clays ( $H > 25$  feet with plasticity index  $PI > 75$ )
- Very thick soft/medium stiff clay ( $H > 120$  feet)

Based on the above criteria and the conclusions of CUSEC, all eight states of the NMSZ study region contained some Site Class F soils, with the exception of Kentucky.

*Thick Soft Soils (Soil Site Class E):* Thick soft soils are defined as soils having soft clay layers with depth greater than 10 ft (3 m). Soft clays are defined by a moisture content level ( $w$ ) of 40% or greater and plastic limit (PL) greater than 20. If soil layers satisfy the above criteria, the site is classified as Site Class E.

*Thin Soils:* According to International Building Codes, soils less than ten feet thick between the top of bedrock and building foundations are excluded from consideration in the soil site class maps. As a result, regions where soil thickness is less than ten feet are classified according to the corresponding bedrock properties.

Typically, soil site class maps were previously produced using local site conditions based on the average shear wave velocity of the upper 30 meters (98 feet) of the local site geology. In this case, CUSEC State Geologists used the entire column of soils material down to bedrock and did not include any bedrock in the calculation of the average shear wave velocity for the column. Bedrock properties were not included due to the fact that it is the soil column and the difference in shear wave velocity of the soils in comparison to the bedrock which influences much of the amplification. Based on the outlined procedures, along with the Fullerton et al. (2003) map, a single combined soil site class map was produced for the eight NMSZ states and it is illustrated in Figure 7.

Soil Site Class Map

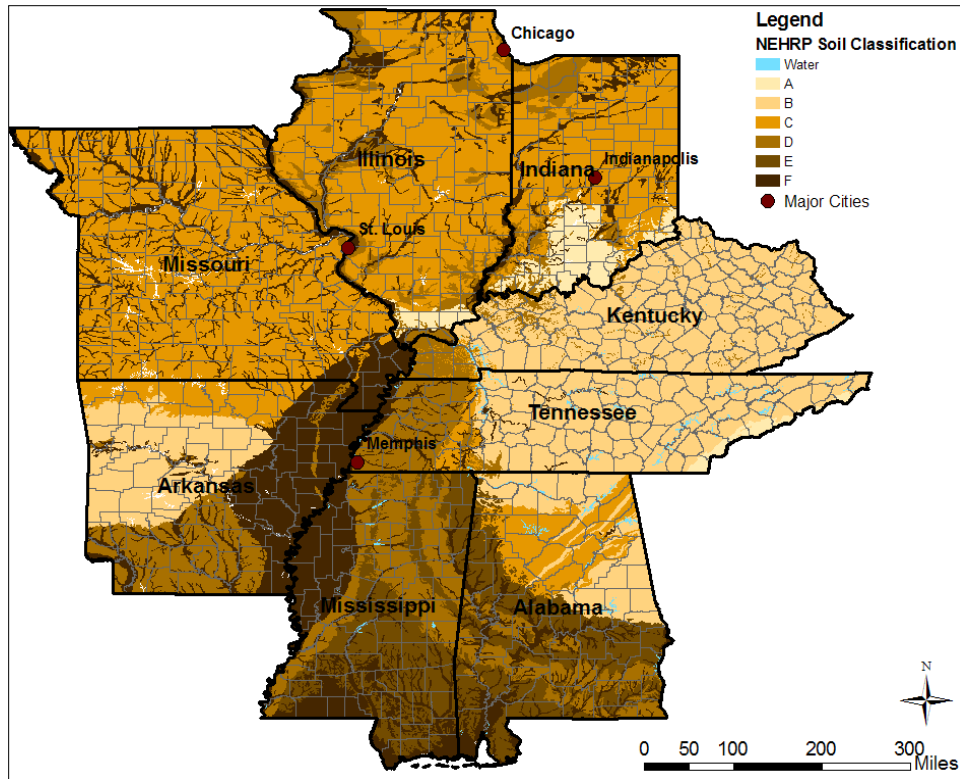


**Figure 7. Soil Site Class Map**

#### 3.1.4.2 Liquefaction Susceptibility Map

As discussed, the liquefaction susceptibility HAZUS is characterized through the work by Youd and Perkins (1978). The classification of liquefiable soils and their susceptibility is shown in Table 2. The new liquefaction susceptibility map developed by the CUSEC State Geologists utilized comparisons with the map developed by Fullerton et al. (2003) and additional expert interpretations of the state geological surveys. The resulting liquefaction susceptibility map that is utilized in the user-defined hazard definition of the project implemented in HAZUS is presented in Figure 8.

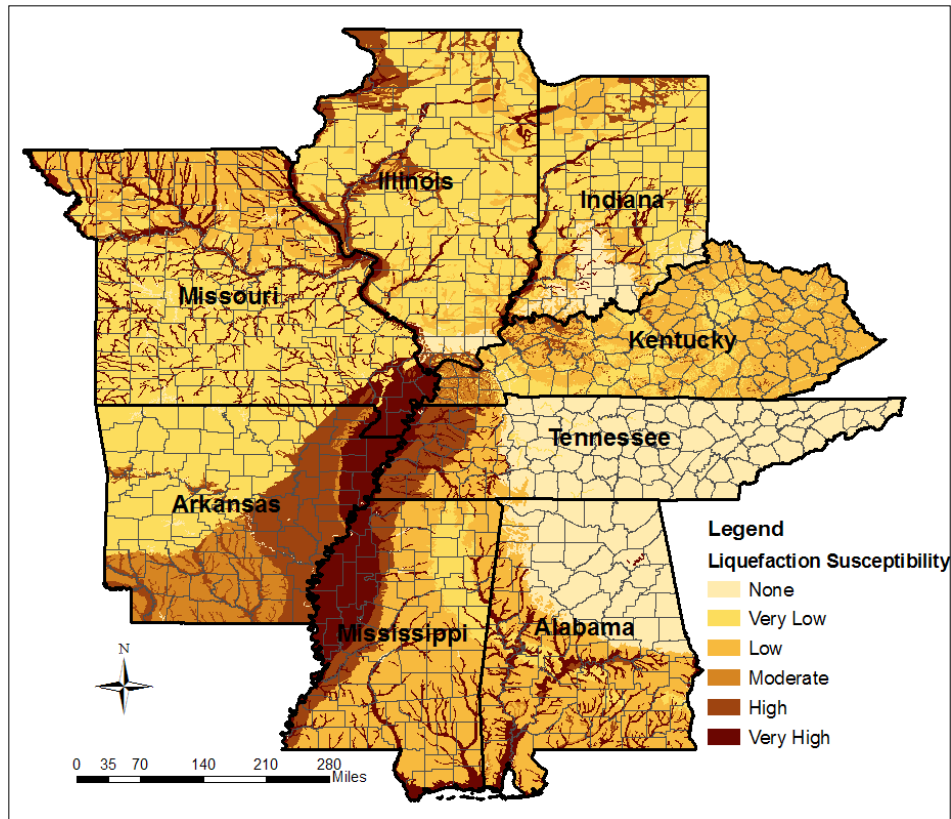


**Figure 8. Liquefaction Susceptibility Map for NMSZ Scenario Event**

#### 3.1.4.3 Soil Response Map

One of the major limitations in HAZUS deals with the extent of analysis; analysis in HAZUS is limited to a distance of 200 km from the source. At distances greater than 200 km HAZUS assigns to shaking parameters by default values of zero. In regions like the Central US ground shaking is attenuated to much greater distances than the maximum default distances, thus the necessity of having improved soil maps to account for this discrepancy.

The CUSEC State Geologists originally produced a soil site classification map for the eight CUSEC states as outlined previously. The soil site class map is used, along with an earthquake magnitude and location, to calculate the surface ground motions throughout the study region. Due to various limitations in HAZUS, all ground motion maps are developed externally and include soil amplification according to the soil site

class information from the CUSEC State Geologists. Dr. Chris Cramer from the University of Memphis created the scenario ground motion maps using the methodology outlined in Cramer (2006). The Cramer (2006) methodology used earthquake events on all three segments of the New Madrid faults along with ground motions modified by soil site amplification based on a soil response map and reference shear wave velocity profiles for each soil type (Figure 9).

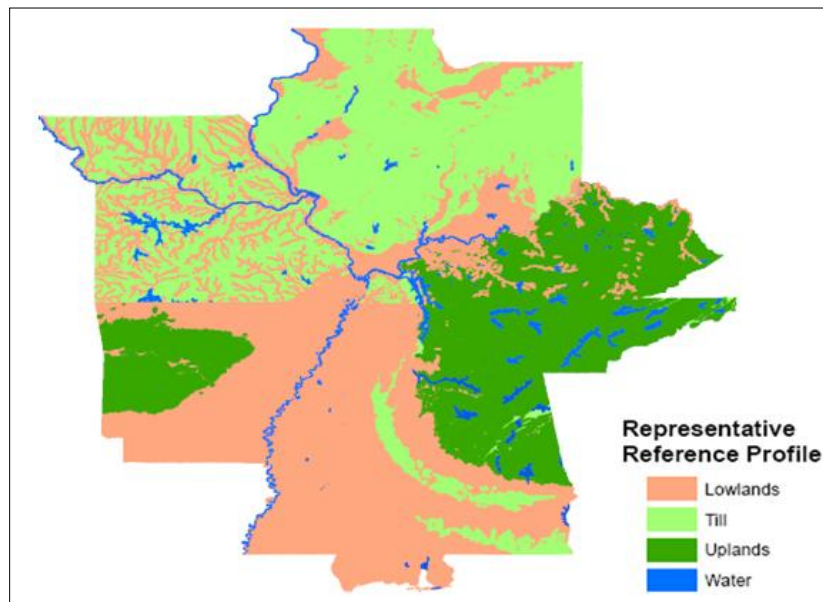


**Figure 9. Soil Response Map (Cramer, 2006; Toro and Silva, 2001)**

The maps created for the NMSZ sequential rupture still utilize the procedure outlined in Cramer (2006), though it is applied to a total rupture length that includes the northeast, central, and southwest segments of the New Madrid Fault. Each individual fault segment rupture was assigned a magnitude of 7.7 and it is assumed that the magnitude is maintained throughout the simultaneous rupture. It is possible that the impacts estimated in the simultaneous rupture scenario are less than the impacts that result from the sequential rupture scenario, since partially damaged structures from one event could be greatly affected by the second and third events. Currently, however, it is impossible to determine damage level or even whether cumulative damage would

increase or decrease for successive earthquake events due to a lack of fragility relationships for damaged infrastructure.

As a result, all the ground motion maps were developed considering a sequential rupture of the three NMSZ segments, meaning that the ground motion maps represent the combined ground motion caused by the rupture of all three segments in a sequence. Figure 10 illustrates the three segments of the NMSZ. The ground motion was propagated horizontally through rock layer and then propagated vertically through soil layers above the bedrock. The ground motion maps that were developed for the 7.7 magnitude sequential rupture event are included at the end of this appendix. Scenario ground shaking maps for PGA, PGV, and both  $S_{a03}$  and  $S_{a10}$  are illustrated in Figure 11 thru Figure 14.

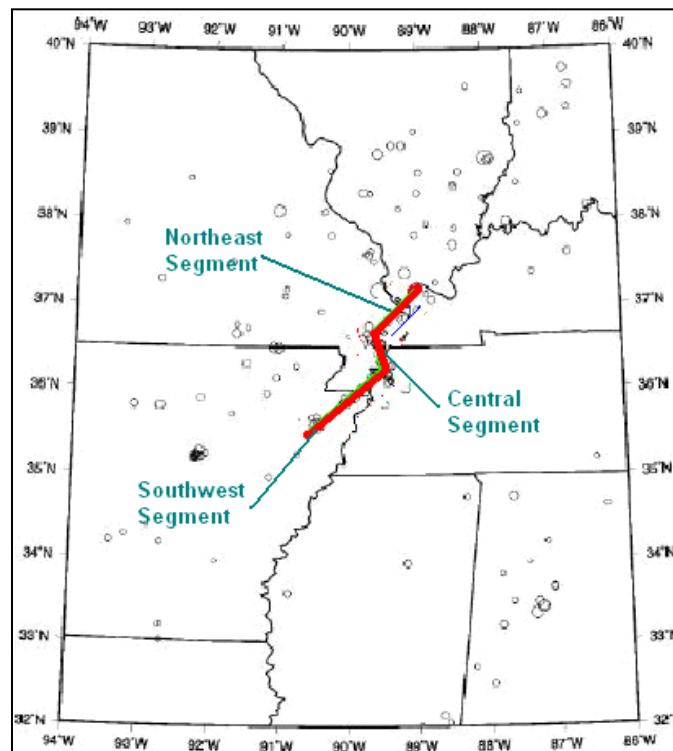


**Figure 10. NMSZ Fault Segments**

All new soil classification, liquefaction susceptibility, and ground motion maps are regionally-comprehensive and represent a substantial improvement upon previous maps that characterize hazard throughout a small portion of the eight-state study region.

Additionally, soil characterization maps and soil classifications utilize a consistent procedure as outlined in the NEHRP provisions or Youd and Perkins (1978), which was not available previously. These substantial improvements to the characterization of regional hazard greatly improve the overall quality and accuracy of Central US earthquake impact assessments as the most current and regionally-comprehensive hazard.

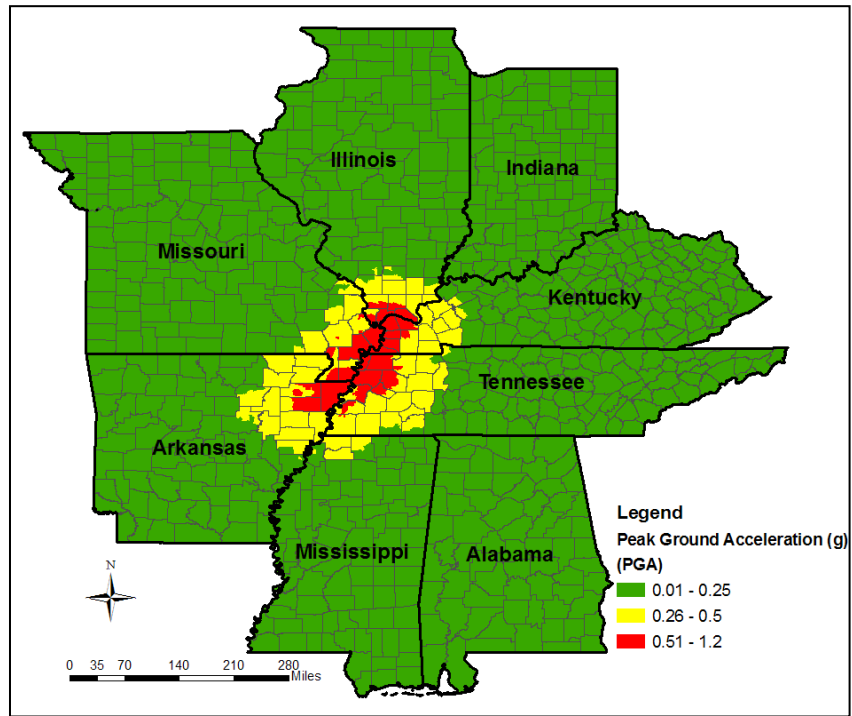


**Figure 11. PGA for NMSZ Scenario Event**



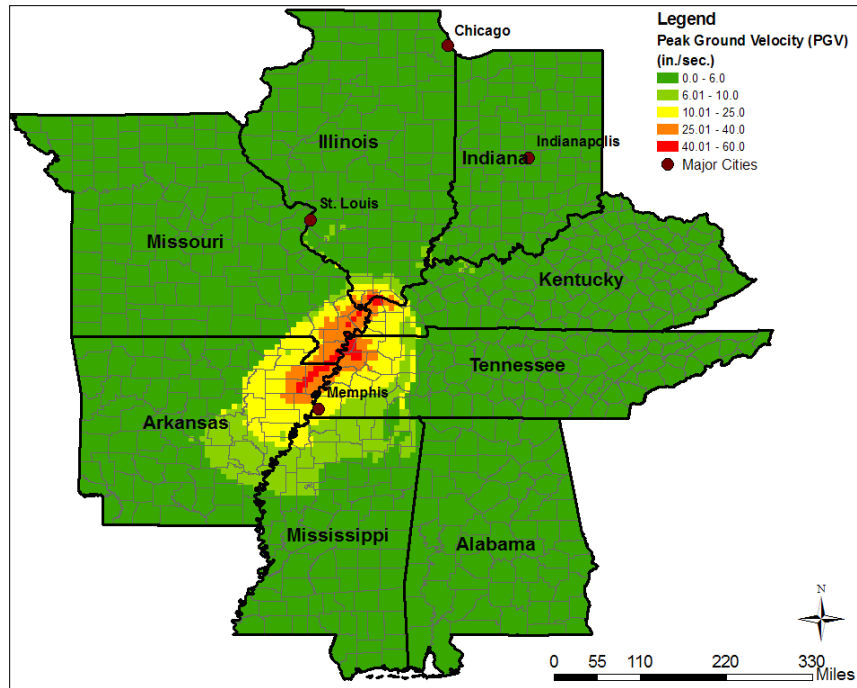


Figure 12. PGV for NMSZ Scenario Event

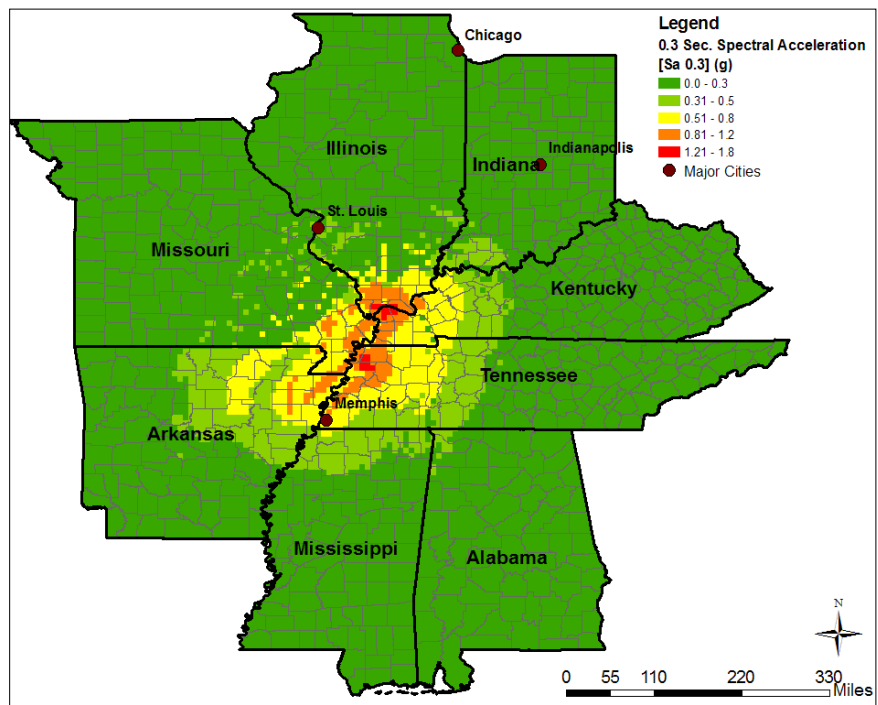
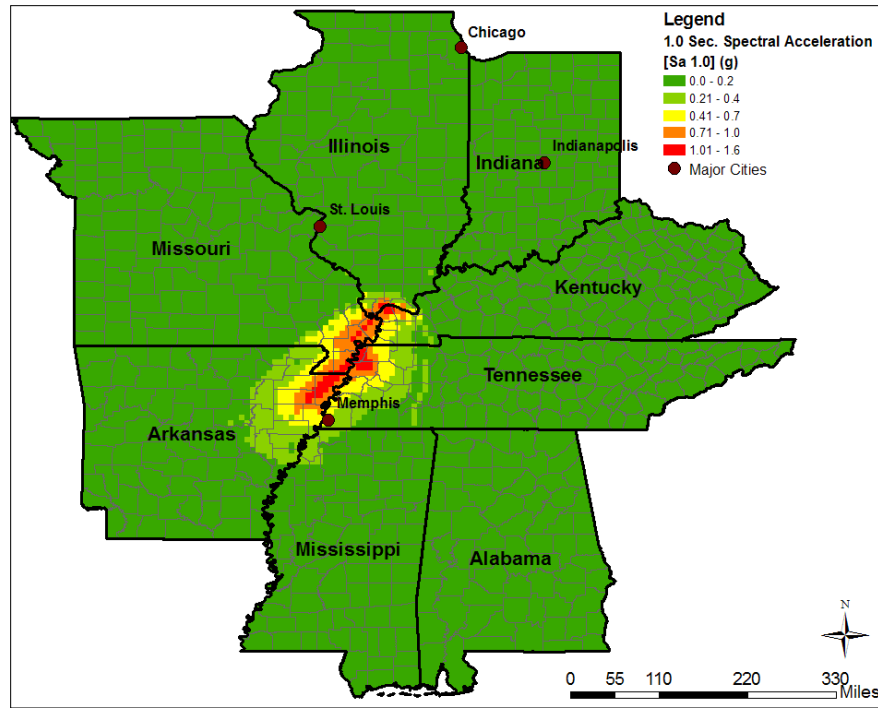


Figure 13. Short-Period (0.3 sec) Spectral Acceleration for NMSZ Scenario Event



**Figure 14. Long-Period (1.0 sec) Spectral Acceleration for NMSZ Scenario Event**

## 3.2 Assets

### 3.2.1 Definition and Categorization

Inventory or assets could be categorized into two major groups: population and infrastructure. Population inventory involves information regarding regional demographics such as age, gender, ethnicity, and socio-economic status. Infrastructure assets relate to all manmade structures ranging from buildings, bridges, roadways, generation plants, transportation systems, utility lifelines, etc. Inventory is an essential part of seismic risk assessment, thus it is important to identify several methodologies of inventory capture and respective uncertainties.

### **3.2.2 Inventory Capture Methods**

There are two main inventory capture methodologies, field survey and remote sensing. The third method is a hybrid combination of physical and remote sensing data capture methods.

Field survey, as the name indicates, relates to collection of inventory data through physical surveys. This type of inventory capture is very useful for demographics data collection and very small regions due to the level of details and amount of information that can be obtained. For example, significant amount of information regarding individual structures can be achieved by existing structural drawings or field observations. Additionally, particularly informative data can be collected for mass movements such as landslides (Njagih, 2003). However, the efficiency of this methodology gradually reduces as the size of study region increases, since it is unfeasible to have access of a large amount of surveyors, in terms of time and financial resources. The inefficiency gap widens to the point of impossibility, especially for significantly large regions such as the NMSZ which encompasses eight states with a total population that nears 44 million. The accuracy of field surveying also depends considerably on expert opinion, especially in cases where observational data is collected in the absence of structural documentation; subjectivity is not only present, but also very hard to quantitatively account for during uncertainty analysis.

Remote sensing relates to inventory capture through aerial methods such as aerial videography, photography, satellite imagery, and several other sensors. A general overview of remote sensing and height ranges are presented in Figure 15.

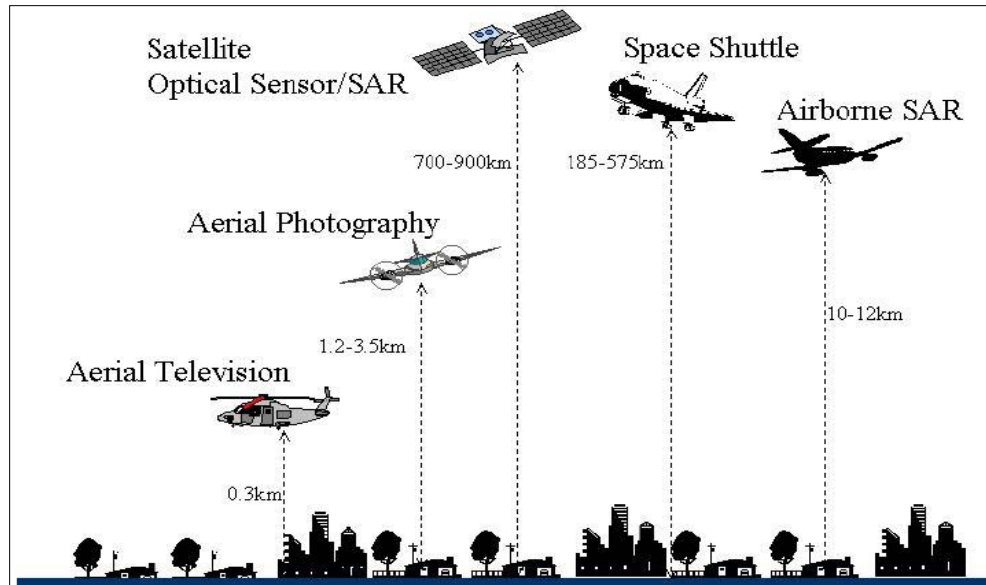


**Figure 15. Remote Sensing Methodologies (Yamazaki, 2001)**

As illustrated above, there are numerous methods that can be implemented to remotely capture inventory. The selection of a specific technique is influenced by several factors: financial resources, time, area coverage, urgency, and data resolution. Upon deciding the priority of each component, an adequate procedure can be decided to for data gathering. For instance, if a large area needs to be surveyed with low resolution and non-urgent data availability, satellite imagery represents an excellent choice. Conversely, for a small area and high resolution, aerial photography might be more efficient. Time of day is also an important factor to consider especially in urban areas, since results can be dependent on the time the images are obtained. In the case when data compilation is exercised during morning hours, many large transportation objects such as delivery trucks can impede the complete capture of structural characteristics (Montoya, 2003). Additional considerations such as meteorological conditions are required for some imagery techniques like Synthetic Aperture Radar (SAR). SAR results are extremely sensitive to unfavorable weather conditions: cloudy skies and poor sunlight filtration.

Remote sensing offers apparent advantages such as providing data in relatively short times, cover large surface areas, provide high resolution information, and easily obtain pre- and post-event data. Remote sensing can provide very useful information that could be effortlessly implemented in impact assessment software. On the other hand,

some major disadvantages relate to the quantification of uncertainty of remote sensing. Uncertainty sources and levels vary and depend on the utilized technique, thus hindering a unified uncertainty quantification approach. Additionally, trivial issues can noticeably influence the data accuracy, such as weather conditions or time of day. Furthermore, these factors cannot always be controlled and minimized.

The final technique of inventory data capture is the combination of both field and remote sensing methods. The interception of two methods when adequately applied produces superior results, since it takes advantage of the best components from both previously mentioned methodologies. In fact, the hybrid technique is recommended to reduce the uncertainty of inventory data, which is otherwise very difficult to accurately account for. The overlapping of the field survey data and remote sensing will aid in the elimination of user and mapping errors, since they are typical for only one of the methodologies. Regardless of the used methodology, the user needs to identify uncertainty sources for inventory capture in order to implement the adequate models that account for corresponding uncertainty levels.

### **3.2.3 Overview of HAZUS Inventory Classification**

This section describes the default classification of inventory in HAZUS. As previously mentioned, inventory can be separated into two distinct groups: infrastructure, which represents the physical inventory such as buildings and lifelines, and demographics, which quantifies population parameters. As stated, socio-economical impacts other than direct economic losses are not considered in this study; therefore, the demographics aspect of inventory is not discussed. As a result, hereinafter use of “inventory” will generally imply only infrastructure or physical assets, such as buildings and lifelines.

Comprehensive descriptions include the explanation of default classification of buildings and lifelines for the following inventory categories: general buildings, essential facilities, high potential loss facilities, transportation, and utilities. Additional information is provided regarding specific inventory classifications and relevant attributes such as determining which attributes are required or optional, and recognizing already provided fields versus the data the user can provide to advance the quality of inventory data set and the accuracy of impact assessment overall.

In terms of assessing damage to inventory through fragility functions, HAZUS considers two types of inventory distributions: aggregated and point-wise data. Aggregated data involves the grouping of inventory based on a census tract level, while point-wise data signifies just that: each facility is represented as an entity through its geographical coordinates and other relevant attributes. HAZUS treats general buildings and most pipelines as aggregated data, while the majority of facilities from inventory classes of essential facilities, high potential loss facilities, transportation, and utilities are represented on a point-by-point basis.

### 3.2.3.1 General Buildings

General building classifications can be mapped in terms of occupancy type and in terms of building models. Regarding the occupancy type classification, buildings can be categorized into seven general classes by occupancy type: residential, commercial, industrial, agricultural, religious, government, and educational buildings. In total, there are 33 specific occupancy types which are illustrated in Table 5.

- . The general building stock contains the following databases (FEMA, 2008):
  - Square Footage by occupancy – The estimated floor area by specific occupancy (e.g., COM1). For viewing by the user, these data are also rolled up to the general occupancies (e.g., Residential).
  - Full Replacement Value by occupancy – The estimated replacement values by specific occupancy (e.g., RES1).
  - Building Count by occupancy – The estimated building count by specific occupancy (e.g., IND1).
  - General Occupancy Mapping – A general mapping for the general building stock inventory data from the specific occupancy to general building type (e.g., Wood).
  - Demographics – Housing and population statistics for the study region.

Model buildings classification mainly attempts to group structures with similar structural parameters that will eventually result in similar structural damage patterns during an earthquake. An optimal categorization of model types is necessary, since it

directly impacts the number of fragility functions used in assessing structural damage. Consequentially, an adequate categorization of building model types will result in a more accurate damage assessment. Table 6 shows all building model types as presented in HAZUS-MH MR3 Technical Manual, while a more detailed description for each model type is included in HAZUS-MH MR3 Technical Manual.

**Table 5. HAZUS Building Classification by Occupancy Type**

Label	Occupancy Class	Example Description
<b>Residential</b>		
RES1	Single Family	House
RES2	Mobile Home	Mobile Home
RES3	Multi Family	Apartment/Condominium
	RES3A Duplex	
	RES3B 3-4 Units	
	RES3C 5-9 Units	
	RES3D 10-19 Units	
	RES3E 20-49 Units	
	RES3F 50+ Units	
RES4	Temporary Lodging	Hotel/Motel
RES5	Institutional Dormitory	Group Housing (military, college), Jails
RES6	Nursing Home	
<b>Commercial</b>		
COM1	Retail Trade	Store
COM2	Wholesale Trade	Warehouse
COM3	Personal and Repair Services	Service Station/Shop
COM4	Professional/Technical Services	Offices
COM5	Banks	
COM6	Hospital	
COM7	Medical Office/Clinic	
COM8	Entertainment and Recreation	Restaurants/bars
COM9	Theaters	Theaters
COM10	Parking	Garages
<b>Industrial</b>		
IND1	Heavy	Factory
IND2	Light	Factory
IND3	Food/Drugs/Chemicals	Factory
IND4	Metals/Minerals Processing	Factory
IND5	High Technology	Factory
IND6	Construction	Office
<b>Agriculture</b>		
AGR1	Agriculture	
<b>Religion/Non Profit</b>		
REL1	Church/Non-Profit	
<b>Government</b>		
GOV1	General Services	Office
GOV2	Emergency Response	Police/Fire Station/EOC
<b>Education</b>		
EDU1	Grade Schools	
EDU2	Colleges/Universities	Does not include group housing



**Table 6. Building Model Types**

No.	Label	Description	Height			
			Range		Typical	
			Name	Stories	Stories	Feet
1	W1	Wood, Light Frame ( $\leq 5,000$ sq. ft)		1 - 2	1	14
2	W2	Wood, Commercial and Industrial ( $> 5,000$ sq. ft)		All	2	24
3	S1L	Steel Moment Frame	Low-Rise	1 – 3	2	24
4	S1M		Mid-Rise	4 – 7	5	60
5	S1H		High-Rise	8+	13	156
6	S2L	Steel Braced Frame	Low-Rise	All	2	24
7	S2M		Mid-Rise	1 – 3	5	60
8	S2H		High-Rise	4 – 7	13	156
9	S3	Steel Light Frame		8+	1	15
10	S4L	Steel Frame with Cast-in-Place Concrete Shear Walls	Low-Rise	1 – 3	2	24
11	S4M		Mid-Rise	4 – 7	5	60
12	S4H		High-Rise	8+	13	156
13	S5L	Steel Frame with Unreinforced Masonry Infill Walls	Low-Rise	1 – 3	2	24
14	S5M		Mid-Rise	4 – 7	5	60
15	S5H		High-Rise	8+	13	156
16	C1L	Concrete Moment Frame	Low-Rise	1 – 3	2	20
17	C1M		Mid-Rise	4 – 7	5	50
18	C1H		High-Rise	8+	12	120
19	C2L	Concrete Shear Walls	Low-Rise	1 – 3	2	20
20	C2M		Mid-Rise	4 – 7	5	50
21	C2H		High-Rise	8+	12	120
22	C3L	Concrete Frame with Unreinforced Masonry Infill Walls	Low-Rise	1 – 3	2	20
23	C3M		Mid-Rise	4 – 7	5	50
24	C3H		High-Rise	8+	12	120
25	PC1	Precast Concrete Tilt-Up Walls		All	1	15
26	PC2L	Precast Concrete Frames with Concrete Shear Walls	Low-Rise	1 – 3	2	20
27	PC2M		Mid-Rise	4 – 7	5	50
28	PC2H		High-Rise	8+	12	120
29	RM1L	Reinforced Masonry Bearing Walls with Wood or Metal Decks Diaphragms	Low-Rise	1 – 3	2	20
30	RM1M		Mid-Rise	4 – 7	5	50
31	RM2L	Reinforced Masonry Bearing Walls with Precast Concrete Diaphragms	Low-Rise	1 – 3	2	20
32	RM2M		Mid-Rise	4 – 7	5	50
33	RM2H		High-Rise	8+	12	120
34	URML	Unreinforced Masonry Bearing Walls	Low-Rise	1 – 3	2	20
35	URMM		Mid-Rise	4 – 7	5	50
36	MH	Mobile Homes		All	1	10

Several parameters are considered in determining the building model types. The major considered parameters include (FEMA, 2008):

- Structural parameters affecting structural capacity and response
  - Basic structural system (steel moment frame)
  - Building height (low-rise, mid-rise, high-rise)
  - Seismic design criteria (seismic zone) (Refer to Chapter 5)
- Nonstructural elements affecting nonstructural damage
- Occupancy (affecting casualties, business interruption and contents damage)
- Regional building practices (Refer to Chapter 5)
- Variability of building characteristics within the classification

To account for these parameters, the building inventory classification system consists of a two-dimensional matrix relating building structure (model building) types grouped in terms of basic structural systems and occupancy classes. As mentioned, HAZUS utilizes aggregated data at the level of census tracts in the process of estimating damage. The overall distribution of general building types is represented by a lumped model at the center of each census tract. To determine the probability of damage to general buildings, HAZUS employs a relationship between specific occupancy type and building model type.

Two-dimensional matrices are developed for different regions of the US (West Coast, Mid-West, and East Coast) and in terms of building height (low-, mid-, and high-rise structures). Table 7 illustrates an example for Mid-West United States and low-rise structures, while all combinations of occupancy-model type mappings can be found in Appendix 3A of HAZUS-MH MR3 Technical Manual. As stated, these tables relay the relationship between specific model types and occupancy types through relating the percentage distribution of floor area square footage.

The building replacement cost database is associated with occupancy types and it is imperative in determining the total economic loss. In HAZUS default inventory, the replacement costs are evaluated based on industry-standard cost-estimation models published in Means Square Foot Costs (R.S. Means, 2002) (FEMA, 2008). Replacement costs are evaluated at the census tract level for each occupancy type in terms of full

replacement cost per square foot. An extensive list illustrating the replacement costs for each several occupancy types is included in Appendix 2, while the complete information for all occupancy types can be found in Appendix 3 of HAZUS Technical Manual.

**Table 7. Mapping of Occupancy-Model Type for Low-rise Buildings in Mid-west US**

Specific Occup. Class	Model Building type															
	1	2	3	6	9	10	13	16	19	22	25	26	29	31	34	36
	W1	W2	S1L	S2L	S3	S4L	S5L	C1L	C2L	C3L	PC1	PC2L	RM1L	RM2L	URML	MH
RES2																100
RES3	75												2		23	
RES4	50												3	2	45	
RES5	20							4	13	2	22	4	2		33	
RES6	90														10	
COM1		30	2	4	11	6	7		5		5		2		28	
COM2		10	2	4	11	6	7	2	10	2	14	2	2		28	
COM3		30	2	4	11	6	7		5		5		2		28	
COM4		30	2	4	11	6	7		5		5		2		28	
COM5		30	2	4	11	6	7		5		5		2		28	
COM6				2	4	2	2	6	21	4	33	6	2		18	
COM7		30	2	4	11	6	7		5		5		2		28	
COM8		30	2	4	11	6	7		5		5		2		28	
COM9			2	6	14	8	10	4	13	2	22	4			15	
COM10			2	4	11	6	7	6	21	4	33	6				
IND1			5	10	25	13	17	2	7	2	12	2			5	
IND2		10	2	4	11	6	7	2	10	2	14	2	3		27	
IND3		10	2	4	11	6	7	2	10	2	14	2	3		27	
IND4			5	10	25	13	17	2	7	2	12	2			5	
IND5		10	2	4	11	6	7	2	10	2	14	2	2		28	
IND6		30	2	4	11	6	7		5		5		2		28	
AGR1		10	2	4	11	6	7	2	10	2	14	2	2		28	
REL1	30			3	5	3	4		5		5		2	2	41	
GOV1		15	14	21				7	6		4		3		30	
GOV2		14	7	17				4	12					3	43	
EDU1		10	5	12				5	7						50	
EDU2		14	6	12			2	8	11					10	37	

### 3.2.3.2 Essential Facilities

Essential facilities include those facilities that service the community thus it is imperative to know whether these facilities are operational or not as well as know the level of their functionality after an event. Essential facilities consist of five main groups: medical care, police stations, fire stations, emergency operating centers (EOC), and schools. Similarly to general buildings, essential facilities require a mapping relationship between occupancy type and building model types. Additional required data in the damage assessment include design level and construction quality factor. For medical care facilities, the number of bed for each hospital is also required for the analysis. The occupancy mapping of building model types is illustrated in Table 8. The replacement cost of essential facilities is included in the replacement cost estimation from the general building stock, corresponding to general building stock occupancy classes 12, 26, 27 and 28, as defined in HAZUS Technical Manual.

**Table 8. Classification of Essential Facilities**

<b>Label</b>	<b>Occupancy Class</b>	<b>Description</b>
<b>Medical Care Facilities</b>		
EFHS	Small Hospital	Hospital with less than 50 beds
EFHM	Medium Hospital	Hospital with beds between 50 and 150
EGHL	Large Hospital	Hospital with greater than 150 beds
EGMC	Medical Clinics	Clinics, Labs, Blood Banks
<b>Emergency Response</b>		
EFFS	Fire Station	
EFPS	Police Station	
EFEO	Emergency Operation Centers	
<b>Schools</b>		
EFS1	Grade Schools	Primary/High Schools
EFS2	Colleges/Universities	

### 3.2.3.3 High Potential Loss Facilities

High potential loss facilities (HPLF) category indicates facilities that have high probability of causing significant additional impact if damaged during an earthquake. By default definition, HPL consists of dams, hazardous materials (hazmat), nuclear power plants, and military installations. The minimum required inventory fields for damage estimation of HPLF are geographical location. Though HPLF are included in inventory, the loss estimation is not calculated as part of the default methodology. The classification of dams, nuclear power facilities and military installations is represented in Table 9.

**Table 9. Classification of High Potential Loss Facilities**

<b>Label</b>	<b>Description</b>
<b>Dams</b>	
HPDE	Earth
HPDR	Rock fill
HPDG	Gravity
HPDB	Buttress
HPDA	Arch
HPDU	Multi-Arch
HPDC	Concrete
HPCM	Masonry
HPDS	Stone
HPDT	Timber Crib
HPDZ	Miscellaneous
<b>Nuclear Power Facilities</b>	
HPNP	Nuclear Power Facilities
<b>Military Installations</b>	
HPMI	Military Installations

Hazardous materials (hazmat) facilities can contain substances that pose significant toxic, radioactive, flammable, explosive, or reactive hazard, when damaged.

Hazmat facilities have the potential to cause significant casualties or infrastructural damage even from a small release amount of hazardous material. Additionally, the extent of the impact due to hazmat damage could vary significantly based on type of material, meteorological conditions, and time effectiveness of the emergency response (FEMA, 2008). Similar to dams, military installation, and nuclear power plants, the damage to hazardous materials is not conducted in the default methodology. Rather, these facilities are included in the inventory to give the user the ability to superimpose their location to damaged areas or hazard maps, in order to identify facilities at risk. A similar methodology of threshold values is utilized by the MAE Center to estimate damage to HLPF and it is discussed later in this document.

#### 3.2.3.4 Transportation Systems

Transportation systems are also classified with the objective of categorizing structures with similar predispositions of structural damage and loss characteristics. Major classes of transportation inventory include highways, railways, airports, light rail, ports, and ferries. Generally, transportation lifelines are represented on a point-wise format; therefore, one of the minimal attribute requirements involves geographical location: latitude and longitude.

Highway systems involve highway bridges, segments, and tunnels. Required attributes for analysis involve the definition of location, classification, and replacement cost. Classification of highway bridges considers material and construction type, span length, number of spans, connection type, and so on. In the analysis of highway segments, the length of highway segment needs to be defined as well.

Railways consist of tracks, bridges, tunnels, stations, and fuel, dispatch and maintenance facilities (FEMA, 2008). Similarly, required inventory data for estimates involves longitude and latitude, classification of facility, and replacement cost. For rail tracks damage assessment, additional information regarding track segment length is necessary.

Airport systems involve control towers, runways, terminal buildings, parking, fuel facilities, and maintenance facilities, while the necessary inventory data for impact

assessment consist of longitude, latitude, classification type, and replacement costs of facilities.

Bus transportation systems consist of public stations, fuel facilities, dispatch, and maintenance facilities. Geographical location, type of category, and replacement cost of facilities are required for damage analysis of bus transportation systems.

Port and harbor transportation systems are composed of waterfront structures, cargo management equipment, storage structures such as warehouses and fuel facilities. The required data for loss assessment of ports involves information regarding geographical coordinates, facility classification, and facility replacement cost.

Ferry systems are comprised of waterfront structures, passenger terminals, fuel facilities, and dispatch and maintenance facilities. The required information for damage estimation includes latitude, longitude, facility classification and replacement cost of facilities.

Similar to railway systems, light rail infrastructure involves bridges, facilities, tunnels, and tracks. The important difference between the two regards the type of power supply; the light rail systems function with DC power substations. The required inventory data consists of geographical location, classification, and replacement cost of infrastructure. In addition, segment length information is necessary for the estimation of damage for tracks only.

Detailed classifications for each transportation class can be found in Appendix 2.

### 3.2.3.5 Utilities Lifelines

Utility systems include electric power systems, communication systems, oil, natural gas, potable water, and waste water systems. HAZUS treats most utility facilities as point-wise data, while most pipelines are considered in an average level, aggregated at the census track level. This section briefly explains the contents of each utility system along with the necessary attributes to run the impact analysis.

Electric power systems are comprised of substations, distribution network, and power generation plants. For each category, distinctions are made regarding components with or without anchors. The required inventory information for loss assessment includes

the geographic coordinates, facility classification, and facility replacement cost. Classification of electric power systems is illustrated in Table 10.

**Table 10. Classification of Electric Power Systems**

<b>Label</b>	<b>Description</b>
<b>Transmission Substations</b>	
ESSL	Low Voltage (115 KV) Substation
ESSM	Medium Voltage (230 KV) Substation
ESSH	High Voltage (500 KV) Substation
<b>Distribution Circuits</b>	
EDC	Distribution Circuits (Seismic or standard design of components)
<b>Generation Plants</b>	
EPPL	Large Power Plants (> 500 MW)
EPPM	Medium Power Plants (100 - 500 MW)
EPPS	Small Power Plants (< 100 MW)

Default communication systems consist of telephone central offices (facilities only) and the required information for estimating losses due to earthquakes includes the geographical coordinates and type of classification system as illustrated in Table 11. For further reference regarding classification of other communication system classes, refer to Appendix 3 of HAZUS Technical Manual.

**Table 11. Classification of Communication Systems**

<b>Label</b>	<b>Description</b>
<b>Central Offices</b>	
CCO	Central Offices (different combination for with or without anchored components and/or with or without backup power)
<b>Stations or Transmitters</b>	
CBR	AM or FM radio stations or transmitters
CBT	TV stations or transmitters
CBW	Weather stations or transmitters
CBO	Other stations or transmitters



Oil systems are composed of pipelines, refineries, pumping plants, and tank farms. The required inventory data for loss assessment includes the latitude, longitude, and classification of system components. Additional required information involves replacement cost of facilities and repair cost of pipelines.

Natural gas systems include pipelines and compressor stations. The necessary data for impact assessment consists of geographical location and classification of infrastructure. Similar to oil systems, replacement cost of facilities and repair cost of pipelines are additional required inventory information.

Potable water systems consist of pipelines, water treatment plants, wells, storage tanks, and pumping stations. The required inventory data includes the knowledge of geographical location and system classification. Additionally, replacement cost for facilities and repair cost for pipelines information is required for loss assessment.

Waste water systems involve comparable components to potable water systems such as pipelines, water treatment plants, and lift stations. The required inventory data includes the identification of geographical location, classification of system components, replacement cost of facilities, and repair cost of pipelines.

For supplementary information and detailed classification for each utility system component, please refer to Appendix 3 of HAZUS-MH MR3 Technical Manual.

### **3.2.4 Inventory Additions**

As previously stated, in HAZUS, inventory is represented through two distinct formats: aggregated and point-wise. General building stock and most of pipelines are considered in aggregated form, while essential facilities, transportation, and the majority of utility facilities are represented on a singular point basis. The inventory improvement for this study was done only on point-wise data. The main challenge during the inventory additions process was encountered while including inventory additions from several sources. While the data format were all similar, different databases have different number of layers, so the initial phase of inventory additions concerned the mapping of the relevant inventory layers (or types) into the respective HAZUS inventory layers. The numerous sources of inventory ranged from national inventory data to private and facility type-specific inventory studies. Private inventory studies were conducted for Illinois and

Indiana by the Mid-America Earthquake (MAE) Center at the University of Illinois at Urbana-Champaign, and the POLIS Center at the University of Purdue, respectively. The Homeland Security Infrastructure Program (HSIP) Gold 2007 and 2008 Databases were largely used for the updates related to essential facilities, transportation systems and utility lifelines. Data regarding other critical infrastructure such as levees and tanks were obtained from additional sources such as US Army Corps of Engineers. Finally, an internal research project from the MAE Center was conducted to collect inventory information regarding major river crossings. Major river crossings were not included in the HSIP inventory, but due to their important infrastructure role in the mid-west, they were included in the overall impact assessment.

The continuing process of inventory additions initiated with the identification of relevant layers from other data sources that needed to be added to HAZUS inventory. The selected layers then needed to be formatted to corresponding HAZUS layers. Any additional metadata that was not required but available was imported into HAZUS. For required metadata that was not available, HAZUS default values were assigned. Often, multiple new layers from additional sources corresponded to a single layer in HAZUS. Subsequently, screening parameters such as buffers based on geographical location were utilized in GIS to compare and avoid duplicity of inventory data. Simultaneously, constant physical checks were conducted by comparing infrastructure information such as facility names or addresses in order to account for structures that were not screened during location buffers. Though great measures were taken to avoid the inclusion of an asset twice, there is still the possibility that the problem is not fully avoided; however, this number would be so small that it would not have the ability to significantly affect the outcome of impact assessment results. Furthermore, it is estimated that inventory of the region is underrepresented, thus it could be argued that the total estimated impact would still be less than the realistic impact that could be expected during a similar event.

#### 3.2.4.1 Buildings

As previously mentioned, general buildings are represented in an aggregated manner in HAZUS; therefore, no inventory updates were performed on general buildings, since the focus of inventory update was concentrated on point-wise data. Part of the

point-wise representation, are the essential facilities that consist of medical care, police stations, fire stations, emergency operating centers (EOC), and school facilities. The inventory improvements were based on the additions of datasets from the HSIP Gold 2008.

Hospital inventory improvements included the addition of hospitals and urgent care facilities. HAZUS methodology classifies the hospitals based on the bed capacity. If the number of beds information is not available, the facilities are classified as medical clinics. Structure type is required for the impact assessment of hospitals, and, since HSIP does not include this information, default HAZUS values are used for this field. Additionally, default assumptions are made regarding seismic design level, which is assumed as pre-code. Similar to facility classification, the replacement cost of facilities is estimated for each state based on the bed capacity. Exceptions regarding default assumptions are made for Illinois, where information regarding structure type and seismic design level were obtained from the MAE Center project in Illinois. The calculated replacement costs are presented in Table 12.

**Table 12. Hospital Replacement Cost**

<b>State</b>	<b>Hospital Replacement Cost (in thousands of dollars/ bed)</b>
Alabama	201.170
Arkansas	193.184
Illinois	262.308
Indiana	227.044
Kentucky	217.747
Mississippi	186.743
Missouri	235.430
Tennessee	205.911

HAZUS classifies all fire stations into one category of essential facilities; therefore, all additional fire stations are added to one category. For all updated fire station inventory, structure type was assumed as low-rise unreinforced masonry (URML) and seismic design level was assigned as pre-code. Default assumptions were not necessary

for Illinois, since relevant information from MAE Center Project in Illinois was used to substitute the HAZUS default values. The replacement cost was adapted from HAZUS default cost data, shown in Table 13.

**Table 13. Fire Station Replacement Cost**

<b>State</b>	<b>Fire Station Replacement Cost (in thousands of dollars)</b>
Alabama	1,205
Arkansas	1,200
Illinois	1,613
Indiana	1,425
Kentucky	1,318
Mississippi	1,137
Missouri	1,470
Tennessee	1,252

Police station additional inventory includes local, state, and university police stations. The new facilities are classified under the single essential facility category for police stations (EFPS), while the structure type is assigned as URML by default and seismic design level is assumed as pre-code. For the state of Illinois, structure type and seismic design level default values were substituted with respective information collected during the MAE Center project in Illinois. HAZUS default replacement costs were applied to the new inventory and are illustrated in Table 14.

**Table 14. Police Station Replacement Cost**

<b>State</b>	<b>Police Station Replacement Cost (in thousands of dollars)</b>
Alabama	1,251
Arkansas	1,201
Illinois	1,613
Indiana	1,425
Kentucky	1,318
Mississippi	1,138
Missouri	1,470
Tennessee	1,252

In HAZUS, schools are categorized into grade schools or colleges/universities, so new HSIP inventory was added into the corresponding HAZUS layers. Default structure type of URML was assigned along with pre-code seismic design level. The replacement cost was estimated by averaging the cost of all schools in a specific state. Table 15 illustrates the calculated replacement costs.

**Table 15. Schools Replacement Cost**

<b>State</b>	<b>Schools Replacement Cost (in thousands of dollars)</b>
Alabama	1,251
Arkansas	1,201
Illinois	1,613
Indiana	1,425
Kentucky	1,318
Mississippi	1,138
Missouri	1,470
Tennessee	1,252

The new emergency operation centers (EOC) included emergency operation centers, state emergency operation centers, and 911 call centers from HSIP database. Similar to other default assumptions, structure type and design level were assigned as

URML and pre-code, respectively. Values from Illinois were substituted with information from the MAE Center project in Illinois. Default replacement values were assumed and are presented in Table 16.

**Table 16. EOC Replacement Cost**

<b>State</b>	<b>EOC Replacement Cost (in thousands of dollars)</b>
Alabama	900
Arkansas	870
Illinois	1,110
Indiana	1,030
Kentucky	980
Mississippi	850
Missouri	1,030
Tennessee	880

#### 3.2.4.2 Transportation Systems

Inventory additions of transportation consist of highway bridges, railway systems, airport facilities, bus facilities, light rail facilities, ports, and ferries. In addition, 127 major river crossings were identified for the region and included in the analysis.

Highway bridges were added from HSIP inventory, which obtained the information from National Bridge Inventory (NIB). As a result, all the added bridge types from NIB were correlated to the highway bridge types in HAZUS. Among the included properties were length, width, number of spans, and skew angle. A default seismic level of low-code was assigned to the new bridges. When available data such as width of the bridge were not provided, and average width was assigned for cost replacement calculations only. The replacement costs based on average widths are presented in Table 17.

**Table 17. Replacement Cost of Highway Bridges**

<b>State</b>	<b>Highway Bridge Replacement Cost (in dollars/m<sup>2</sup>)</b>	<b>Average Width (in m)</b>
Alabama	1.458	11.90
Arkansas	1.409	9.54
Illinois	1.798	28.95
Indiana	1.669	30.08
Kentucky	1.588	11.20
Mississippi	1.377	9.70
Missouri	1.669	N/A
Tennessee	1.426	14.90

The improvement of railway bridges followed the same process as highway bridges. Railway bridge types were correlated to HAZUS railway bridge categories. The entire new infrastructure obtained default low-code assignments of seismic design level. The replacement cost of railway bridges is expressed in terms of dollars per tenths of linear meters.

Table 18 illustrates replacement cost for each state. It is necessary to notice that both replacement costs for highway and railway bridge costs were required to be converted to unit measures of English units (\$/ft<sup>2</sup> and \$/ft).

**Table 18. Railway Bridge Replacement Cost**

<b>State</b>	<b>Railway Bridge Replacement Cost (in dollars/tenths of meters)</b>
Alabama	2.70
Arkansas	2.61
Illinois	3.33
Indiana	3.09
Kentucky	2.94
Mississippi	2.55
Missouri	3.09
Tennessee	2959.20

All the HSIP railway facilities were added to railway facilities with the exception of two layers which were added to the light rail facilities. As with railway facilities, low-code seismic design level was assigned along with default replacement costs, which are shown in Table 19.

**Table 19. Light Rail Facility Replacement Cost**

<b>State</b>	<b>Light Rail Facility Replacement Cost (in thousands of dollars)</b>
Alabama	1,962.00
Arkansas	1,896.60
Illinois	2,419.80
Indiana	2,245.40
Kentucky	2,136.40
Mississippi	1,853.00
Missouri	2,245.50
Tennessee	1,918.40

Railway tunnels and railway facilities from HSIP were all applied to the corresponding categories in HAZUS concerning their respective infrastructure types. Default assumptions for low-code seismic level design and replacement costs were assumed. Replacement cost for railway tunnels in HAZUS is a fixed value of \$11/meter, while replacement costs for railway facilities are the same as for light rail facilities are shown in Table 19.

The updates of bus facilities were obtained from HSIP data and they were assigned to the corresponding group of bus facilities in HAZUS. Default assumptions of low-code seismic level and replacement costs were applied to the new facilities. The replacement costs are shown in Table 20.



**Table 20. Bus Facility Replacement Cost**

<b>State</b>	<b>Bus Facility Replacement Cost (in thousands of dollars)</b>
Alabama	981.00
Arkansas	948.30
Illinois	1,209.90
Indiana	1,122.70
Kentucky	1,068.20
Mississippi	926.50
Missouri	1,122.70
Tennessee	981.00

Ports inventory data was obtained from a single HSIP layer and assigned to its respective HAZUS layer. Default assumptions of low-code seismic design level and replacement costs were assigned. The replacement costs are presented in Table 21.

**Table 21. Port Facility Replacement Cost**

<b>State</b>	<b>Port Facility Replacement Cost (in thousands of dollars)</b>
Alabama	1,962.00
Arkansas	1,896.60
Illinois	2,245.40
Indiana	2,158.20
Kentucky	1,940.20
Mississippi	2,245.40
Missouri	2,158.20
Tennessee	1,940.20

Ferry additions were subtracted from the single HSIP layer concerning ferry structures and added to the corresponding HAZUS layer. Low-code seismic design level and default replacement costs were applied. Replacement costs are included in Table 22.

**Table 22. Ferry Replacement Cost**

<b>State</b>	<b>Ferry Facility Replacement Cost (in thousands of dollars)</b>
Alabama	1,122.70
Arkansas	948.30
Illinois	1,209.90
Indiana	1,122.70
Kentucky	1,068.20
Mississippi	926.50
Missouri	1,122.70
Tennessee	959.20

Airport additions were also obtained from HSIP sources. Multiple layers needed to be mapped into the analogous HAZUS layers. All airport facilities were assigned low-code seismic level design and default replacement costs, which are shown in Table 23.

**Table 23. Airport Facility Replacement Cost**

<b>State</b>	<b>Airport Facility Replacement Cost (in thousands of dollars)</b>
Alabama	4,905.00
Arkansas	4,741.50
Illinois	6,049.50
Indiana	5,613.50
Kentucky	5,341.00
Mississippi	4,632.50
Missouri	5,613.50
Tennessee	4,796.00

### 3.2.4.3 Utility Systems

Utility systems are comprised of communication, electric power, potable water, waste water, oil, and natural gas facilities. HSIP inventory does not contain potable water facilities; therefore, no updates were included for potable water systems.

Regarding communication facilities, multiple layers of HSIP data were mapped into the HAZUS classification data, in order to obtain data compatibility. Default assumptions were applied to the new inventory by assigning to all facilities a low-code seismic design level. Replacement costs were adapted from HAZUS default estimations and are shown in Table 24.

**Table 24. Communication Facilities Replacement Cost**

<b>State</b>	<b>Communication Facilities Replacement Cost (in thousands of dollars)</b>
Alabama	90
Arkansas	87
Illinois	111
Indiana	103
Kentucky	98
Mississippi	85
Missouri	103
Tennessee	88

Electric power facilities update involved the classification of substations and power plants from HSIP layers into their respective categories based on their voltage and power generation capacities, as outlined in Table 10. Default seismic design level of low-code and facility replacement cost were assigned to the new inventory; replacement costs are shown in Table 25.

**Table 25. Electric Power Facilities Replacement Cost**

<b>State</b>	<b>Electric Power Facilities Replacement Cost (in thousands of dollars)</b>
Alabama	99,000
Arkansas	95,700
Illinois	122,100
Indiana	113,300
Kentucky	107,800
Mississippi	93,500
Missouri	113,300
Tennessee	96,800

New waste water facilities were assigned to the single HAZUS layer corresponding waste water facilities, WDFLT. All new facilities were assigned a seismic design level of low-code and default replacement costs by state were assumed.

Table 26 illustrates default replacement costs.

**Table 26. Waste Water Facilities Replacement Cost**

<b>State</b>	<b>Waste Water Facilities Replacement Cost (in thousands of dollars)</b>
Alabama	59,940
Arkansas	57,942
Illinois	73,926
Indiana	68,598
Kentucky	65,268
Mississippi	56,610
Missouri	68,598
Tennessee	58,608

Oil and natural gas facilities have multiple HSIP layers corresponding to the respective HAZUS layers. Facilities such as wells, terminals, and refineries are added to default inventory. Refineries are classified according to their capacity, small or medium. Only active layers were added. Low-code seismic design level is assigned to all new facilities and default replacement costs are applied. HAZUS replacement cost for oil and natural gas facilities are presented in Table 27 and Table 28.

**Table 27. Oil Facilities Replacement Cost**

<b>State</b>	<b>Oil Facilities Replacement Cost (in thousands of dollars)</b>
Alabama	90
Arkansas	87
Illinois	111
Indiana	103
Kentucky	98
Mississippi	85
Missouri	103
Tennessee	88

**Table 28. Natural Gas Facilities Replacement Cost**

<b>State</b>	<b>Natural Gas Facilities Replacement Cost (in thousands of dollars)</b>
Alabama	981.00
Arkansas	948.30
Illinois	1,209.90
Indiana	1,122.70
Kentucky	1,068.20
Mississippi	926.50
Missouri	1,122.70
Tennessee	959.20

#### 3.2.4.4 High Potential Loss Facilities

The dam data used to update HAZUS inventory was taken from HSIP database. Since multiple layers for dam classifications existed both in HSIP and HAZUS, a mapping relation was necessary. By default, HAZUS does not implement the calculation of replacement costs in the assessment methodology; therefore, no replacement cost for dams were included.

Nuclear power facilities and hazmat facilities are not analyzed in HAZUS as mentioned, though they are included in the inventory. Thus, the added data from HSIP was not utilized during the impact assessment.

Levee damage was assessed not implementing HAZUS methodology; rather, pass-fail criteria were established through the threshold values determined during a MAE Center study specifically for critical structures such as levees.

#### 3.2.4.5 Regional Overview of Inventory Improvements

Through a rigorous process of inventory additions, a total of over 400,000 new assets were added to the default HAZUS inventory, thus increasing the total inventory entities to over 600,000. Significant improvements were made to all point-wise represented inventory categories. Specifically, major improvements were achieved for communication facilities, oil facilities, highway bridges, hospitals, waste water facilities, and so on. A summary of all regional inventory additions and comparison with baseline data are presented in Table 29.

**Table 29. Regional Inventory Improvements Summary**

<b>Infrastructure Category</b>	<b>Default Inventory</b>	<b>Improved Inventory</b>	<b>Differential Infrastructure</b>
<b>Essential Facilities</b>			
Emergency Operation Centers	1,074	2,825	1,751
Fire Stations	18,455	20,291	1,836
Hospitals	5,032	10,346	5,314
Police Stations	3,982	4,480	498
Schools	353	1,182	829
<b>Total</b>	<b>28,896</b>	<b>39,124</b>	<b>10,228</b>
<b>Transportation Facilities</b>			
Highway Bridges	104,048	165,771	61,723
Highway Tunnels	11	11	0
Railway Bridges	1,663	1,888	225
Railway Facilities	990	1,118	128
Railway Tunnels	2	72	70
Bus Facilities	310	405	95
Port Facilities	1,738	1,904	166
Ferry Facilities	6	52	46
Airport Facilities	2,435	3,773	1,338
Light Rail Facilities	0	537	537
Light Rail Bridges	38	38	0
<b>Total</b>	<b>111,241</b>	<b>175,569</b>	<b>64,328</b>
<b>Utility Facilities</b>			
Communication Facilities	3,160	145,722	142,562
Electric Power Facilities	554	10,893	10,339
Natural Gas Facilities	464	34,339	33,875
Oil Facilities	138	89,621	89,483
Potable Water Facilities	918	1,195	277
Waste Water Facilities	4,518	48,430	43,912
<b>Total</b>	<b>9,752</b>	<b>330,200</b>	<b>320,448</b>
<b>High Potential Loss Facilities</b>			
Dams	15,098	17,573	2,475
Levees	20,153	39,939	19,786
Hazmat Facilities	0	1,326	1,326
Nuclear Power Plants	15	25	10
<b>Total</b>	<b>35,266</b>	<b>58,863</b>	<b>23,597</b>
<b>Total Number of Facilities</b>	<b>185,155</b>	<b>603,756</b>	<b>418,601</b>

### 3.3 Vulnerability Functions

#### 3.3.1 Definition

Fragility, or vulnerability, functions relate the severity of shaking to the probability of reaching or exceeding pre-determined damage limit states. The shaking intensity is defined by peak ground parameters or spectral values of acceleration, velocity, or displacement. The maximum structural performance is estimated through capacity curves, specific to building or other infrastructure types. Furthermore, the intensity measure selected in fragility derivations is dependent upon the type of structure that the fragility relationships are developed for. It is generally recognized that structures with long natural periods, such as long span bridges or pipelines, are more sensitive to displacement; thus, peak ground displacement is a suitable choice as an intensity measure for the derivation of fragility relationships. Conversely, structures with short periods of vibration such as low rise masonry buildings are more sensitive to acceleration; hence in this case peak ground acceleration is a better choice as an intensity measure.

Limit states are essential in fragility curve derivation. HAZUS limit states include slight, moderate, extensive, and complete damage. The probability of reaching a defined limit state is given the following equation:

$$P[LS] = \sum P[LS|D = d] P[D = d] \quad (5)$$

where

$D$  = a variable that describes the demand imposed on the system

$P[LS|D = d]$  = the conditional probability for the exceedance of the limit state (LS), given that  $D = d$ , and the summation is taken over all possible values of  $D$

$P[D = d]$  = probability that defines the hazard.

$d$  = the control, or interface, variable



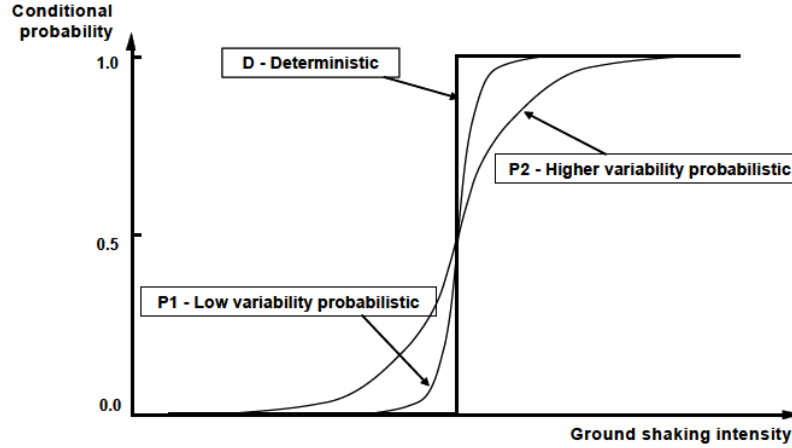


Figure 16. Conventional Fragility Curves (MAEC, 2007)

Figure 16 illustrates a typical fragility curve. The vertical line represents a system with deterministic limit state, while the other two curves represent probabilistic limit states with different variability. The curve closer to the vertical line (deterministic) has lower uncertainty than the curve that is farther from the vertical line.

### 3.3.2 HAZUS Building Fragility Relationships

HAZUS implements four damage limit states (slight, moderate, extensive, and complete), which correspond to four fragility curves per building type. Fragilities are represented with lognormal cumulative distribution functions that estimate the probability of reaching or exceeding a certain damage state, for a certain level of ground shaking or ground deformation. Equation (2) expresses the mathematical relationship utilized to describe the fragility curves:

$$P[\text{Exceedance}_i | S_d] = \Phi \left[ \frac{1}{\beta_{\text{TOT}i}} \ln \left( \frac{S_d}{LS_i} \right) \right] \quad (6)$$

where

$\Phi$  = the standard normal cumulative distribution function

$\beta_{\text{TOT}i}$  = the total uncertainty associated with damage state,  $i$

$S_d$  = spectral displacement

$LS_i$  = the median value of  $S_d$  at which the building achieves the damage limit state,  $i$

Typical fragility curves implemented in HAZUS depicting the four limit states: slight, moderate, extensive, and complete damage are illustrated in Figure 17.

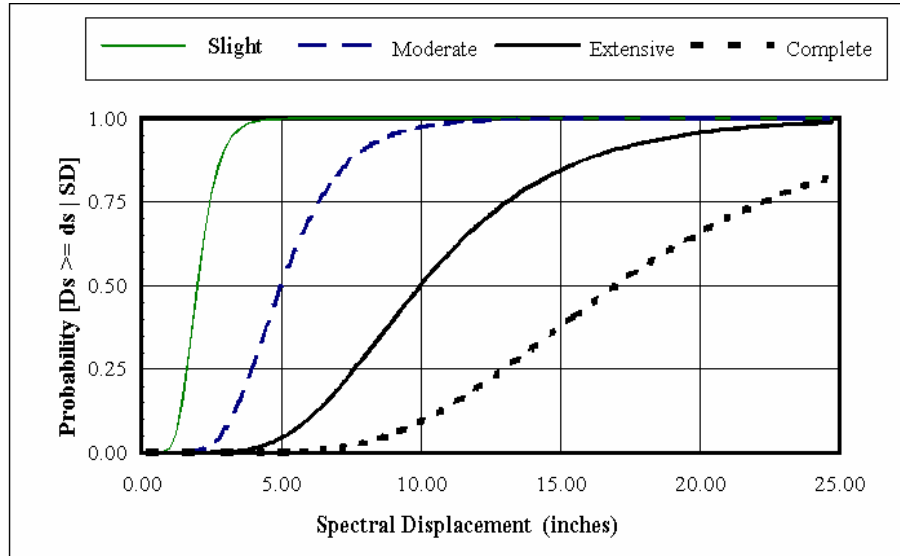


**Figure 17: Characteristic Fragility Relationships (FEMA, 2008)**

Damage functions require various metadata to properly apply building fragilities including, the construction material, the building height (low, medium, or high rise), and the response spectrum of the structure. There are 36 model building types defined in HAZUS, as previously shown in Table 6. The fragility curves implemented in HAZUS are functions of the structural response. The structural response required to utilize the vulnerability functions is determined by applying the capacity spectrum approach, thus requiring the derivation of the capacity, defined by pushover curves.

Fragility curves are further characterized by the level of seismic design inherent in building construction. The four seismic design levels in HAZUS correspond to pre-, low-, moderate-, and high-code, and are applicable to each building type. There are a total of 144 combinations of building types and seismic design levels in HAZUS representing 144 individual capacity curves. The capacity spectrum method (CSM) and building

capacity curves provide reasonable structural damage estimates adequate for structural loss assessment.

A capacity curve relates the lateral displacement to the lateral force. Typically, lateral displacement is top (roof) displacement, while base shear is utilized for a static-equivalent lateral force representation. In order to obtain HAZUS-compatible relationships, total base shear is converted to spectral acceleration ( $S_a$ ) and roof displacement is converted to spectral displacement ( $S_d$ ), by applying the following equations:

$$S_a = \frac{V/W}{\alpha_1} \quad (7)$$

$$\alpha_1 = \frac{\left[ \sum_{i=1}^N w_i \phi_{i1} / g \right]^2}{\left[ \sum_{i=1}^N w_i / g \right] \left[ \sum_{i=1}^N (w_i \phi_{i1}^2) / g \right]} \quad (8)$$

$$S_d = \frac{\Delta_{\text{roof}}}{PF_1 \phi_{\text{roof},1}} \quad (9)$$

$$PF_1 = \frac{\left[ \sum_{i=1}^N w_i \phi_{i1} / g \right]}{\left[ \sum_{i=1}^N (w_i \phi_{i1}^2) / g \right]} \quad (10)$$

where

$V$  = the base shear

$W$  = total building weight

$g$  = the acceleration of gravity

$w_i$  = the weight of  $i$ -th story

$\phi_i$  = the magnitude of the fundamental mode shape at story,  $i$

The parameters  $\alpha_1$  and  $PF_1$  are defined by equations (4) and (6), respectively, while the applied methodology is adapted from Applied Technology Council Report, ATC-40 (1996).

The building capacity curves are constructed based on estimates of engineering properties that affect the design, i.e. the yield and the ultimate capacities of each model building type. The parameters required to define the limit states are as follows (FEMA, 2008):

- $C_s$  – Design strength coefficient (fraction of building’s weight)
- $T_e$  – True “elastic” fundamental-mode period of building (seconds)
- $\alpha_1$  – Fraction of building weight effective in push-over mode
- $\alpha_2$  – Fraction of building height at location of push-over mode displacement
- $\gamma$  – Overstrength factor relating “true” yield strength to design strength
- $\lambda$  – Overstrength factor relating ultimate strength to yield strength
- $\mu$  – Ductility factor relating ultimate displacement to  $\lambda$  times the yield displacement (i.e., assumed point of significant yielding of the structure)

The design strength,  $C_s$ , is approximately based on the lateral-force design requirements of current seismic codes (e.g., 1994 NEHRP Provisions). These requirements are functions of the building seismic zone location and other factors such as the type of lateral force resisting systems, the local soil conditions, and the building fundamental period. In the HAZUS Technical Manual (FEMA, 2008), Tables 5.4, 5.5, and 5.6 provide values for the parameters  $C_s$ ,  $T_e$ , the response factors  $\alpha_1$  and  $\alpha_2$ , the overstrength factors  $\lambda$  and  $\gamma$ , and the ductility factor  $\mu$ . Figure 18 illustrates the derivation procedure for HAZUS fragility curves and relates the definition of the yield and ultimate points to the previously discussed parameters.

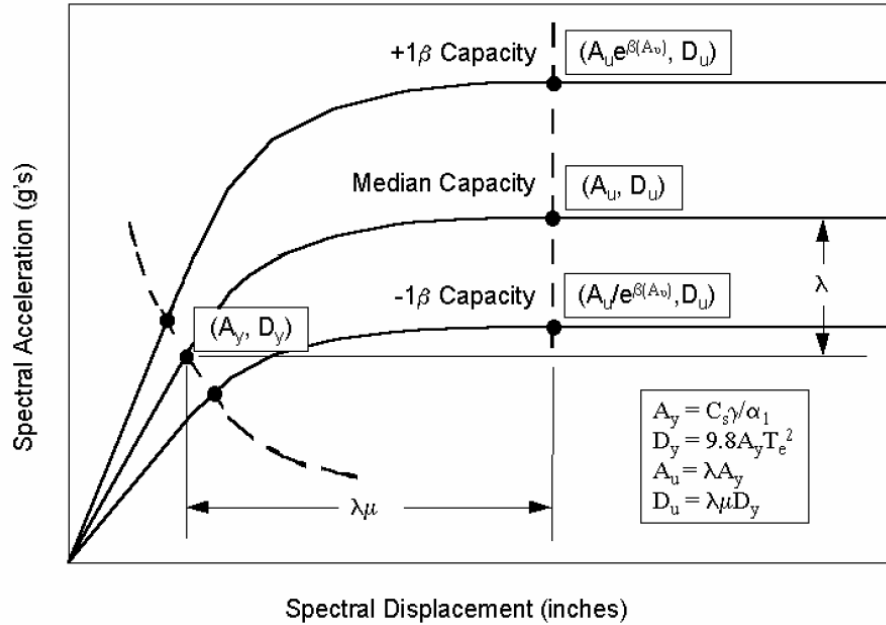


**Figure 18: Derivation of HAZUS Fragilities (FEMA, 2008)**

The four damage states (slight, moderate, extensive, and complete) are defined through drift threshold median values of buildings. Comprehensive drift values for different building types, seismic design levels, and heights are included in the HAZUS Technical Manual, Tables 5.9a-d. Though drift threshold values vary depending upon construction materials, building height, and seismic level, general assumptions are applied for specific categories as follows:

- Drift ratio values of complete damage of moderate-code buildings are assumed to be 75% of drift ratio values that define complete damage of high-code buildings.
- Drift ratio values of complete damage of low-code buildings are assumed to be 63% of drift ratio values that define complete damage of high-code buildings
- Slight damage ratios are assumed to have approximately same drift ratio values for all code design levels.

The previous statements are based on the assumption that low- and moderate-code structures have lower ductility capacity than high-code buildings, thus having lower post-yield capacity. Most structures still exhibit elastic behavior even when slightly damaged that leads to the assumption of equal drift ratio for all code levels. For pre-code buildings, low-code parameters are reduced to 80% of the original values, in order to account for inferior seismic design. For all damage states, drift ratios are reduced as building height increases. Drift ratio values of mid-rise buildings are reduced to 67% of the low-rise building values, while high-rise building values are assumed to be 50% of the low-rise building drift ratios.

The uncertainty associated with damage levels in fragility relationships is obtained by the combination of three lognormal standard deviation values. The total variability for each limit state is evaluated using the following equation:

$$\beta_{Sds} = \sqrt{(\text{CONV}[\beta_C, \beta_D, \bar{S}_{d,Sds}])^2 + (\beta_{M(Sds)})^2} \quad (11)$$

where

$\beta_{Sds}$  = the lognormal standard deviation that describes the total variability in structural damage state, ds,

$\beta_C$  = the lognormal standard deviation parameter that describes the variability in the capacity curve,

$\beta_D$  = the lognormal standard deviation parameter that describes the variability in the demand spectrum,

$\bar{S}_{d,Sds}$  = the median value of spectral displacement, in inches, of structural components for damage state, ds,

$\beta_{M(Sds)}$  = the lognormal standard deviation parameter that describes the uncertainty in the estimate of the median value of the threshold of structural damage state, ds.

CONV refers to a convolution function which is necessary to account for the interdependency between the lognormal standard deviations of capacity and demand values.  $\beta_{M(Sds)}$  is assumed as 0.4 for all buildings, while the lognormal standard deviation

parameter,  $\beta_C$ , takes the values of 0.3 for pre-code structures and 0.25 for all post-code seismic design levels. The  $\beta_D$  term is taken as 0.45 for short periods and 0.5 for long periods (FEMA, 2008).

The resulting fragilities are applied to the entire U.S. even though they are not specific to the Central US; therefore, the uncertainty associated with the default fragilities is high. In order to reduce the uncertainty and provide more accurate and structure-specific fragilities, new fragilities derived by the MAE Center and implemented in the earthquake impact assessment conducted in this study.

### **3.3.3 Building Fragility Improvements**

A new method to derive fragilities is used to improve upon the HAZUS default fragility functions. The methodology employed to develop the new building fragilities allows for a more accurate damage assessment and is used to derive sets of fragility curves for all building types. The HAZUS fragility derivation methodology developed by Gencturk et al. (2007) consists of three main components: capacity, demand, and structural analysis and fragility curve generation.

The capacity of structures is represented by either analytical (for wood frame structures) or expert opinion (for other building types) pushover curves. Demand refers to the earthquake event a structure is subjected to and represented using artificially generated earthquake ground motions. HAZUS provides default capacity for all infrastructure types, though the demand curves are adjusted to represent Central US event during the development of new building fragilities. Capacity and demand are critical to the process of fragility relationship derivations. A better representation of the real behavior both in terms of building capacity and earthquake demand generate more dependable results. The fragility derivation method produces fragility relationships that are easily implemented in loss assessment methodology. A similar methodology as described in HAZUS Technical Manual was implemented to estimate building capacity.

The spectral displacement ground motion parameter is employed in HAZUS building fragility curves and thus is the basis for all new HAZUS-compatible fragility relationships incorporated in this study. Building capacity curves for all building types included in the HAZUS program were not modified for these HAZUS-compatible

fragilities. In other words, fragility curves are derived using the default capacity curves as provided by HAZUS, the site specific ground motions for Central U.S. and the developed method for structural assessment, i.e. advanced CSM.

Ground motion processes are highly unpredictable and variable, thus they are responsible for a large portion of the uncertainty in the derivation of fragility relationships. This emphasizes the importance of earthquake record selection, since the accuracy of the representation of the demand is directly related to the reliability of fragility derivation. Due to the lack of natural records in the Central US, synthetic artificial records were used.

The derived fragilities take into account regional differences in ground motion. As previously mentioned, attenuation of strong motion can differ significantly for inter-plate and intra-plate regions. In intra-plate regions such as CEUS, ground motion takes longer to attenuate due to geological conditions. One example of a cohesive intra-plate region is the Upper Mississippi Embayment. The Upper Mississippi Embayment has unique ground motion attenuation due to the soft soil sediments located on top of the bedrock. Thickness varies from only a few feet up to 4,000 feet throughout the Embayment. With this in mind, attenuation relationships were derived for two soil profiles, uplands and lowlands. The Upland profile represents extremely stiff soils or rock, while the lowland profile represents soft soil conditions (Gencurk et al., 2007). Figure 19 (Fernandez and Rix, 2006) illustrates the soil profile of the Upper Mississippi Embayment and the cities for which synthetic ground motions were developed.



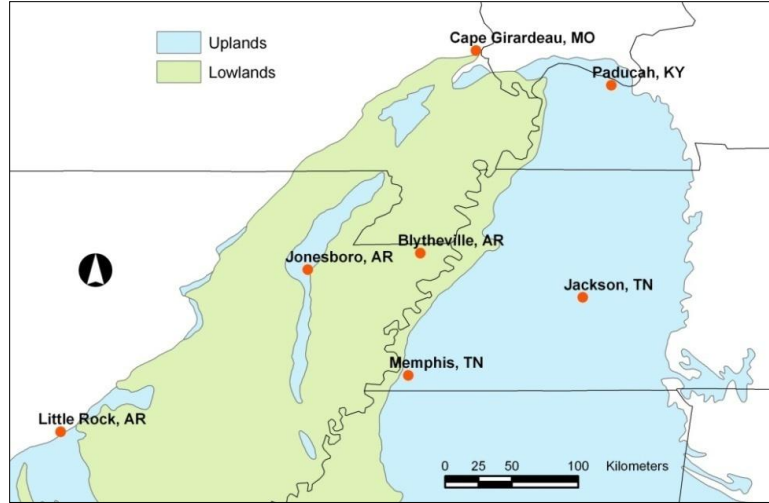


**Figure 19: Soil Profiles for the Upper Mississippi Embayment**

A set of ground motions consistent with hazard levels of 10%, 5% and 2% probabilities of exceedance in 50 years were considered and the ground motions representing the 975 year return period event were selected; each set includes ten acceleration time histories for both upland and lowland profiles. Table 30 (Gencturk et al., 2007) illustrates the ground motion parameters for both soil profiles.

**Table 30: Single Value Representations of Earthquake Record Sets**

Record #	Lowlands			Uplands		
	PGA (g)	PGV (in/sec)	PGD (in)	PGA (g)	PGV (in/sec)	PGD (in)
1	0.204	13.580	6.938	0.201	9.007	3.851
2	0.212	10.733	5.884	0.224	12.048	7.554
3	0.185	8.785	6.902	0.230	17.364	11.546
4	0.207	10.870	7.034	0.226	11.240	6.176
5	0.198	9.821	11.615	0.198	9.808	12.338
6	0.237	17.385	18.182	0.239	13.772	23.945
7	0.192	7.812	6.120	0.275	9.737	8.396
8	0.208	9.511	10.684	0.223	13.614	14.424
9	0.178	17.592	7.321	0.213	13.490	5.489
10	0.213	16.352	6.444	0.250	15.601	13.397
Mean	0.203	12.244	8.712	0.228	12.568	10.712
Standard Deviation	0.017	3.694	3.845	0.023	2.707	5.866

NMSZ is a low probability high consequence event. This signifies that strong motion events are rare. In fact, the last major event was the 1811-1812 earthquake series.

As a result, there is a lack of natural strong motion records in the region. Furthermore, there are very few records in the world that have similar characteristics to the NMSZ. Obviously, it is important that the used ground motions represent the characteristics of NMSZ; therefore, in the absence of natural records, synthetically generated ground motion records compatible with the seismo-tectonic and geotechnical characteristics (magnitude, distance, and site conditions) of the NMSZ are utilized.

The improved methodology also introduces an advanced capacity spectrum method (CSM) to more accurately predict displacement response. This advanced method is utilized to analyze structures, whose pushover curves are available, under any desired ground motion without convergence problems even under very severe ground motions. Additionally, the methodology provides a reliable alternative to computationally expensive inelastic dynamic analysis of multiple degree of freedom (MDOF) structures (Gencturk et al., 2008).

Fragility relationships are generated by conducting statistical analysis of the results obtained from the structural response of buildings under the variations of ground motions using the proposed methodology for structural response assessment. This final component of the proposed framework for fragility analysis yields the desired relationships and completes the whole procedure.

Conventional fragilities differ from HAZUS fragilities in terms of intensity measures. The majority of conventional fragilities utilize peak ground parameters (PGA, PGV, or PGD) or spectral values to represent the ground shaking intensity. In HAZUS, the fragility relationships are expressed by damage state exceedance probabilities related to structural response and the only parameter required to derive the HAZUS compatible fragility curves is the combined uncertainty of capacity and demand, which is obtained through the convolution process (Gencturk et al., 2008).

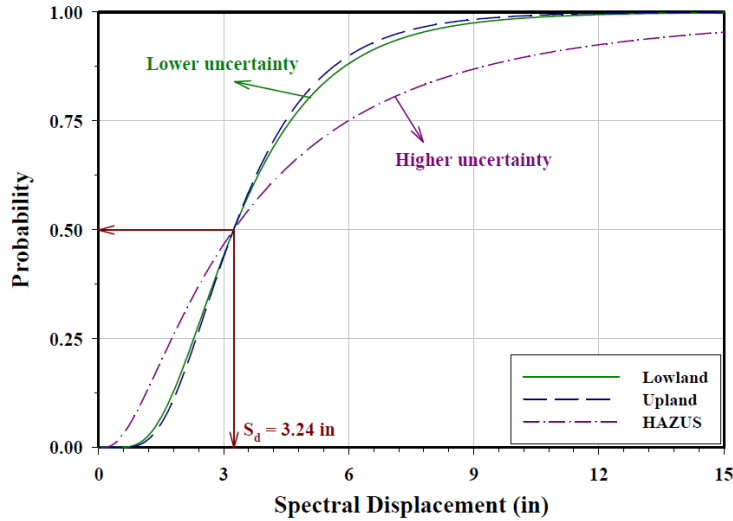


**Figure 20: Improved Fragility Relationships (Gencturk et al., 2008)**

Figure 20 illustrates the improved fragility curves for upland and lowland soil profiles as well as the HAZUS default damage function for building type S3, high-code, for the extensive damage state. Both upland and lowland profiles are illustrated in Figure 20 and show a lesser level of uncertainty than the HAZUS default fragility. By reducing the level of uncertainty in the building fragility relationships, better estimates of the building damage for the Central US are obtained.

### **3.3.4 Threshold Limit States**

Though state-of-the art fragilities are implemented for buildings and bridges, there are other critical infrastructure components that do not have adequate vulnerability functions. Such critical infrastructure involves major river crossings, which are essential to river navigation in major rivers such as the Mississippi and Ohio rivers. Adequate fragilities are also deficient for dams, levees, and tanks. Due to time constraints, developing fragility relationships for all the above infrastructure categories was unfeasible and extremely time-consuming. However, these components play important roles in the functionality of the region, thus it is necessary to conduct some type of impact assessment that can be supported scientifically. For example, information on

damaged dams can be further used to conduct secondary analysis such as floods following earthquakes.

A compromising solution to the problem is the application of two limit states rather than the four limit states that were previously mentioned. The two proposed limit states can define whether a structure is likely damaged or likely undamaged. The pass-fail methodology produces threshold values. Threshold values represent parameter values below which a structure is likely undamaged and above which the structure is considered damaged.

Threshold values are developed for critical infrastructure such as major river crossings, dams, levees, and hazmat storage tanks. For simplicity and feasibility, each infrastructure type was divided into general groups and PGA was used as the parameters to derive pass-fail limit states. The general process followed to develop threshold values consists of selection of intensity measure, consideration of fragility curves, and determination of lower bounds. In this study, PGA was selected as the intensity measure due to its availability from ground shaking maps. Fragility curves are considered to reduce uncertainties and more accurately predict limit states. In the absence of fragility curves, previous damage information and field data were utilized in damage assessment. Finally, after close consideration, realistic lower bound threshold values were selected for the respective infrastructure components. Additionally, damage limit states from HAZUS are considered during the damage evaluation of the infrastructure.

Classification of inventory components was important especially for major river crossings, which were included through a research conducted within the MAE Center, since HSIP data did not include information on this type of infrastructure. The classification of major river crossings was based on construction type and materials, while dams and storage tanks are categorized in terms of materials only.

The resulting threshold values of peak ground accelerations utilized in the latest NMSZ impact assessment are presented in

. Threshold limit values are based on systematic research and expert opinions and, though not as scientifically accurate as limit states fragilities, they provide a general understanding of the performance of critical infrastructure for which fragility functions generally do not exist.

**Table 31: Threshold Values**

<b>Structure Type</b>	<b>Slight (g)</b>	<b>Moderate (g)</b>	<b>Extensive (g)</b>	<b>Complete (g)</b>
<b>Bridges</b>				
Cable-Stayed & Suspension	--	0.15	--	--
Multispan Continuous Steel Truss	0.18	0.31	0.39	0.5
Multispan Simply Supported Steel Truss	0.2	0.33	0.47	0.61
Multispan Continuous Steel Girder	0.18	0.31	0.39	0.5
Multispan Simply Supported Steel Girder	0.2	0.33	0.47	0.61
Multispan Simply Supported Concrete Girder	0.28	0.61	0.73	1
<b>Dams &amp; Levees</b>				
Earth Dams	0.5	0.63	1.25	--
Concrete Gravity & Arch Dams	0.63	1.25	--	--
Levees	0.33	--	--	--
<b>Hazmat Facilities</b>				
Tanks	0.7	1.1	1.29	1.35

### 3.4 Additional Modeling – Flood Risk Analysis

The flood risk model utilizes a threshold methodology regarding dam damage. The two categories are defined as “damaged” or “not damaged” and the threshold limit is based on the “at least moderate incurred damage” level; that is, any dam that is determined to be moderately damaged or worse is defined as “damaged”, while dams that have been classified as having incurred no or slight damage are considered as “not damaged” during the flood risk modeling.

Once the dams are classified into the two aforementioned categories (damaged or not damaged), the selected flood risk methodology can be applied to determine areas at risk. According to the selected model, parameters such as dam height and elevation, and maximum storage capacity can be used to determine the danger zones by determining a danger reach length (relevant distance that water travels after dam fails) and width of the overflowing water. By combining the two, an area or surface is created, thus determining

a danger zone. Respective elevations are then assigned to each danger zone created for each damaged dam, based on dam elevation information (the elevation at the bottom of the dam is assigned as the elevation of the respective danger zone).

After the danger zones are drawn and respective elevations are assigned, the created surfaces are intersected with a 3D elevation map of the study region, the eight states, and a cut-fill analysis is performed to determine which areas are at risk. Based on the analysis results, areas from the elevation map that are found below the danger zone elevations are considered to experience flood risks. Once the areas that exhibit flood risk potential are identified, the inventory of these areas is studied to determine the affected buildings and critical infrastructure. As previously discussed, a pass/fail criteria is used to identify the damaged dams that present flood risk. Danger reach length and water overflow width are utilized to identify danger zones.

Regarding methodology and procedure, pass/fail criteria is employed to determine whether dam structures are likely to be damaged or undamaged, based on established threshold values and experienced peak ground acceleration values, as previously discussed. The damaged dams are utilized in determining the danger zone areas, which are defined using danger reach length and water overflow width. Danger reach length is a very important parameter, since it determines how far downstream the flood analysis should continue; therefore, it states the extent of flood risk. There are two parameters that are absolutely required to determine the danger reach length; the parameters involve the height of the dam under consideration and maximum storage capacity. Next, the peak discharge of dam is calculated based on the following equation:

$$Q_{\max} = 3.2 H_w^{2.5} \quad (12)$$

where,

$Q_{\max}$  = peak discharge (cfs)

$H_w$  = water depth at failure (ft)

The peak discharge parameter is utilized in the implemented methodology of dam failure to estimate flood risk. The implemented method pertaining to this project was

adapted from information contained in the Soil Conservation Service TSC Engineering-UD-16, 1969 (Johnson, 1998). According to the methodology, the dam is assumed to fail at maximum capacity, that is, when the water height is at the top of the dam. The water height, the maximum storage capacity, and 100 year flood plain valley width are utilized to approximate the danger length (in feet) from a derived graph. For feasibility and assumption of worst case scenario, the water height was assumed to be equal to dam height (the maximum possible water height). A brief example outlining the determination of danger reach length is included in Appendix 4.

The second essential parameter in determining danger zones is the water width. It initiates with determining the breach width. In this analysis, the valley width is used as the initial width. Subsequently, a slope of 1:3 is used to progress the lateral water flow until the danger reach length limit is reached. The selected slope is implemented as the average of two slopes; a 1:2 slope used for an area populated by houses, and a 1:4 slope used for open areas such as roadways (Johnson, 1998).

The two dimensions (length and width) create the surface area of the danger zone. Using GIS software, polygons are drawn on top of the regional elevation map to approximate the danger zones. Consequently, an elevation signifying the elevation at the bottom of the dam is assigned to the drawn polygon. Once all the polygons are drawn, elevation information obtained from dam inventory is assigned to each polygon. Consequently, the polygons are converted to triangulated surfaces or “tin”-s and the GIS cut-fill analysis is performed and a raster is obtained. Resulting from the analysis, regions that exhibit flood potential or regions that result under water are presented in red color, while danger zone areas that are tentatively above water level are illustrated in blue. A simulated example of the result of creation of tin surfaces and cut-fill analysis is shown in Figure 21 (Unen, 2009). The red location in the figure represents the initiation of flood region, which in this case would correspond to the dam elevation. The blue surface identifies submerged areas. After the flood potential areas are identified, further analysis and observations are needed to determine the danger to critical structures and infrastructure. Inventory layers are overlapped with the cut-fill analysis results, allowing for the classification and prioritization of the areas at risk.

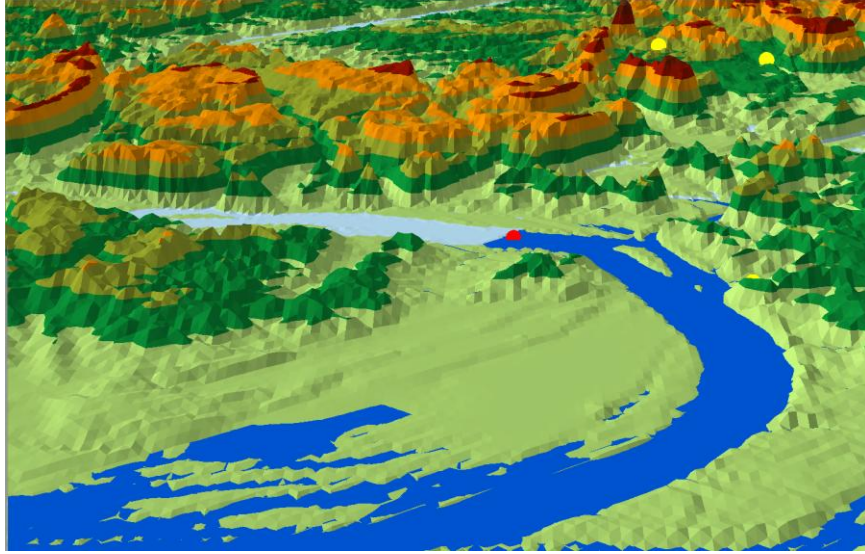


**Figure 21. Simulated Illustration of Flood Risk Analysis Methodology**

The uncertainty of the methodology is significant, especially in identifying the danger zones and the pass/fail criteria that are implemented in determining dam damage. These two components can lead to improvements in future phases of the project. Additionally, in future phases, improved breach and flow models and utilization of appropriate software are important to increase the accuracy of the flood risk analysis. Future work can be extended to identifying different levels of damage to buildings and infrastructure based on water depth and damage can focus more on quantitative levels rather than qualitative attributes.



## **CHAPTER 4: Assessment Results and Discussion**

This chapter concerns the results of the impact assessment for the NMSZ. Due to the large region, the risk analysis was conducted for each of the eight states separately, and the final results were assembled to summarize and present the overall regional impact. The earthquake scenario assuming a moment magnitude of 7.7 and sequential ruptures of all three NMSZ segments was applied to all eight states, along with the implementation of developed liquefaction susceptibility map. The same approaches and assumptions were applied throughout the modeling, analysis, and post-processing procedures; therefore, the consistency in the conduction of the impact assessment simplified the aggregation of results. As previously stated, the presented results only include loss assessments based on direct structural damage. Indirect losses or socio-economical losses are not included in the report. Subsequent sections will discuss damage of all main inventory categories previously discussed; general buildings, essential facilities, transportation systems, utility lifelines, and high potential loss facilities. Damage to structures is estimated and presented in terms of occupancy type and type of construction. Generated amount of debris, total casualties, and economic losses estimated by HAZUS are also included. Finally, results from post-processing flood risk analysis are also presented.

Based on cumulative damage results, a list of impacted counties was assembled. The criteria of determining impacted counties consisted of cumulative damage based on structural damage to facilities, functionality of infrastructure systems (transportation and utilities), and direct economic losses. It is important to note, however, that the damage and loss of functionality of essential facilities and lifelines are not limited to the list of impacted counties. Instead, the impacted counties are significantly affected and impaired. Moreover, they would probably require some type of intervention to recuperate and regain operational potential. Among the impact results for the eight states, Alabama incurred the least amount of damage, resulting in having no ‘impacted counties’ based on the general established criteria for classifying impacted counties. However, assuming that Alabama would not experience significant damage could be a misconception, since even slight or moderate structural damage could result in inoperable critical lifelines or essential facilities, thus resulting in interruption of normal activities. The list of the

impacted counties by state is outlined below and illustrated in Figure 22. Figures illustrating damage distribution for each infrastructure type are included in Appendix 3.

### **Arkansas**

- |              |                |               |                 |
|--------------|----------------|---------------|-----------------|
| • Arkansas   | • Greene       | • Mississippi | • Randolph      |
| • Clay       | • Independence | • Monroe      | • Saint Francis |
| • Craighead  | • Jackson      | • Phillips    | • White         |
| • Crittenden | • Lawrence     | • Poinsett    | • Woodruff      |
| • Cross      | • Lee          | • Prairie     |                 |

### **Illinois**

- |             |             |               |              |
|-------------|-------------|---------------|--------------|
| • Alexander | • Hardin    | • Massac      | • Saline     |
| • Bond      | • Jackson   | • Monroe      | • Union      |
| • Clinton   | • Jefferson | • Perry       | • Washington |
| • Fayette   | • Johnson   | • Pope        | • Wayne      |
| • Franklin  | • Lawrence  | • Pulaski     | • White      |
| • Gallatin  | • Madison   | • Randolph    | • Williamson |
| • Hamilton  | • Marion    | • Saint Clair |              |

### **Indiana**

- |            |            |           |               |
|------------|------------|-----------|---------------|
| • Crawford | • Knox     | • Perry   | • Vanderburgh |
| • Dubois   | • Lawrence | • Pike    | • Warrick     |
| • Gibson   | • Martin   | • Posey   |               |
| • Harrison | • Orange   | • Spencer |               |

## **Kentucky**

- Ballard
- Caldwell
- Calloway
- Carlisle
- Crittenden
- Daviess
- Fulton
- Graves
- Henderson
- Hickman
- Hopkins
- Livingston
- Lyon
- McCracken
- Marshall
- Muhlenberg
- Trigg
- Union
- Webster

## **Mississippi**

- Alcorn
- Benton
- Bolivar
- Coahoma
- Desoto
- Lafayette
- Marshall
- Panola
- Pontotoc
- Prentiss
- Quitman
- Sunflower
- Tallahatchie
- Tate
- Tippah
- Tishomingo
- Tunica
- Union
- Yalobusha

## **Missouri**

- Bollinger
- Butler
- Cape Girardeau
- Carter
- Dunklin
- Iron
- Jefferson
- Madison
- Mississippi
- New Madrid
- Oregon
- Pemiscot
- Perry
- Reynolds
- Ripley
- St. Charles
- St. Francois
- St. Louis
- Ste. Genevieve
- Scott
- Stoddard
- Wayne
- City of St. Louis

## **Tennessee**

- Benton
- Carroll
- Chester
- Crockett
- Dyer
- Fayette
- Gibson
- Hardeman
- Hardin
- Haywood
- Henderson
- Henry
- Lake
- Lauderdale
- Madison
- McNairy
- Obion
- Shelby
- Tipton
- Weakley

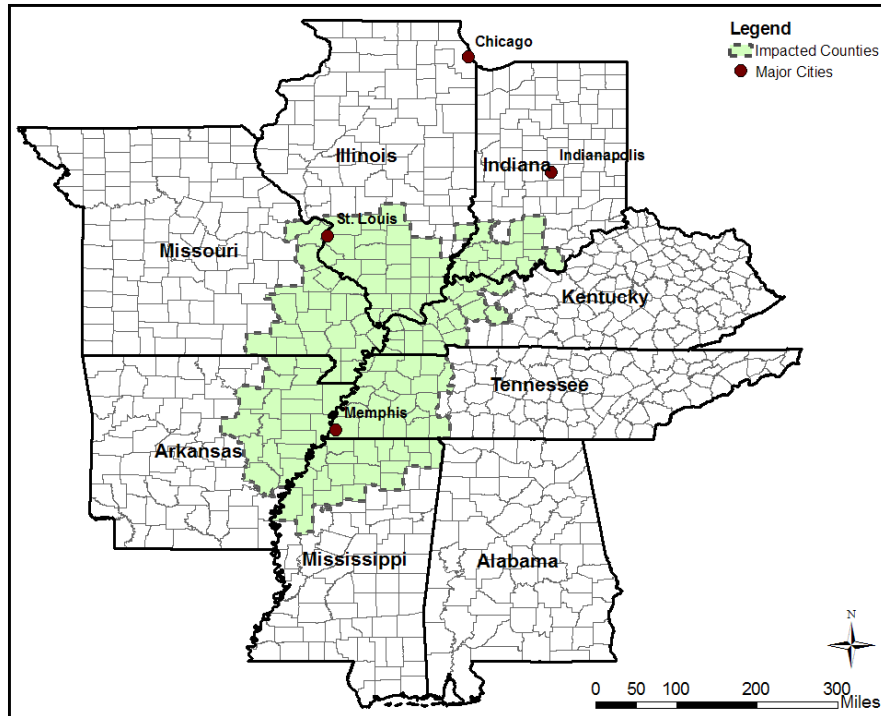


**Figure 22. Impacted Counties for the Eight-State NMSZ Region**

## 4.1 General Buildings

The general building stock was the only major inventory category that was not improved with new data, due to its aggregated representation methodology, since the focus of inventory additions were the point-wise data. Based on HAZUS default inventory, there are approximately 15.8 million general buildings in the eight-state region of interest. A distribution of individual state building inventory and damage both in absolute numbers and percentages is presented in Table 32. Definition of damaged structures throughout this document is defined as structures that incur at least moderate damage of 50% or more. In addition, complete damage for each state is presented. Table 33 shows the damage of general buildings based on the occupancy type, while Table 34 shows the regional damage in terms of construction material. Table 35 further illustrates the distribution of damage for wood and unreinforced masonry (URM) structures in terms

of total damaged wood and total damaged URM structures, respectively, and in terms of the total number of damaged buildings in the eight-state region.

**Table 32: Building Damage Distribution by State**

<b>State</b>	<b>Total Buildings</b>	<b>% of Total Buildings</b>	<b>Damaged Buildings</b>	<b>% of Total Damaged Buildings</b>
Alabama	1,758,300	11.1	15,400	2.2
Arkansas	1,325,400	8.4	162,200	22.7
Illinois	3,655,800	23.2	44,500	6.2
Indiana	2,202,000	14.0	14,200	2.0
Kentucky	1,543,900	9.8	68,400	9.6
Mississippi	1,064,000	6.7	57,400	8.0
Missouri	2,101,800	13.3	86,800	12.2
Tennessee	2,126,600	13.5	264,200	37.0
<b>Total</b>	<b>15,777,800</b>	<b>100.0</b>	<b>713,100</b>	<b>100.0</b>

**Table 33: Building Damage by Occupancy Type**

<b>General Occupancy Type</b>	<b>Total Buildings</b>	<b>At Least Moderate Damage</b>	<b>Complete Damage</b>
Single Family	12,617,800	426,300	210,900
Other Residential	2,652,600	240,100	71,700
Commercial	323,200	29,600	11,000
Industrial	91,700	8,400	2,900
Other	92,700	8,800	3,700
<b>Total</b>	<b>15,778,000</b>	<b>713,200</b>	<b>300,200</b>

Table 32 illustrates that over 713,000 buildings are damaged throughout the eight states and over 300,000 are completely damaged. Tennessee experiences the most damage in terms of total damaged buildings and percentage. Tennessee accounts for about 37% of the total damage, while it includes only over 13% of the total general building inventory. This is largely due to the high density of buildings in Memphis, Tennessee, and the high levels of ground shaking and substantial ground deformations.

Arkansas is also seriously affected with a total of nearly 23% damaged buildings, while it accounts only for 8% of the total inventory. Missouri is the third most impacted state with damaged percentage of about 12% and it accounts for about 13% of the total assets. Alabama, Indiana, Illinois, Kentucky, and Mississippi are relatively less impacted.

Table 33 details the number of damaged structures by building use group throughout the eight-state study region. Based on Table 33, residential buildings comprise a significant portion of all building damage in the eight-state study region. Single family homes incur the majority of the total damage based on occupancy type, while other residential structures also experience significant damage. Overall, about 90% of the damage occurs in residential buildings.

Table 34 displays building damage by structure type for the entire study region. Referring to Table 34, wood structures by far incur the most damage, followed by unreinforced masonry structures. Wood structures account for about half of the total damaged structures, while unreinforced masonry amount to almost 20% of the total damaged buildings for at least moderate damage.

More detailed results for each state are presented in Table 35 for wood and unreinforced masonry. Once again, Tennessee is the most affected in terms of construction materials as well as occupancy types. Figure 23 illustrates the damage distribution in terms of number of damaged buildings for the eight-state region.

**Table 34: Building Damage by Building Type**

<b>General Building Type</b>	<b>Total Buildings</b>	<b>At Least Moderate Damage</b>	<b>Complete Damage</b>
Wood	11,370,700	354,000	180,500
Steel	167,800	19,600	6,500
Concrete	77,300	5,000	2,000
Precast	43,500	4,600	1,700
Reinforced Masonry	34,200	2,400	1,000
Unreinforced Masonry	2,373,800	132,300	59,200
Manufactured Housing	1,710,700	195,300	49,300
<b>Total</b>	<b>15,778,000</b>	<b>713,200</b>	<b>300,200</b>

**Table 35. Building Damage Distribution by State for Wood and URM**

State	Damaged Buildings	URM Damage			Wood Damage		
		Total	% of Total URM	% of Total Damaged	Total	% of Total Wood	% of Total Damaged
Alabama	15,400	400	0.3	0.1	3,000	0.8	0.4
Arkansas	162,200	29,100	22.0	4.1	68,800	19.4	9.6
Illinois	44,500	10,100	7.6	1.4	17,700	5.0	2.5
Indiana	14,200	2,600	2.0	0.4	4,800	1.4	0.7
Kentucky	68,400	9,400	7.1	1.3	36,100	10.2	5.1
Mississippi	57,400	5,000	3.8	0.7	19,900	5.6	2.8
Missouri	86,800	26,800	20.3	3.8	40,200	11.4	5.6
Tennessee	264,200	48,900	37.0	6.9	163,600	46.2	22.9
<b>Total</b>	<b>713,100</b>	<b>132,300</b>	<b>100.0</b>	<b>18.6</b>	<b>354,100</b>	<b>100.0</b>	<b>49.7</b>

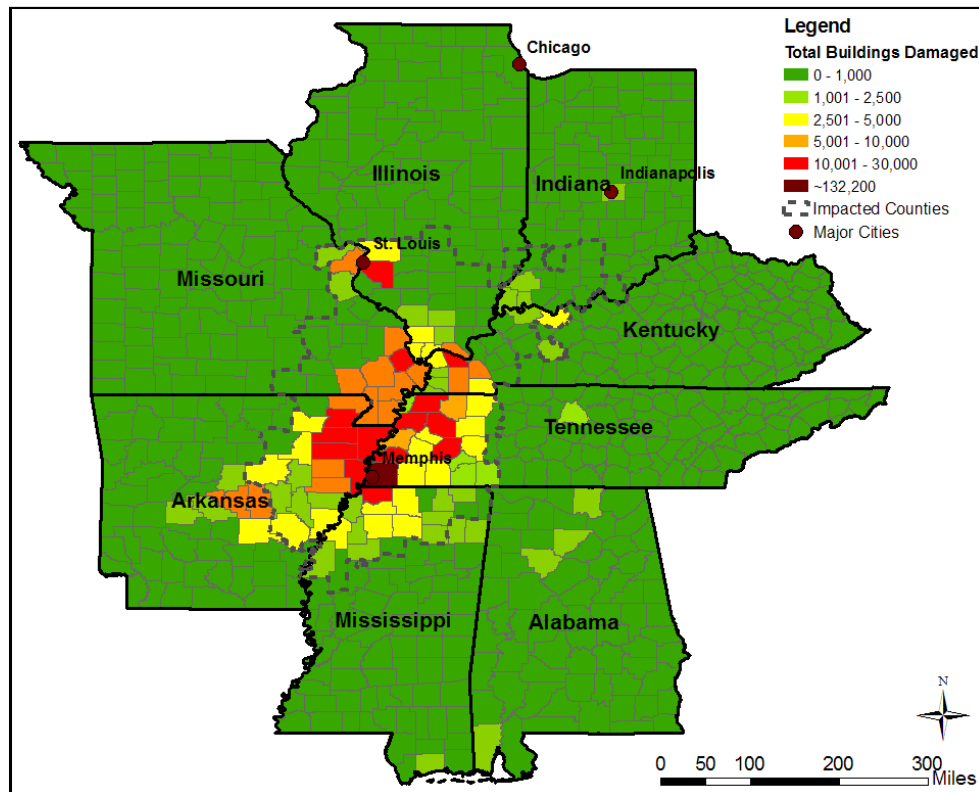


**Figure 23. General Building Damage for NMSZ Region**

## 4.2 Essential Facilities

Essential facilities are significantly affected after the earthquake event. Table 36 illustrates the overall damage results for the eight-state study region. Over 10% of the regional EOCs incur at least moderate damage. Approximately 130 medical care facilities have acquired damage, with the majority of the damage situated in western Tennessee, as it can be observed from Figure 24. This is due to the highly populated region in that part of Tennessee as well as the intensity of the strong motion. Arkansas and Mississippi each also experience moderate damage to hospitals. Due to the severe impact to hospitals in the 140 critical counties, it is obvious that the critical counties will not have the capability to remedy the situation without additional assistance from neighboring counties or higher government agencies. Most probably, help will be required to relocate the injured and medical-seeking patients to safer, less affected areas where the necessary medical care can be provided without compromising lives.

**Table 36: Regional Essential Facilities Damage**

<b>Essential Facility</b>	<b>Total Facilities</b>	<b>At Least Moderate Damage</b>	<b>Complete Damage</b>
EOC	1,093	116	44
Fire Stations	10,346	729	177
Hospitals	2,825	129	32
Police Stations	4,480	379	136
Schools	20,291	1,322	277

Operational capacity of fire and police stations is also compromised due to the scenario event. From Table 36, it is observed that nearly 730 fire stations and 380 police stations are at least moderately damaged, which signifies that most probably these facilities will be nonfunctional. As it was the case with EOCs and hospitals, damage is concentrated in Tennessee and Arkansas, followed by moderately affected states of Illinois, Mississippi, and Missouri. In terms of fire station damage, about a third of damaged fire stations are located in western Tennessee, which may cause significant



issues regarding cascading effects of fires following earthquakes. Significant damage to fires stations also occur in Illinois, Kentucky, Mississippi, and Missouri.

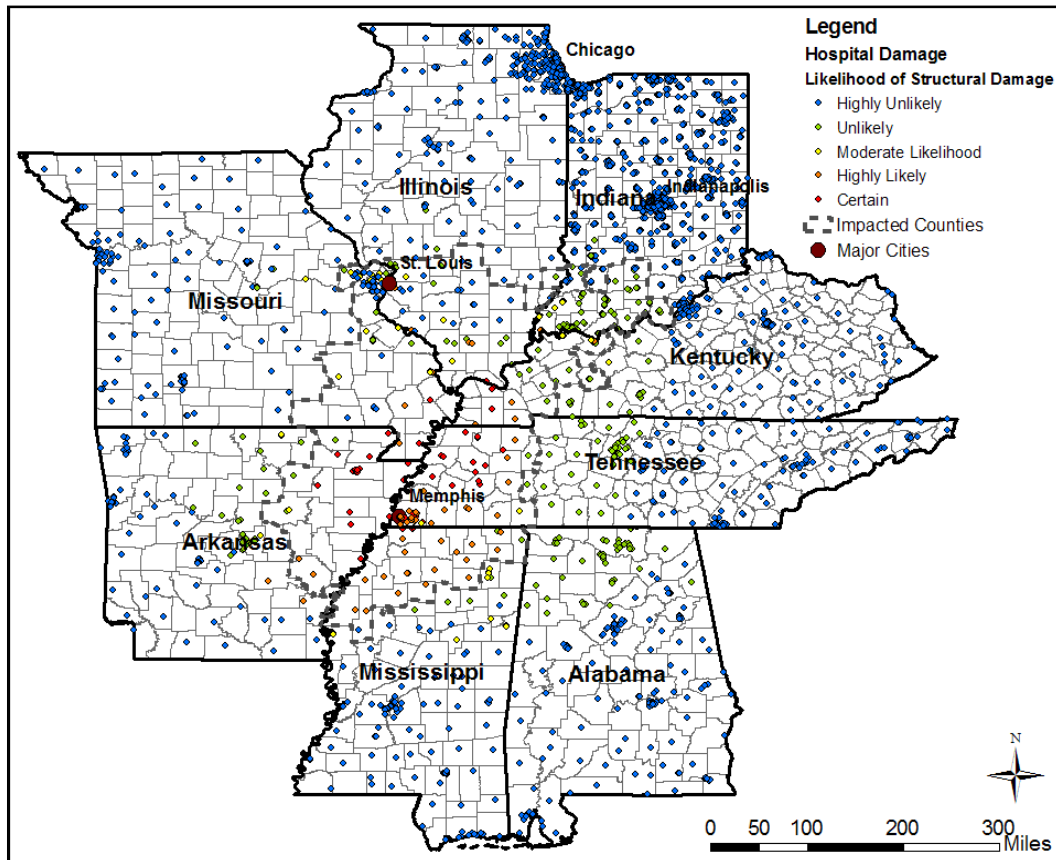


**Figure 24. Hospital Damage for Eight-State Study Region**

Schools are also severely impacted by the scenario earthquake, totaling in over 1,300 damaged facilities. Impact to schools affects post-event response in two aspects. Firstly, if an actual event would occur during the day, a significant number of casualties would be comprised by children. Additionally, schools are generally identified as emergency shelters during emergency situations, and damaged schools would considerably reduce the capacity of the emergency shelters and increase response emergency and recovery times for the critically impacted areas. Western Tennessee is once more the most affected with nearly half of school damages occurring in this region. As previously noted, this is partially due to the highly populated urban area and partially due to the strong ground motion that this region experiences. Significant school damage

is observed in northeastern Arkansas and moderate damage occurs in Illinois, Kentucky, Mississippi, and Missouri.

### **4.3 Transportation Systems**

Transportation systems functionality is vital in the emergency response and recovery operations after an earthquake event in terms of ingress routes, which assure that no unnecessary delays are experienced while providing emergency help, and in terms of egress routes, which allow for safe evacuation from severely damaged zones. Logically, damage to transportation lifelines influences the emergency response operations in a negative manner. Overview of damage to transportation systems for the eight-state study region is presented in Table 37. The most severe damage occurs to highway bridges with over 3,500 damaged bridges and over 1,200 completely damaged structures. Most of the damage is observed in the vicinity of fault ruptures, thus the most damage is located in Arkansas, Missouri, and Tennessee, which exhibit over 1,000 damaged bridges for each state. Though roads are not analyzed in this project, it can still be determined that considerable travel interruptions will arise due to the large number of damaged bridges.

In addition to land travel, air travel will be severely impacted, since about 150 airport facilities result as at least moderately damaged, that is, most probably nonfunctional. Tennessee is the most greatly affected state in the region with a third of the total airport facilities damage located in the western part of the state. This level of expected damage would significantly affect air emergency operations, especially in the heavily impacted areas. Bus facility, railway facility, and railway facility damages are included in Table 37

**Table 37: Regional Transportation Systems Damage**

<b>Transportation Lifelines</b>	<b>Total Facilities</b>	<b>At Least Moderate Damage</b>	<b>Complete Damage</b>
Highway Bridges	165,771	3,547	1,255
Airport Facilities	3,773	143	0
Bus Facilities	405	16	0
Railway Bridges	1,888	29	0
Railway Facilities	1,118	119	0
Port Facilities	2,004	232	0

As previously discussed, a study conducted by the MAE Center involved the analysis of 127 major river crossing in the Central US based on threshold values. These bridges were included due to their important role in transportation systems. Based on threshold values, about 15 major river crossings were estimated as likely damaged during the scenario event. The damage distribution of the major river crossings is illustrated in Figure 25. Estimated damage shows interruption of transportation from one side of the Mississippi River to the other near the fault zones, which will cause significant problems in rescue and recovery emergency operations.

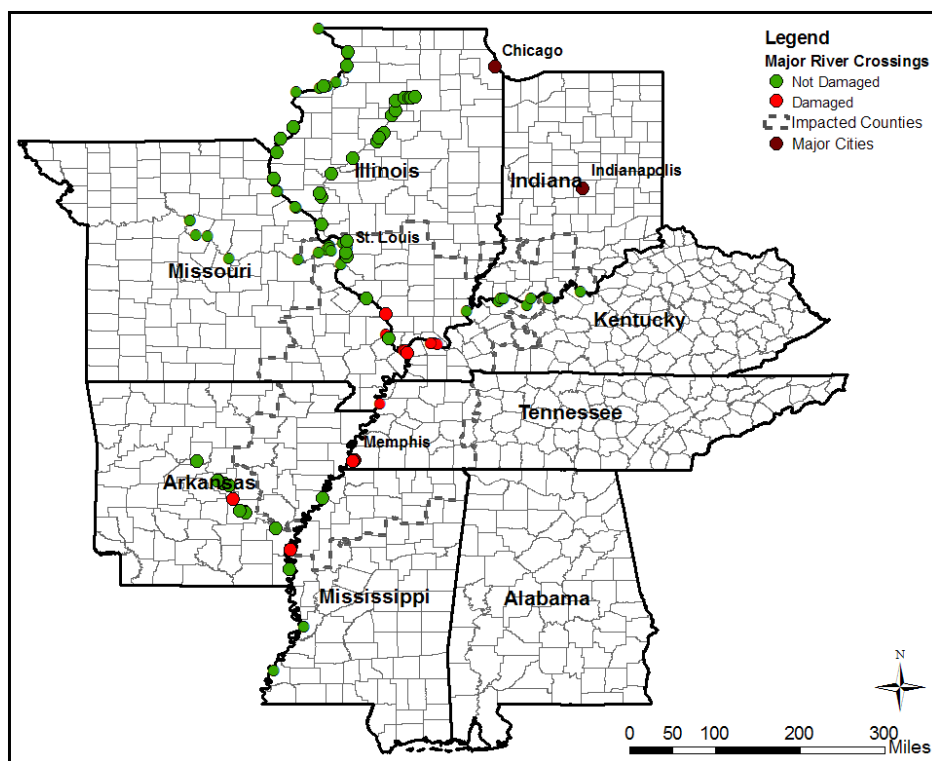


**Figure 25. Major River Crossing Damage for Eight-State Study Region**

## 4.4 Utility Lifelines

Utility networks represent a vital component of survival after a disastrous event. Overall impacts on the utility facilities for the eight-state region are presented in Table 38, while damage to pipelines is included in Table 39. As observed from summarized results, utility systems experience severe damage in all infrastructure categories. A significant factor that should be considered would also be prolonged repair times due to the extent of the damage and limited available resources of workers. Damage to communication facilities nears 10,000 facilities, with the most damage located in the impacted counties. Due to the extent of the damage as well as travel impairments, the effectiveness of response operations will be substantially reduced, since disabled communication tools will impede efficient operation coordination. Almost half of the communication damage occurs in western Tennessee, while significant impact is experienced in Illinois and Missouri as well.

Additional impacts to utility networks include severe damage to waste water facilities, oil facilities, electric power facilities, natural gas facilities, and, finally, potable water facilities. The extent of damage follows the same pattern as the degree of communication facilities damage.

**Table 38: Regional Utility Facilities Damage**

<b>Utility Facilities</b>	<b>Total Facilities</b>	<b>At Least Moderate Damage</b>	<b>Complete Damage</b>
Communication Facilities	145,722	9,748	115
Electric Facilities	10,893	673	4
Natural Gas Facilities	34,339	418	3
Oil Facilities	89,621	998	0
Potable Water Facilities	1,195	76	1
Waste Water Facilities	48,430	2,732	17

**Table 39: Utility Pipeline Damage for Study Region**

<b>Pipeline Systems</b>	<b>Total Miles</b>	<b>Leaks</b>	<b>Breaks</b>	<b>Total Repairs</b>
Natural Gas Local	413,200	55,273	77,829	133,102
Natural Gas Interstate	66,500	1,534	4,841	6,375
Oil Interstate	29,100	310	1,015	1,325
Potable Water Local	1,030,000	65,452	92,094	157,546
Waste Water Local	607,100	51,776	72,837	124,613

Referring to results in Table 39, considerable damage occurs to both local and interstate pipelines for natural gas, oil, potable water, and waste water pipeline systems. Among the most substantially damaged, potable water local pipelines, natural gas local pipelines, and waste water local pipelines require considerable total amounts of repairs, which include leaks and breaks. Assuming reduced capability of repairs due to the damage extent and large number of required repairs, it is estimated that all the repairs would extend over a period of several months. Delays in utility pipeline repairs would cause backup during the recuperation or restoration period, when functionality of vital

utility components cannot be restored, even though regions might be structurally safe. Further issues arise for natural gas and oil pipelines, since the natural flow of these pipelines follows a southwest-northeast direction. Fuel interruptions would cause cascading effects and the impacted areas would include northeastern states like Michigan and Ohio, which could experience serious absences of fuel. These interruptions would cause significant problems in terms of sheltering, especially during the winter period, since these states will no longer be able to provide shelter services. Instead they will require additional assistance of their own, thus reducing shelter and recovery capacity of the region even further than estimated. To avoid such a situation, system redundancies and alternative paths should be specified prior to seismic events.

Substantial service interruptions occur throughout the region in terms of loss of electric power and potable water. As shown in Table 40, approximately 2.6 million households will be without power at day 1 of the event, while nearly 1.1 million households will have no potable water services. Regarding electric power, severe damage is experienced throughout the eight-state region, as shown in Figure 26. Population of the impacted counties might experience the loss of these services for months, due to potentially reduced resources and possibly inaccessibility.

**Table 40: Service Outages at Day 1 for Eight-State Study Region**

	<b>Total Households</b>	<b>Electric Power</b>	<b>Potable Water</b>
Service Outages at Day 1 (Households)	16,773,000	2,598,000	1,090,000

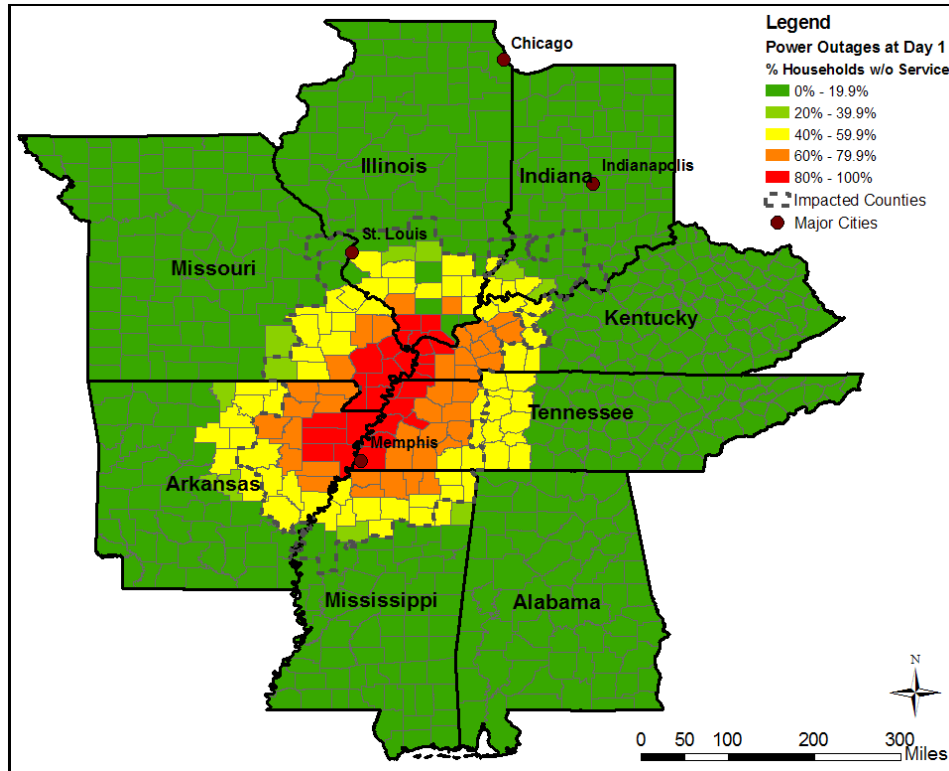


Figure 26. Electric Power Outages at Day 1 for Impacted Region

## 4.5 High Potential Loss Facilities

Impact on high potential loss facilities includes damage to dams, levees, and hazardous materials (hazmat) facilities. These infrastructure components are critical not only due to their direct damage, but rather due to secondary effects that may take place due to damaged infrastructure. As expected, most of the damage to high potential loss facilities occurs near the fault rupture, or where the shaking intensity is the greatest. Overview of damaged infrastructure is outlined in Table 41. Based on pass-fail criteria, it results that near 330 dams and 100 levees are likely to be damaged. Secondary effects such as floods following earthquakes due to dam and levee failures can follow and should be considered in the overall impact assessment. Also, about 250 hazmat facilities (mainly tanks) incur damages and possible leaks of hazardous materials can occur.

**Table 41: Other Critical Facilities Damage for Eight-State Study Region**

<b>Facility Type</b>	<b>Total Facilities</b>	<b>Damaged</b>
Dams	17,573	327
Levees	1,326	96
Hazardous Materials	39,759	253

## 4.6 Induced Damage, Casualties, and Economic Losses

Induced damage, casualties, and economic losses are based impact due to direct losses, while social and indirect losses are not considered. The total amount of generated debris for the eight-state region is illustrated in Table 42, based on debris material.

**Table 42: Regional Total Debris Generation**

	<b>Steel and Concrete (Tons)</b>	<b>Wood, Brick, or Other (Tons)</b>	<b>Total Debris (Tons)</b>	<b>Removal Truckloads (25-ton truck)</b>
Debris Generation	21,943,000	28,113,000	50,056,000	2,002,240

Over 50 million tons of debris need to be removed, requiring the capacity of over 2 million 25-ton trucks. Over half of the generated debris contains wood, brick, or other materials, while the rest of the generated debris consists of steel and concrete materials. Most of all debris is generated in Arkansas, followed by Tennessee and Kentucky. Consequently, most of the debris amount is generated in the most impacted areas within each state.

Casualties from the NMSZ scenario event result in over 85.7 thousand casualties. Casualties were calculated at 2:00AM which corresponds to the time the event occurs based on the selected scenario. Table 43 represents overall regional impacts based on the severity of injuries starting from Level 1, which involves minor injuries, up to Level 4, which includes fatalities.



**Table 43: Casualties at 2:00AM for Eight-State Study Region**

	Level 1	Level 2	Level 3	Level 4	Total
Casualties at 2:00AM	63,266	17,121	1,882	3,496	85,765

Tennessee is severely impacted by casualties, attributing over 35% of total casualties to the western part of the state. Considerable casualties occur in Arkansas and Missouri with roughly 20% of casualties each, while the rest of the eight states are relatively less affected. The regional distribution of casualties is illustrated in Figure 27 for the eight-state study region.

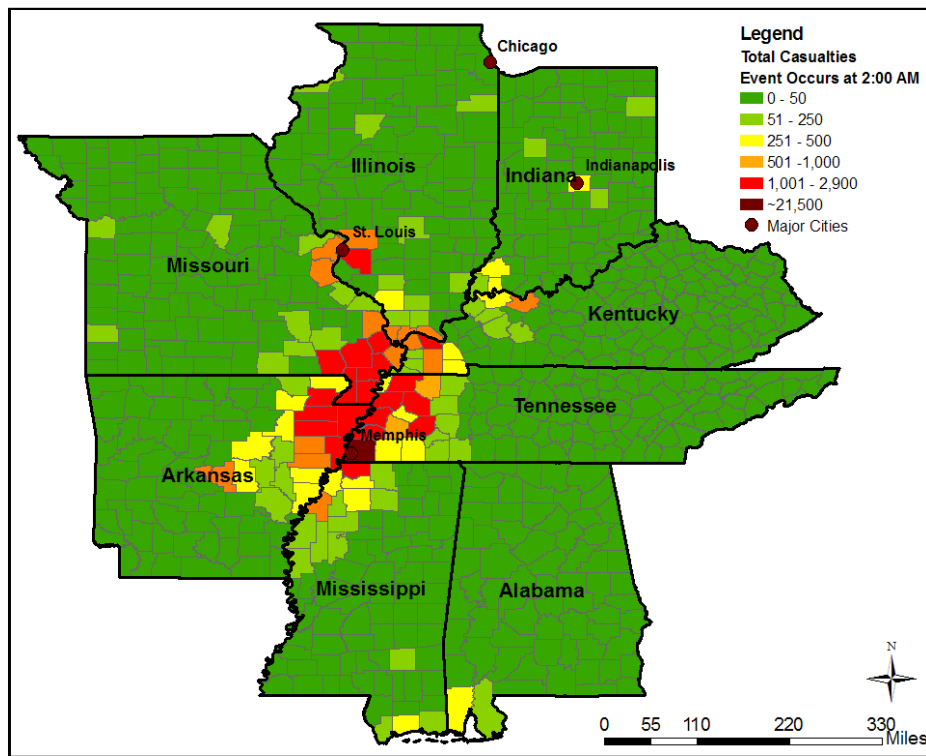


**Figure 27. Total Casualties for 2:00 AM Event in Study Region**

The overall direct economic losses due to the NMSZ scenario event amount to nearly \$ 300 billion, as shown in Table 44. Over half of the total incurred economic losses concern utilities, while direct economic loss due to building damage account for less than 40% of the total losses. Losses due to transportation system damages are relatively low in comparison to the other two inventory categories.

**Table 44: Direct Economic Loss for Eight-State Study Region (\$ millions)**

	<b>Buildings</b>	<b>Transportation</b>	<b>Utilities</b>	<b>Total</b>
Direct Economic Loss	\$113,080	\$10,866	\$172,101	\$296,047

Based on default replacement costs of all infrastructures, the study region encompasses an inventory value of approximately \$8.6 trillion. The damage distribution is not necessarily proportional to inventory data. For example, Illinois accounts for 25% of total assets in the study region, however only 15% of total losses are experienced in this state. Tennessee which is the most gravely affected state in the region, accounts for only about 8% of total regional assets, while it incurs about 25% of total losses. Arkansas is also a heavily hit state, since it includes about 5% of total asset values, but experiences about 13% of total losses.

## **4.7 Flood Potential**

Flood risk modeling involved the identification of danger zones through utilizing available dam inventory data such as height and maximum storage capacity. Consequently, a cut-fill analysis was performed to locate potentially flooded areas. Lastly, inventory was mapped on top of potentially flooded areas and infrastructure that exhibited flood potential was physically identified.

Based on the flood analysis results, out of the eight-state study region, only five states contain flood risk potential. The five states that will potentially be affected by floods due to dam damage following the selected earthquake scenario consist of Arkansas, Illinois, Kentucky, Missouri, and Tennessee. An inclusive list of impacted counties for each state is shown in Table 45, while the identified potentially flooded regions are presented in Figure 28.

**Table 45. List of Counties with Flood Potential**

State	County
Arkansas	Poinsett
Illinois	Massac
	Pope
	Pulaski
Kentucky	Ballard
	Carlisle
	Hickman
Missouri	Scott
Tennessee	Dyer
	Gibson
	Obion

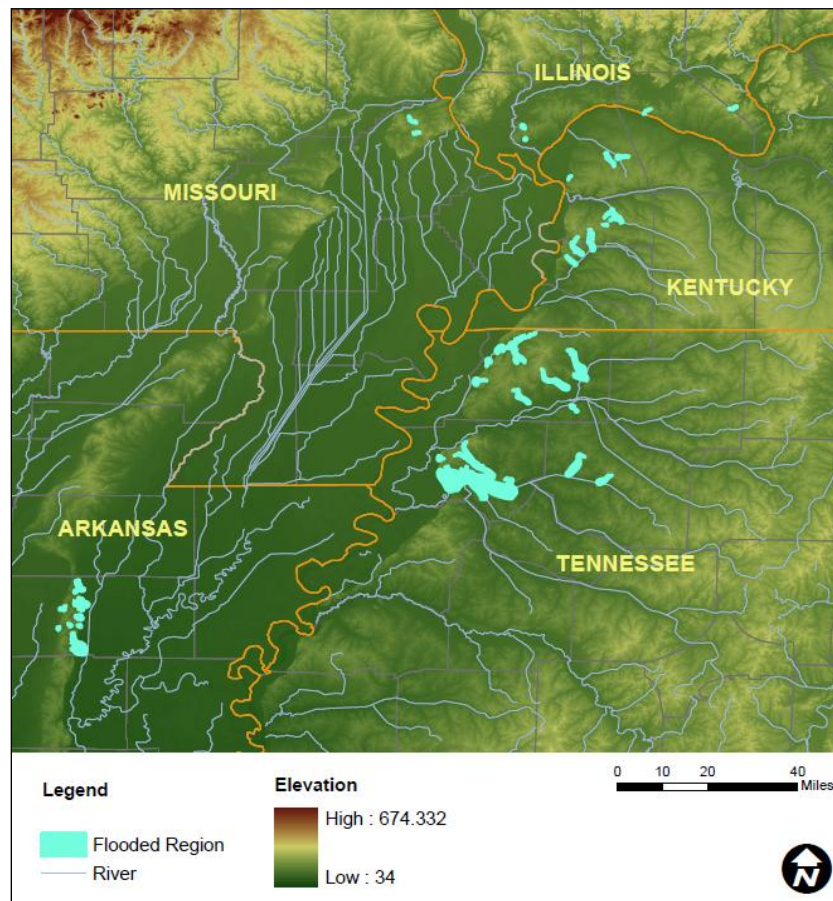


**Figure 28. New Madrid Seismic Zone Flood Risk**

To determine the flood risk potential on critical infrastructure, flooded regions and inventory were mapped and intersected. Inventory that was located either completely or partially inside a flooded region boundary was determined as potentially flooded. Overall, the most impacted facilities involved communication facilities, fire stations, waste water facilities, and highway bridges. Regarding the five states, Tennessee had the most serious damage regarding flood risk due to dam damage, by a large margin in comparison to the other four states. An example of flood risk methodology through intersecting inventory with flooded areas is illustrated in Figure 29 for essential facilities in the state of Illinois.

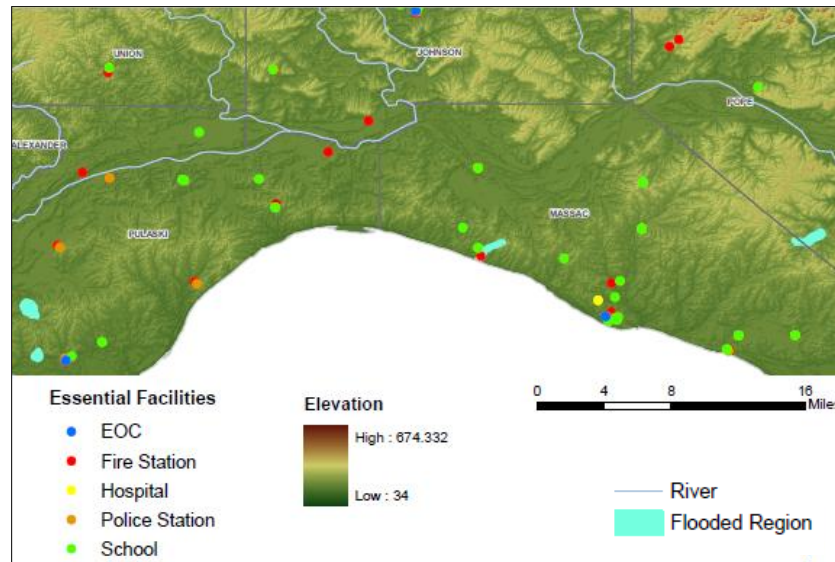


**Figure 29. Illinois Essential Facilities Flood Potential**

Generally, over 300 facilities were recognized as at risk in terms of flood potential. The region summary regarding potentially flooded facilities is presented in Table 46 at the end of this section. Results of infrastructure at risk were summarized in tabular form for each state. Additionally, flood risk assessment results were presented graphically through mapping flooded regions and facility categories simultaneously. Maps expressing flood risk potential for essential facilities, transportation systems, and utility systems were developed. Detailed results for each state are included in Appendix 4.

Arkansas is moderately affected regarding flood potential with Poinsett County as the only impacted county. Highway bridges are the most critical infrastructure for this state with 25 bridges potentially flooded out of a total of 27 facilities affected. The other two facilities belong to fire stations; while utility lifelines are possibly not significantly impacted by flood potential.

Illinois is relatively one of the least impacted states due to dam failure flood potential. Three counties are affected in the state of Illinois with a total of 6 flooded facilities state-wide, while the affected infrastructure and facility types involve fire stations, schools, highway bridges, and waste water facilities.

Kentucky experiences moderate impact of flood risk due to dam damage from an earthquake event. Impacted facilities and infrastructure include highway bridges, while slighter impact is observed in fire stations, communication facilities, and waste water facilities.

Missouri is the second relatively impacted state based on flood potential, with one impacted county and 6 facilities. The infrastructure at risk includes schools, highway bridges, communication facilities, and natural gas facilities.

Tennessee incurs by far the highest flood risk in the region. Nearly 250 facilities out of 309 facilities at risk occur in Tennessee. While flood potential in other states is limited to a few facility types, in Tennessee all facility and infrastructure types are affected by flood risk, with the exception of ports, railway facilities and railroad bridges.

In terms of facility type, highway bridges are majorly at greater risk with over 180 structures at risk. Moderately affected facilities include communication facilities and waste water facilities.

Completing a flood risk analysis for the region has important theoretical value, since secondary effects due to earthquakes need to be seriously considered, since they can cause significant damage comparable to damage caused by primary effects. While the implemented methodology is simplistic, it is very valuable in terms of having an overall view of the flood potential. Additionally, with model improvement and ease of implementation, the accuracy of analysis can be increased and the analysis can be extended to other critical infrastructure like levees.

**Table 46. Regional Summary of Flood Risk Results**

Facility Type	Number of Potentially Flooded Facilities					Total by Facility Type
	AR	IL	KY	MO	TN	
Essential Facilities						
EOC	0	0	0	0	2	2
Fire Stations	2	1	1	0	7	11
Hospitals	0	0	0	0	1	1
Police Stations	0	0	0	0	7	7
Schools	0	1	0	1	8	10
Transportation Systems						
Airports	0	0	0	0	2	2
Bus Facilities	0	0	0	0	1	1
Highway Bridges	25	2	23	2	132	184
Ports	0	0	0	0	0	0
Railway Bridges	0	0	0	0	0	0
Railway Facilities	0	0	0	0	0	0
Utility Systems						
Communication Facilities	0	0	4	1	59	64
Electric Power Facilities	0	0	0	0	1	1
Natural Gas Facilities	0	0	0	2	1	3
Oil Facilities	0	0	0	0	1	1
Potable Water Facilities	0	0	0	0	2	2
Waste Water Facilities	0	2	3	0	15	20
Total Facilities by State						
	27	6	31	6	239	309

## **CHAPTER 5: Concluding Remarks**

### **5.1 Summary**

The earthquake impact assessment in this study provides the most current data available for the Central US. The latest models are used to apply and improve the three components of loss assessment: hazard, inventory, and fragility curves. New soil and liquefaction maps are developed to accurately depict the local soil conditions of the region. Inventory improvements from multiple datasets result in inventory additions of over 400,000 new asset entities. New advanced methodologies are applied to develop more accurate fragility functions specific to regional building characteristics. In absence of multi-level limit states fragilities, threshold values are derived to estimate impact on critical infrastructure such as major river crossings, dams, and levees. HAZUS modeling tool is employed to estimate structural damage, economic loss, and casualties of an impact assessment due to an earthquake scenario based on the 1811-1812 earthquake series. Secondary effects of floods following earthquakes due to dam failures are also considered. Summarized loss assessment results are outlined in the following paragraphs.

Direct structural damage is estimated to reach nearly 715,000 at least moderately damaged buildings. Significant impairments will affect medical care, fire fighting operations, law enforcement response, and emergency operation services in the critical counties region. Furthermore, massive damage will occur to transportation systems with approximately 3,500 at least moderately damaged highway bridges. Severe impacts will be observed in utility systems, too, where over 2.5 million households are without power at day 1 after the event. Massive casualties of over 85,000 are estimated, among which 3,500 are fatalities. Finally, direct economic losses are estimated in the range of \$300 billion.

Eight central states incur direct impacts by the implemented scenario: Alabama, Arkansas, Illinois, Indiana, Kentucky, Mississippi, Missouri, and Tennessee. Utility systems will be severely impacted both in terms of direct damage and restoration times. Major pipeline networks cross paths in the Central US. Interruption of these pipelines will affect a much larger region than the eight immediate states. Many northeastern states depend on the pipelines that cross through the NMSZ to obtain natural gas and oil. The

pipeline services will not be able to operate fully soon after the event. Several months of repairs might be required to restore normal system flows. Also power outages will possibly extend beyond the eight-state region, since only substations are considered in the analysis, while there is not still an accurate methodology to assess the impact of electric grid or distribution network.

Severe damage of transportation systems is caused due to failure of key transportation components such as highway bridges, major river crossings, or airport facilities. Damaged highway bridges limit travel to and from critically impacted areas, thus impeding the arrival of emergency responders and the exit of evacuation operations. Damage to airport facilities limits yet another travel manner; thus isolating damaged areas even more. For areas where river navigation is generally present, major obstructions will be created due to major river crossing failures and debris generation and emergency and business transportations are not going to be possible, probably even for extended periods of time due to the reduced resources and inaccessibility. In general, critical routes would be prioritized to be restored, while repairs for secondary routes would take longer.

The presented impact results give insight into the consequences that would be seen during such an event. Most probably, damages will be even greater than presented in this document. The underestimation of damage is due to several factors such as inventory underrepresentation and inconsideration of system interdependencies. It is very probable that though a network might be in working conditions, due to its dependency on another damaged network, the network is nonfunctional. Additionally, impact effects are likely not comprehensively assessed such as damage to roadways. Assuming that all roadways would be intact is a major understatement, thus damage and overall losses could be significantly affected by just one component. In any case, massive resources will need to be prepared and mobilized. Pre-event planning and mitigation could considerably reduce cascading effects and retrofit of vulnerable critical structures can assure smaller direct loss of life. Though this report presents the most current models for Central US, there are still some significant deficiencies regarding specific infrastructure components. Possible future work and research requirements are discussed in the following section.



## **5.2 Future Research and Development Needs**

The conducted loss assessment implements the best available data for the Central US and provides the most current and scientifically-defensible regional results. However, there are still many components that can and need to be improved in the future with extended research work and advancement of modeling software. Among the most important components are the development of roadway fragilities, dam and levee fragilities, improvements of transportation and utility networks and network interdependencies, uncertainty quantification, development of cumulative fragilities, consideration of secondary effects of fire following earthquake. Additionally, though not specifically discussed in this document, socio-economical models regarding emergency, evacuation, and shelter needs as well as public education and preparation models need to be improved and converted into easily implementable emergency plans.

### **5.2.1 Roadway Fragilities**

There are no existing fragilities for roadways; therefore, no damage assessment is performed for this important infrastructure component. The necessity of roadway impact relates the effect of roadways in several other assessment components. For example, highway bridges might be operational, but if roads are nonfunctional, there is still an interruption in transportation flow. At this point in time, it is impossible to predict this kind of interruption. The capability to estimate roadway damage is imperative, since it will play a major role on determining emergency routes such as for medical emergencies, evacuations, or even public traffic flow. The identification of routes is vital during and prior to an event, since it will facilitate planning initiatives in preparation of a similar event or allow retrofits of critical arteries. The level of functionality of roadways affects directly the immediate and planning responses and the results of loss assessment overall, thus the prioritization of fragilities development.

### **5.2.2 Fragility Relationships for Dams and Levees**

As noted previously, impact to dams and levees was estimated through applying threshold PGA values. Though threshold values provide valuable input in terms of

affected areas, there is high uncertainty linked to this methodology, since there is no determination of the level of damage. The maximum capability of a pass-fail analysis ends at the limit of determining likelihood of damaged or undamaged structure. The boundaries of defining damage and no damage are very vague and highly uncertain, especially when applied to infrastructure with high variability such as dams and levees, in terms of size, material etc. It was also mentioned that the estimation of damage to these structures is crucial in accurately determining secondary flood effects due to damage of dams and levees. Therefore, development of fragilities for dams and levees is very important and should be included as one of the priorities during future progress.

### **5.2.3 Utilities Network Interdependencies**

Utility networks can be improved, especially in terms of damage functions. Additionally, a previously not considered issue would be the interdependency of several networks. For example, the electric power grid significantly affects the performance of several other networks such as potable water and waste water systems. Though these systems might not have incurred significant damage, they are still inoperable since they are controlled by electric power. Existing or new interdependency relationships should be applied to account for damage due to this phenomenon. Superior models should consider two-way dependencies, rather than one-way dependency flow.

### **5.2.4 Uncertainty Modeling**

Though not explicitly discussed in this thesis, independent uncertainty studies were conducted. The applied methodologies represented different processes to assess uncertainty related with each component of loss assessment and how those uncertainties are reflected in an overall uncertainty for the whole impact assessment. Both uncertainty studies were generally implemented to be compared to HAZUS uncertainty quantifications and to distinguish any discrepancies in the default methodology. More improvements and further refinements would increase the value and produce an accurate uncertainty methodology for loss assessment.

### **5.2.5 Cumulative Damage Fragilities**

Up to this point in the project, impact assessment has been based on one single event caused by simultaneous ruptures of the three segments of NMSZ. However, evidence shows that events of NMSZ occur in series over a period of several months. The current limitations are due to modeling restrictions as well as unavailability of fragilities that account for damage accumulation. Ongoing research at the MAE Center is studying the development of new material models that can account for accumulated damage due to multiple earthquake events. For the new models, material and geometric non-linearities are being considered. In the future, the models will be experimentally tested and potentially will be successfully implemented in future loss assessments.

### **5.2.6 Fire Following Earthquakes**

Earthquakes are often followed by subsequent fires that result directly from earthquake damages; however, losses due to fire are not considered in the current loss assessment model. Fires following earthquakes have the potential to cause major damage and can cause losses multiple times bigger than the losses caused by the earthquake event itself. A great example illustrating the fire damage after an earthquake is the losses incurred during the 1906 San Francisco earthquake; it is estimated that up to 90% of the total loss was caused by the fires that erupted subsequently after the earthquake (Tobriner, 2006). Regions with high percentage of wood structures are more prone to fire damage following earthquake. Based on the inventory analysis for the 8 states, about 80% of inventory is comprised of wood buildings, causing the fire damage probability to be high. Therefore, it is essential that in future stages of the assessment adequate FFE models be implemented. FFE models differ from spontaneous fire models because of significant differences in both situations. In FFE model applications there are several factors that significantly affect the fire initiation, spread, and duration. Unlike normal fires, during FFEs, initial structural damage is probable (due to earthquake damage). In addition, it should be taken in consideration that emergency response has incurred damage as well. For example, there could be damaged water pipelines, fire stations, fire engines, etc. Due to these major differences, normal fire models would not be applicable.

FFE models are relatively recent and they could be divided into three main groups: ignition, spread/suppression, and suppression models. Ignition models usually estimate the number, location, and times of fire ignition after an earthquake. Most ignition models relate an earthquake intensity measure to ignition frequency through regression models. Spread/suppression models involve the estimation of fire spread, given the initial ignition locations. The estimate can involve several degree, including the geographic spread or status (e.g, burned or not, percentage burned) as a function of time, with or without suppression measures. Suppression models are used to estimate the suppression time given the burn status. Integrated FFE models incorporate all the three aforementioned models and are preferred because of integrated variables (Lee et al., 2008).

Some limitations that should be taken in consideration are the lack of validation (because models are without precedents) and the accurate physical inventory requirements. During the process of FFE model selection, several factors to be considered would involve input parameters (number of parameters and respective uncertainty), required level of analysis, degree of model verification, and time available to complete the FFE studies. The selected model should represent a scientifically sound FFE application.

## CHAPTER 6: References

Atkinson, G. M., and Boore, D. M. (1995). Ground Motion Relations for Eastern North America. *Bulletin of Seismological Society of America*, 85(1), pp 17-30.

Building Seismic Safety Council (2004). NEHRP Recommended Provisions for Seismic Regulations for New Buildings and Other Structures, 2003 Edition, Part 1 Provisions. FEMA 450, 355.

Cleveland, L. (2006). "Seismic Loss Assessment for the New Madrid Seismic Zone," MS Thesis, Department of Civil and Environmental Engineering, University of Illinois at Urbana-Champaign, Urbana, IL

Cramer, C.H. (2006). Quantifying the Uncertainty in Site Amplification Modeling and Its Effects on Site-Specific Seismic-Hazard Estimation in the Upper Mississippi Embayment and Adjacent Areas. *Bulletin of the Seismological Society of America*, 96 (6), 2008-2020.

CUSEC Association of the State Geologists (2008). CUSEC State Geologists' Procedures for New Madrid Catastrophic Planning Initiative Phase II 8-State Soil Site Class, Liquefaction Susceptibility, and Soil Response Maps. Memphis, TN. CUSEC.

Davis, J. F., Bennet, J. H., Glenn, A. B., James, E. K., Salem, J. R. and Michael, A. S. (1982). *Earthquake Planning Scenario for a Magnitude 8.3 Earthquake on the San Andreas Fault in the San Francisco Bay Area*. California Department of Conservation, Division of Mines and Geology, Sacramento, CA

Earthquake Engineering Research Institute (1996). *Scenario for a Magnitude 7.0 Earthquake on the Hayward Fault*, Oakland, CA

- Earthquake Engineering Research Institute (2005). *Scenario for a Magnitude 6.7 Earthquake on the Seattle Fault*, Oakland, CA
- Elnashai, Amr S. (2008). Perspectives on the History of Seismic Risk Assessment. Risk, Governance and Society, Vol 14. Chapter 3, pp 89-95.
- Federal Emergency Management Agency [FEMA] (2008). HAZUS-MH MR3 Technical Manual. Washington, D.C. FEMA.
- Fernandez, A, and Rix, G. J. (2006). Soil Attenuation Relationships and Seismic Hazard Analyses in the Upper Mississippi Embayment. Proceedings of the 8<sup>th</sup> U.S. National Conference on Earthquake Engineering San Francisco, California, April 18-22, 2006, EERI, Oakland, CA.
- Frankel, A. et al. (1996). National Seismic Hazard Maps: Documentation. *OFR*, pp. 96-532. USGS
- Fullerton, D. S., Bush, C. A., and Pennell, J. N. (2003). Map of Surficial Deposits and Materials in the Eastern and Central United State (East of 102 degrees West Longitude). USGS Geologic Investigation Series I-2789.
- Gencturk, B., Elnashai, A. S., and Song, J. (2007). Fragility Relationships for Populations of Buildings Based on Inelastic Response. Mid-America Earthquake Center Report, August.
- Gencturk, B., Elnashai, A. S., and Song, J. (2008). Improved Fragility Relationships for Populations of Buildings Based on Inelastic Response. *The 14<sup>th</sup> World Conference on Earthquake Engineering*. Beijing, China. October 12-17.
- Hansen, G. (1996) Chronology of the Great Earthquake, and the 1906-1907 Graft Investigations. <<http://www.sfmuseum.org/hisg10/06timeline.html>>.

Homeland Security Infrastructure Program (HSIP) Gold Dataset 2008. Bethesda, MD 20816-5003.

Hunt, R. E. (2005). Geotechnical Engineering Investigation Handbook, Earthquakes, 2<sup>nd</sup> ed. pp 944-947, Boca Raton, FL

International Code Council (2002). 2003 International Building Code, 668.

Johnson, W. (1998). Dam Breach/Hazard Class Analysis Powerpoint Presentation. Frederick, MD.

Kircher et al. (2006). When the Big One Strikes Again – Estimated Losses due to a Repeat of the 1906 San Francisco Earthquake. *Earthquake Spectra*, 22(2), S297-S339. EERI

International Code Council (2002). 2003 International Building Code, 668.

Mid-America Earthquake Center (2007). “Comprehensive Seismic Loss Modeling for the State of Illinois” Report: Appendix III, Fragility Functions. June.

Mogami T, Kubo K (1953). The behavior of soil during vibration. In: Proceedings of the Third International Conference of Soil Mechanics and Foundation Engineering, pp 152–155

Montoya, L. 2003. Geo-Data Acquisition Through Mobile GIS and Digital Video: An Urban Disaster Management Perspective. *Environmental Modeling and Software*, 18, pp 869-876.

Newton Consultants (2007). Geotechnical Liquefaction Image. Retrieved October 11 2009.

<[http://www.newtonconsultants.com/Images/Nwtn\\_Pg\\_Geotech\\_Liqfact.gif](http://www.newtonconsultants.com/Images/Nwtn_Pg_Geotech_Liqfact.gif)>

NGA Office of Americas/North America and Homeland Security Division (PMH) (2007).  
Homeland Security Infrastructure Program (HSIP) Gold Dataset 2007. Bethesda,  
MD 20816-5003. May.

NGA Office of Americas/North America and Homeland Security Division (PMH) (2008).  
Rix, G.J. and J.A. Fernandez-Leon (2004). Synthetic Ground Motions for  
Memphis, TN. Retrieved July 2 2004.  
<[http://www.ce.gatech.edu/research/mae\\_ground\\_motion](http://www.ce.gatech.edu/research/mae_ground_motion)>

Njagih, J. K. (2003). Digital Field Data Capture Technique for Natural Hazard and Risk  
Assessment, MS Thesis, Natural Hazard Studies, International Institute for Geo-  
Information Science and Earth Observation, Enschede, The Netherlands.

Scawthorn, Charles (2008). A Brief History of Seismic Risk Assessment. Risk,  
Governance and Society, Vol 14. Chapter 2, pp 5-81.

Steinbrugge, K. V., Degenkolb, H. J., Lavery, G. L. and McCarty, J. E. (1987).  
*Earthquake planning scenario for a magnitude 7.5 earthquake on the Hayward  
Fault in the San Francisco Bay Area*, California Dept. of Conservation, Division  
of Mines and Geology, Sacramento, CA

Stover, C. W., and Coffman, J. L. (1993). Seismicity of the United States. U.S.  
Geological Survey Professional Paper 1527. United States Government Printing  
Office, Washington, D.C.

Tobriner, S. (2006). What really happened in San Francisco in the earthquake of 1906.  
*Commemorating the 1906 San Francisco Earthquake 100<sup>th</sup> Anniversary  
Earthquake Conference*. San Francisco, CA. April 18-22.



- Toro, G.R. and W.J. Silva, (2001), Scenario Earthquakes for St. Louis, MO, and Memphis, TN, and Seismic Hazard Maps for the Central United States Region Including the Effect of Site Conditions. Final Technical Report, USGS External Grant 1434-HQ-GR-02981, 248 pp.
- Tuttle, M. P., and Schweig, E. S. (1995). Archeological and Pedological Evidence for Large Prehistoric Earthquakes in the New Madrid Seismic Zone, Central United States. *Geology*, 23 (3), 253-256.
- Unen, C. (2009). Private Communication
- US Department of Transportation – Federal Highway Administration (2008). National Bridge Inventory. 1200 New Jersey Avenue SE, Washington, D.C., 20590. (2008).
- U.S. Geological Survey (2007). Earthquake Hazard in the Heart of the Homeland. Fact Sheet 2006–3125. USGS, January 2007.
- U.S. Geological Survey (2009). Earthquake Hazard in the New Madrid Seismic Zone Remains a Concern. Fact Sheet 2009–3071. USGS, August 2009.
- U.S. Geological Survey (2003). The USGS Earthquake Hazards program in NEHRP – Investing in a Safer Future. Fact Sheet 017-03, USGS, March 2003.
- Wang, Yumei (1999). Risk Assessment and Risk Management in Oregon. Proceeding of the 5<sup>th</sup> U.S. Conference on Lifeline Earthquake Engineering, pp. 197-206, Seattle, WA
- Wong et al. (2005). Potential Losses in a Repeat of the 1886 Charleston, South Carolina, Earthquake. *Earthquake Spectra*, 21(4), 1157-1184. EERI

Yamazaki, F. (2001). Application of Remote Sensing and GIS for Damage Assessment, *Structural Safety and Reliability*, Swets and Zeitlinger.

Youd, T. L., and Perkins, D. M., 1978. Mapping of Liquefaction Induced Ground Failure Potential, *Journal of the Geotechnical Engineering Division*, American Society of Civil Engineers, vol. 104, no. 4, pp. 433-446.

## CHAPTER 7: Appendices

### Appendix 1. Hazard

The utilized attenuation relationships for the CEUS are outlined as follows:

**Atkinson and Boore (1995):**

$$\log(y) = C_1 + C_2(M-6) + C_3(M-6)^3 - \log(R) - C_4 R \quad (13)$$

where

y = response parameter (e.g., PGA)

M = moment magnitude

R = distance from site to hypocenter

**Table 47. Atkinson and Boore Regression Coefficients**

	$C_1$	$C_2$	$C_3$	$C_4$
Sa(0.2s)	3.79	0.298	-0.0536	0.00135
Sa(1.0s)	3.75	0.418	-0.0644	0.000457
PGA	2.77	0.620	-0.0409	0.0000

**Toro, Abrahamson, and Schneider**

$$\ln Y = C_1 + C_2(M-6) + C_3(M-6)^2 - C_4 \ln R_M - (C_5 - C_4) \max\left[\ln\left(\frac{R_M}{100}\right), 0\right] - C_6 R_M \quad (14)$$

where:

Y = response parameter (e.g., PGA)

M = moment magnitude

R =  $r_{jb}$ , distance from site to the vertical projection of the fault rupture plane

$$R_M = \sqrt{r_{jb}^2 + C_7^2}$$

**Table 48. Attenuation Coefficients of Toro, Abrahamson, and Schneider**

	$C_1$	$C_2$	$C_3$	$C_4$	$C_5$	$C_6$	$C_7$
Sa(0.2s)	1.73	0.84	0.00	0.98	0.66	0.0042	7.5
Sa(1.0s)	0.09	1.42	-0.20	0.90	0.49	0.0023	6.8
PGA	2.20	0.81	0.00	1.27	1.16	0.0021	9.3

**Campbell (2003)**

$$\ln Y = C_1 + f_1(M) + f_2(M, r_{rup}) + f_3(r) \quad (15)$$

where

Y = mean of response parameter (e.g., PGA)

M = moment magnitude

$r_{rup}$  = Distance from the site to the fault rupture plane

$r_1 = 70$  km

$r_2 = 130$  km

$$f_1(M) = C_2 M + C_3(8.5 - M)^2$$

$$f_2(M, r_{rup}) = C_4 \ln R + (C_5 - C_6 M)r_{rup}$$

$$R = \sqrt{r_{rup}^2 + [C_7 e^{C_8 M}]^2}$$

$$f_3(r) = \begin{cases} 0 & \text{for } r_{rup} \leq r_1 \\ C_7(\ln r_{rup} - \ln r_1) & \text{for } r_1 < r_{rup} \leq r_2 \\ C_7(\ln r_{rup} - \ln r_1) + C_8(\ln r_{rup} - \ln r_2) & \text{for } r_{rup} > r_2 \end{cases}$$

**Table 49. Coefficients of Campbell Attenuation Equation**

	$C_1$	$C_2$	$C_3$	$C_4$	$C_5$	$C_6$	$C_7$	$C_8$
Sa(0.2s)	-0.4328	0.617	-0.0586	-1.320	-0.00460	0.000337	0.399	0.493
Sa(1.0s)	-0.6104	0.451	-0.2090	-1.158	-0.00255	0.000141	0.299	0.503
PGA	0.0305	0.633	-0.0427	-1.591	-0.00428	0.000483	0.683	0.416

**Somerville, Collins, Abrahamson, Braves, and Saikia**

Hard rock:

For  $r < r_1$

$$\ln(S_a(g)) = C_1 + C_2(M - m_1) + C_3 \ln R + C_4(M - m_1) \ln R + C_5 r + C_7(8.5-M)^2 \quad (16)$$

for  $r \geq r_1$

$$C_1 + C_2(M - m_1) + C_3 \ln R_1 + C_4(M - m_1) \ln R + C_5 r + C_6(\ln R - \ln R_1)^2 + C_7(8.5-M)^2 \quad (17)$$

where

$S_a(g)$  = spectral acceleration

$m_1 = 6.4$

$r_1 = 50$  km

$h = 6$  km

$R = \sqrt{r^2 + h^2}$

$R_1 = \sqrt{r_1^2 + h^2}$

$M$  = moment magnitude

$R$  = epicentral distance (km)

**Table 50. Attenuation Coefficients of Somerville et al.**

	$C_1$	$C_2$	$C_3$	$C_4$	$C_5$	$C_6$	$C_7$
Sa(0.2s)	0.793	0.805	-0.679	0.0861	-0.00498	-0.477	0.0000
Sa(1.0s)	-0.307	0.805	-0.696	0.0861	-0.00362	-0.755	-0.1020

## Appendix 2. Inventory

**Table 3.6 Default Full Replacement Cost Models (Means, 2002)**

HAZUS Occupancy Class Description		Sub-category	Means Model Description (Means Model Number)	Means Cost/SF (2002)
RES1	Single Family Dwelling	See Table 14.2		
RES2	Manufactured Housing	Manufactured Housing	Manufactured Housing (N/A) <sup>1</sup>	\$30.90
RES3	Multi Family Dwelling – small	Duplex	SFR Avg 2 St., MF adj, 3000 SF	\$67.24
		Triplex/Quads	SFR Avg 2 St., MF adj, 3000 SF	\$73.08
	Multi Family Dwelling – medium	5-9 units	Apt., 1-3 st., 8,000 SF (M.010)	\$125.63
		10-19 units	Apt., 1-3 st., 12,000 SF (M.010)	\$112.73
		20-49 units	Apt., 4-7 st., 40,000 SF (M.020)	\$108.86
	Multi Family Dwelling – large	50+ units	Apt., 4-7 st., 60,000 SF (M.020)	\$106.13
			Apt., 8-24 st., 145,000 SF (M.030)	\$111.69
RES4	Temp. Lodging	Hotel, medium	Hotel, 4-7 st., 135,000 SF (M.350)	\$104.63
		Hotel, large	Hotel, 8-24 st., 450,000 SF (M.360)	\$93.47
		Motel, small	Motel, 1 st., 8,000 SF (M.420)	\$94.13
		Motel, medium	Motel, 2-3 st., 49,000 SF (M.430)	\$110.03
RES5	Institutional Dormitory	Dorm, medium	College Dorm, 2-3 st, 25,000 SF (M.130)	\$118.82
		Dorm, large	College Dorm, 4-8 st, 85,000 SF (M.140)	\$113.31
		Dorm, small	Frat House, 2 st., 10,000 SF (M.240)	\$99.50
RES6	Nursing Home	Nursing home	Nursing Home, 2 st., 25,000 SF (M.450)	\$104.62
COM1	Retail Trade	Dept Store, 1 st	Store, Dept., 1 st., 110,000 SF (M.610)	\$71.54
		Dept Store, 3 st	Store, Dept., 3 st., 95,000 SF (M.620)	\$88.73
		Store, small	Store, retail, 8,000 SF (M.630)	\$79.23
		Store, medium	Supermarket, 44,000 SF (M.640)	\$69.09
		Store, convenience	Store, Convenience, 4,000 SF (M.600)	\$83.59
		Auto Sales	Garage, Auto Sales, 21,000 SF (M.260)	\$70.84
COM2	Wholesale Trade	Warehouse, medium	Warehouse, 30,000 SF (M.690)	\$61.91
		Warehouse, large	Warehouse, 60,000 SF (M.690)	\$56.58
		Warehouse, small	Warehouse, 15,000 SF (M.690)	\$70.43
COM3	Personal and Repair Services	Garage, Repair	Garage, Repair, 10,000 SF (M.290)	\$86.81
		Garage, Service sta.	Garage, Service sta., 1,400 SF (M.300)	\$113.91
		Funeral Home	Funeral home, 10,000 SF (M.250)	\$97.66
		Laundromat	Laundromat 3,000 SF (M.380)	\$135.64
		Car Wash	Car Wash, 1 st., 800 SF (M.080)	\$198.28
COM4	Prof./ Tech./Business Services	Office, Medium	Office, 5-10 st., 80,000 SF (M.470)	\$98.96
		Office, Small	Office, 2-4 st., 20,000 SF (M.460)	\$102.69
		Office, Large	Office, 11-20 st., 260,000 SF (M.480)	\$88.21
COM5	Banks	Bank	Bank, 1 st., 4100 SF (M.050)	\$153.97

**Table 51. HAZUS Classification of Highway Systems**

<b>Label</b>	<b>Description</b>
<b>Highway Roads</b>	
HRD1	Major Roads
HRD2	Urban Roads
<b>Highway Bridges</b>	
HWB1	Major Bridge - Length > 150m (Conventional Design)
HWB2	Major Bridge - Length > 150m (Seismic Design)
HWB3	Single Span – (Not HWB1 or HWB2) (Conventional Design)
HWB4	Single Span – (Not HWB1 or HWB2) (Seismic Design)
HWB5	Concrete, Multi-Column Bent, Simple Support (Conventional Design), Non-California (Non-CA)
HWB6	Concrete, Multi-Column Bent, Simple Support (Conventional Design), California (CA)
HWB7	Concrete, Multi-Column Bent, Simple Support (Seismic Design)
HWB8	Continuous Concrete, Single Column, Box Girder (Conventional Design)
HWB9	Continuous Concrete, Single Column, Box Girder (Seismic Design)
HWB10	Continuous Concrete, (Not HWB8 or HWB9) (Conventional Design)
HWB11	Continuous Concrete, (Not HWB8 or HWB9) (Seismic Design)
HWB12	Steel, Multi-Column Bent, Simple Support (Conventional Design), Non-California (Non-CA)
HWB13	Steel, Multi-Column Bent, Simple Support (Conventional Design), California (CA)
HWB14	Steel, Multi-Column Bent, Simple Support (Seismic Design)
HWB15	Continuous Steel (Conventional Design)
HWB16	Continuous Steel (Seismic Design)
HWB17	PS Concrete Multi-Column Bent, Simple Support - (Conventional Design), Non-California
HWB18	PS Concrete, Multi-Column Bent, Simple Support (Conventional Design), California (CA)
HWB19	PS Concrete, Multi-Column Bent, Simple Support (Seismic Design)
HWB20	PS Concrete, Single Column, Box Girder (Conventional Design)
HWB21	PS Concrete, Single Column, Box Girder (Seismic Design)
HWB22	Continuous Concrete, (Not HWB20/HWB21) (Conventional Design)
HWB23	Continuous Concrete, (Not HWB20/HWB21) (Seismic Design)
HWB24	Same definition as HWB12 except that the bridge length is less than 20 meters
HWB25	Same definition as HWB13 except that the bridge length is less than 20 meters
HWB26	Same definition as HWB15 except that the bridge length is less than 20 meters and Non-CA
HWB27	Same definition as HWB15 except that the bridge length is less than 20 meters and in CA
HWB28	All other bridges that are not classified (including wooden bridges)
<b>Highway Tunnels</b>	
HTU1	Highway Bored/Drilled Tunnel
HTU2	Highway Cut and Cover Tunnel

**Table 52. HAZUS Classification of Railway Systems**

<b>Label</b>	<b>Description</b>
RTR1	<b>Railway Tracks</b> Railway Tracks
RLB1	<b>Railway Bridges</b> Steel, Multi-Column Bent, Simple Support (Conventional Design), Non-California (Non-CA)
RLB2	Steel, Multi-Column Bent, Simple Support (Conventional Design), California (CA)
RLB3	Steel, Multi-Column Bent, Simple Support (Seismic Design)
RLB4	Continuous Steel (Conventional Design)
RLB5	Continuous Steel (Seismic Design)
RLB6	Same definition as HWB1 except that the bridge length is less than 20 meters
RLB7	Same definition as HWB2 except that the bridge length is less than 20 meters
RLB8	Same definition as HWB4 except that the bridge length is less than 20 meters and Non-CA
RLB9	Same definition as HWB5 except that the bridge length is less than 20 meters and in CA
RLB10	All other bridges that are not classified
RST	<b>Railway Urban Station</b> Rail Urban Station (with all building type options enabled)
	<b>Railway Tunnels</b>
RTU1	Rail Bored/Drilled Tunnel
RTU2	Rail Cut and Cover Tunnel
	<b>Railway Fuel Facility</b>
RFF	Rail Fuel Facility (different combinations for with or without anchored components and/or with or without backup power)
	<b>Railway Dispatch Facility</b>
RDF	Rail Dispatch Facility (different combinations for with or without anchored components and/or with or without backup power)
	<b>Railway Maintenance Facility</b>
RMF	Rail Maintenance Facility (with all building type options enabled)



**Table 53. HAZUS Light Rail Systems Classification**

<b>Label</b>	<b>Description</b>
	<b>Light Rail Tracks</b>
LTR1	Light Rail Track
	<b>Light Rail Bridges</b>
LRB1	Steel, Multi-Column Bent, Simple Support (Conventional Design), Non-California (Non-CA)
LRB2	Steel, Multi-Column Bent, Simple Support (Conventional Design), California (CA)
LRB3	Steel, Multi-Column Bent, Simple Support (Seismic Design)
LRB4	Continuous Steel (Conventional Design)
LRB5	Continuous Steel (Seismic Design)
LRB6	Same definition as HWB1 except that the bridge length is less than 20 meters
LRB7	Same definition as HWB2 except that the bridge length is less than 20 meters
LRB8	Same definition as HWB4 except that the bridge length is less than 20 meters and Non-CA
LRB9	Same definition as HWB5 except that the bridge length is less than 20 meters and in CA
LRB10	All other bridges that are not classified
	<b>Light Rail Tunnels</b>
LTU1	Light Rail Bored/Drilled Tunnel
LTU2	Light Rail Cut and Cover Tunnel
	<b>DC Substation</b>
LDC1	Light Rail DC Substation w/ Anchored Sub-Components
LDC2	Light Rail DC Substation w/ Unanchored Sub-Components
	<b>Dispatch Facility</b>
LDF	Light Rail Dispatch Facility (different combinations for with or without anchored components and/or with or without backup power)
	<b>Maintenance Facility</b>
LMF	Maintenance Facility (with all building type options enabled)

**Table 54. HAZUS Bus Facility Classification**

<b>Label</b>	<b>Description</b>
	<b>Bus Urban Station</b>
BPT	Bus Urban Station (with all building type options enabled)
	<b>Bus Fuel Facility</b>
BFF	Bus Fuel Facility (different combinations for with or without anchored components and/or with or without backup power)
	<b>Bus Dispatch Facility</b>
BDF	Bus Dispatch Facility (different combinations for with or without anchored components and/or with or without backup power)
	<b>Bus Maintenance Facility</b>
BMF	Bus Maintenance Facilities (with all building type options enabled)

**Table 55. HAZUS Port Facility Classification**

<b>Label</b>	<b>Description</b>
	<b>Waterfront Structures</b>
PWS	Waterfront Structures
	<b>Cranes/Cargo Handling Equipment</b>
PEQ1	Stationary Port Handling Equipment
PEQ2	Rail Mounted Port Handling Equipment
	<b>Warehouses</b>
PWH	Port Warehouses (with all building type options enabled)
	<b>Fuel Facility</b>
PFF	Port Fuel Facility Facility (different combinations for with or without anchored components and/or with or without backup power)

**Table 56. HAZUS Ferry Facility Classification**

<b>Label</b>	<b>Description</b>
	<b>Water Front Structures</b>
FWS	Ferry Waterfront Structures
	<b>Ferry Passenger Terminals</b>
FPT	Passenger Terminals (with all building type options enabled)
	<b>Ferry Fuel Facility</b>
FFF	Ferry Fuel Facility (different combinations for with or without anchored components and/or with or without backup power)
	<b>Ferry Dispatch Facility</b>
FDF	Ferry Dispatch Facility (different combinations for with or without anchored components and/or with or without backup power)
	<b>Ferry Maintenance Facility</b>
FMF	Piers and Dock Facilities (with all building type options enabled)

**Table 57. HAZUS Airport Facility Classification**

<b>Label</b>	<b>Description</b>
	<b>Airport Control Towers</b>
ACT	Airport Control Tower (with all building type options enabled)
	<b>Airport Terminal Buildings</b>
ATB	Airport Terminal Building (with all building type options enabled)
	<b>Airport Parking Structures</b>
APS	Airport Parking Structure (with all building type options enabled)
	<b>Fuel Facilities</b>
AFF	Airport Fuel Facility (different combinations for with or without anchored components and/or with or without backup power)
	<b>Airport Maintenance &amp; Hangar Facility</b>
AMF	Airport Maintenance & Hangar Facility (with all building type options enabled)
ARW	Airport Runway
	<b>Airport Facilities - Others</b>
AFO	Gliderport, Seaport, Stolport, Ultralight or Balloonport Facilities
AFH	Heliport Facilities

### Appendix 3. Detailed Damage Results

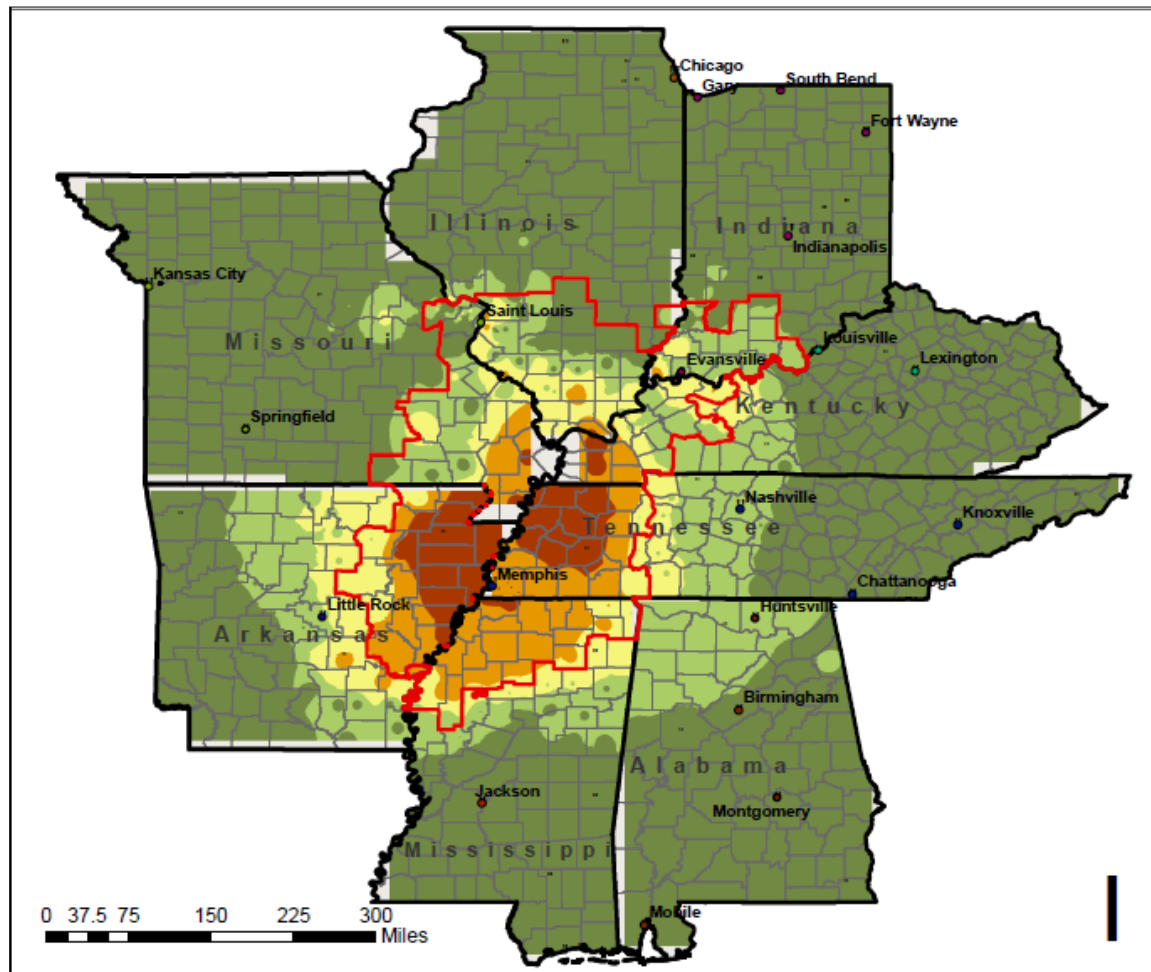
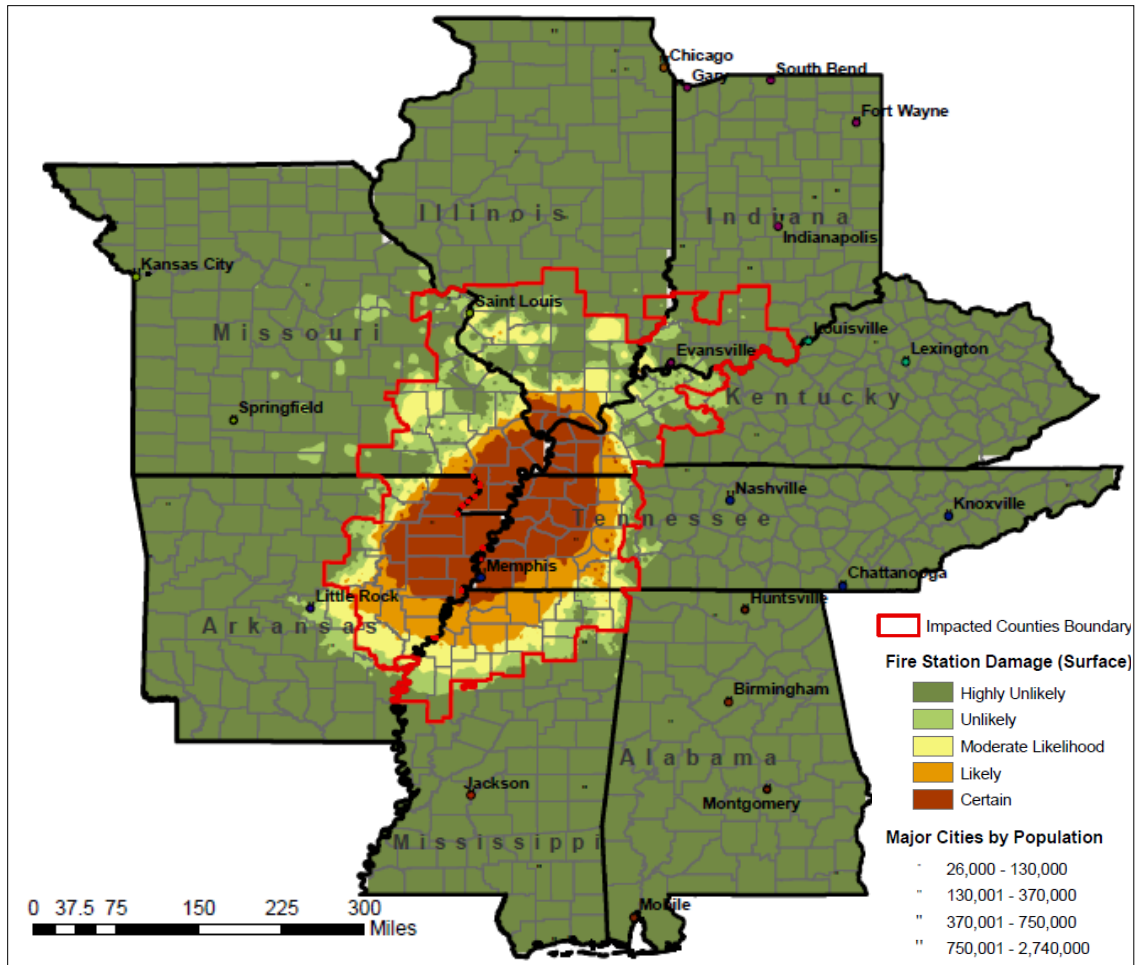


Figure 30. Hospitals Regional Impact



**Figure 31. Fire Stations Regional Impact**

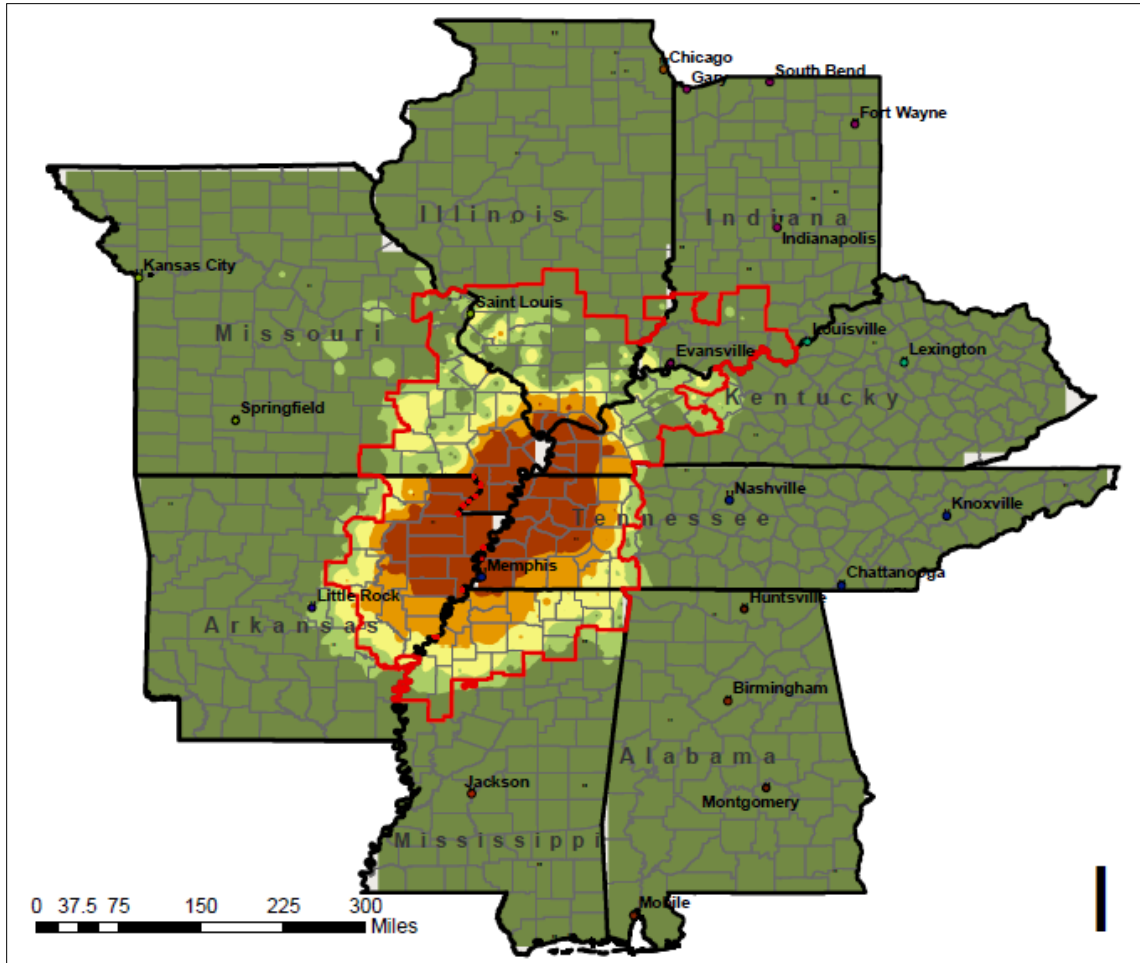


Figure 32. Police Stations Regional Impact

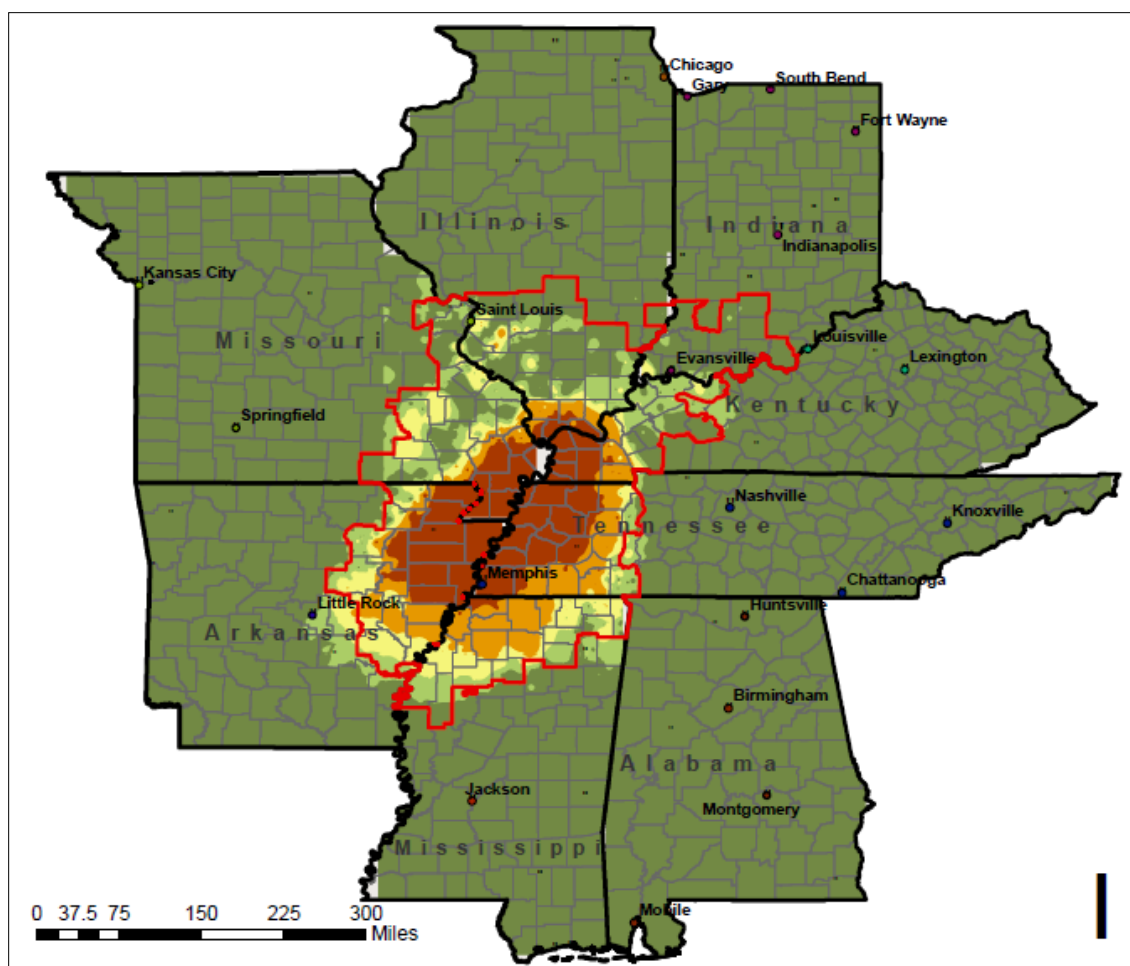


Figure 33. Schools Regional Impact

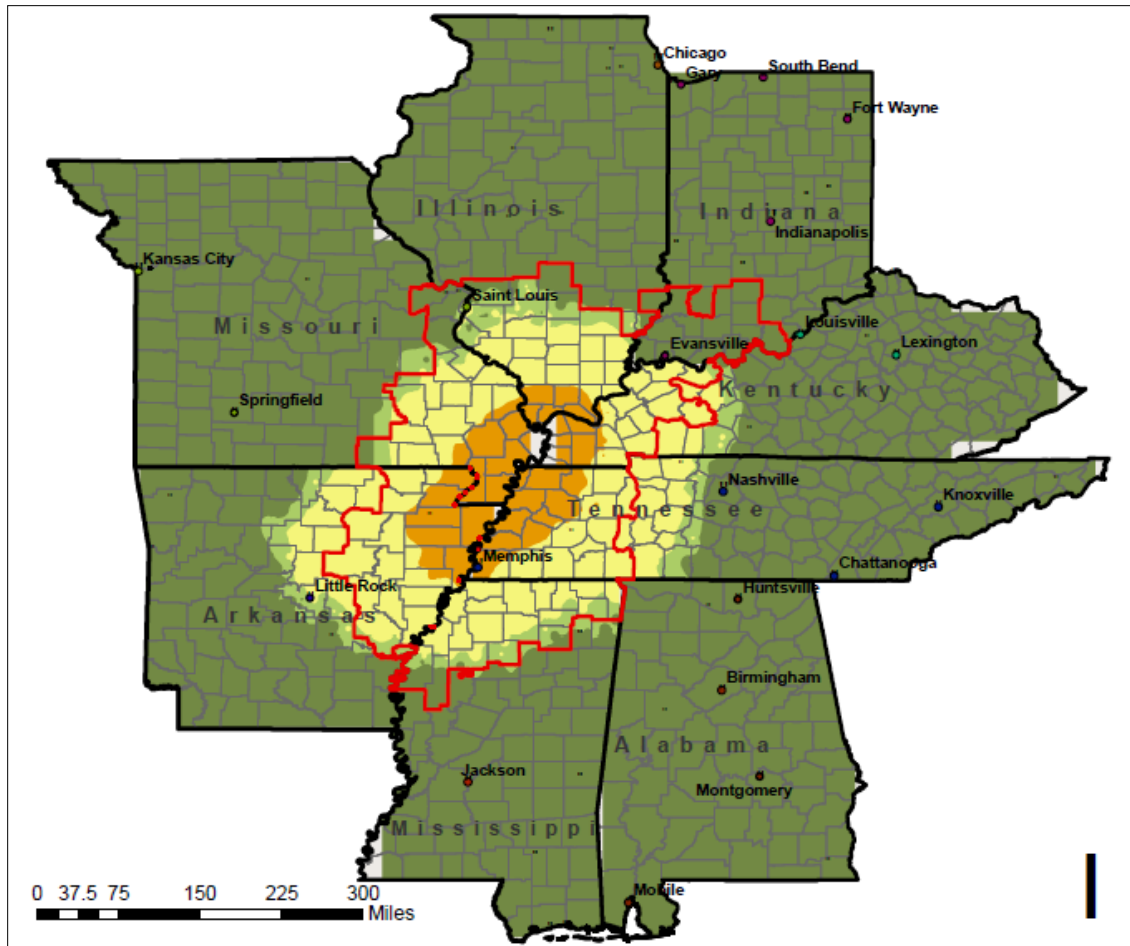


Figure 34. Airports Regional Impact



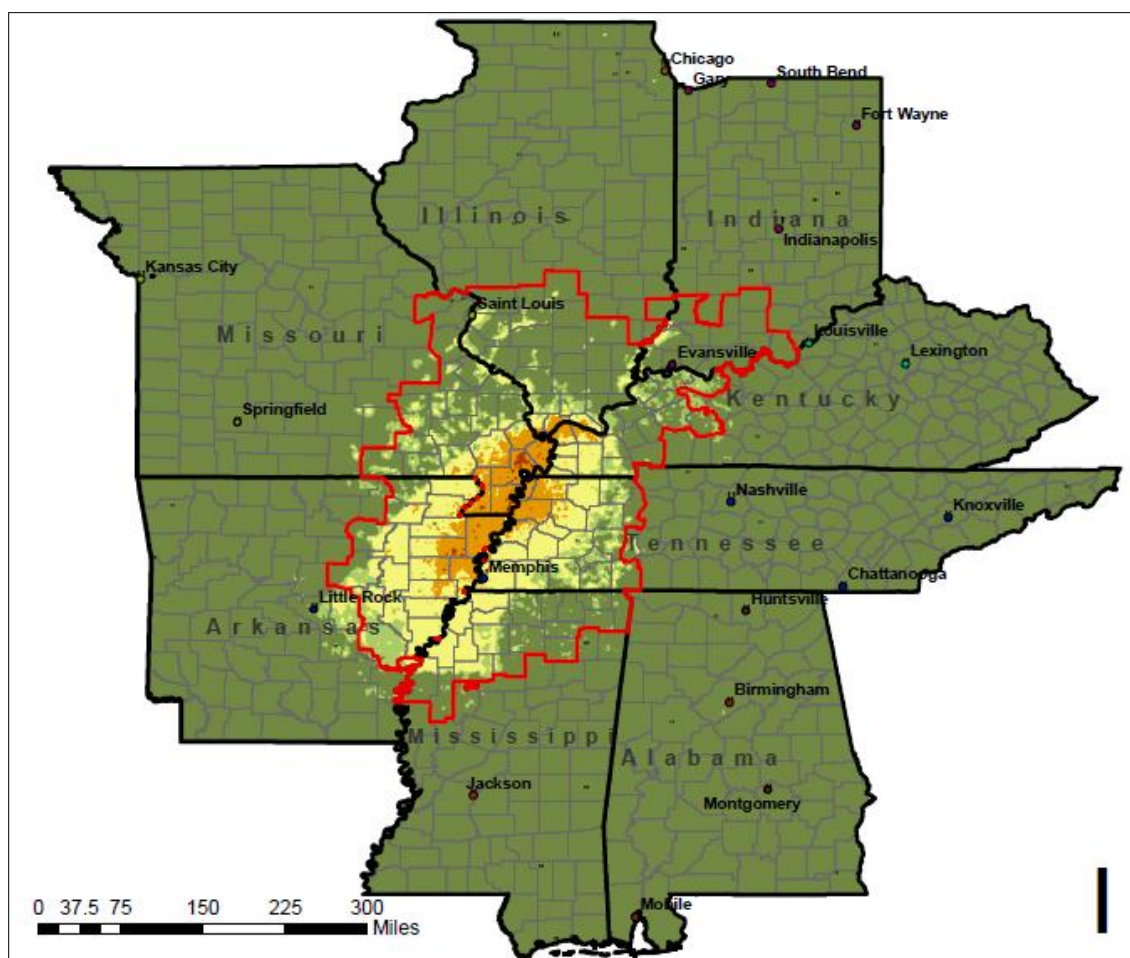


Figure 35. Highway Bridges Regional Impact



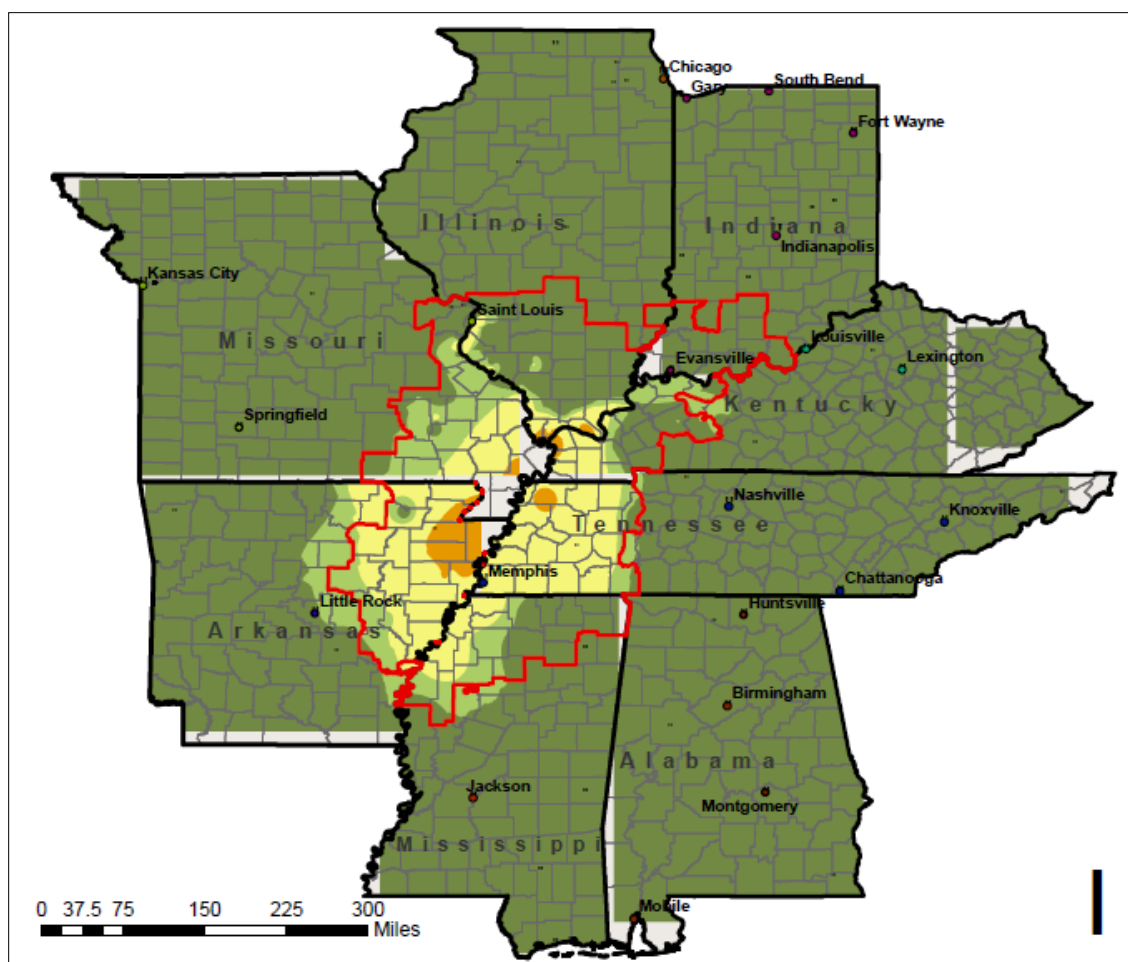


Figure 36. Railway Bridges Regional Impact

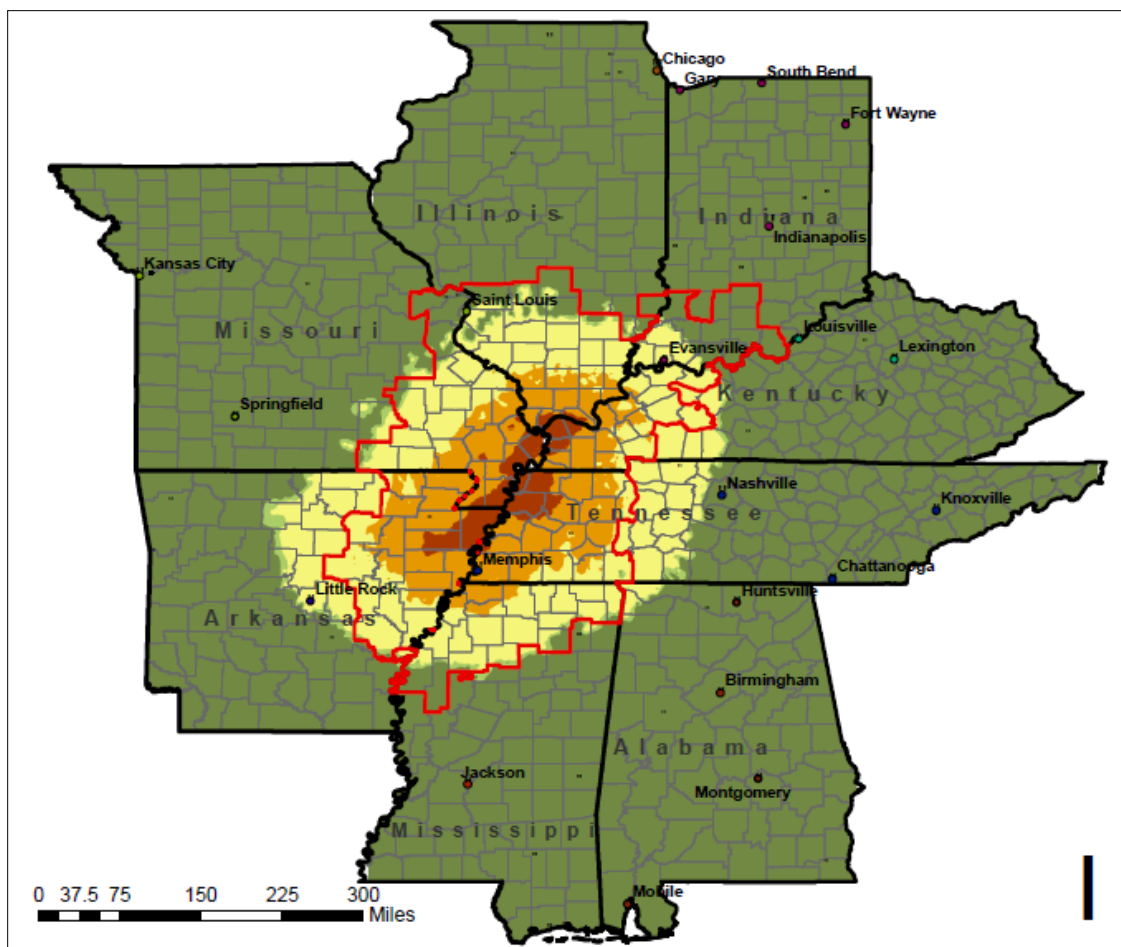


Figure 37. Communication Facilities Regional Impact

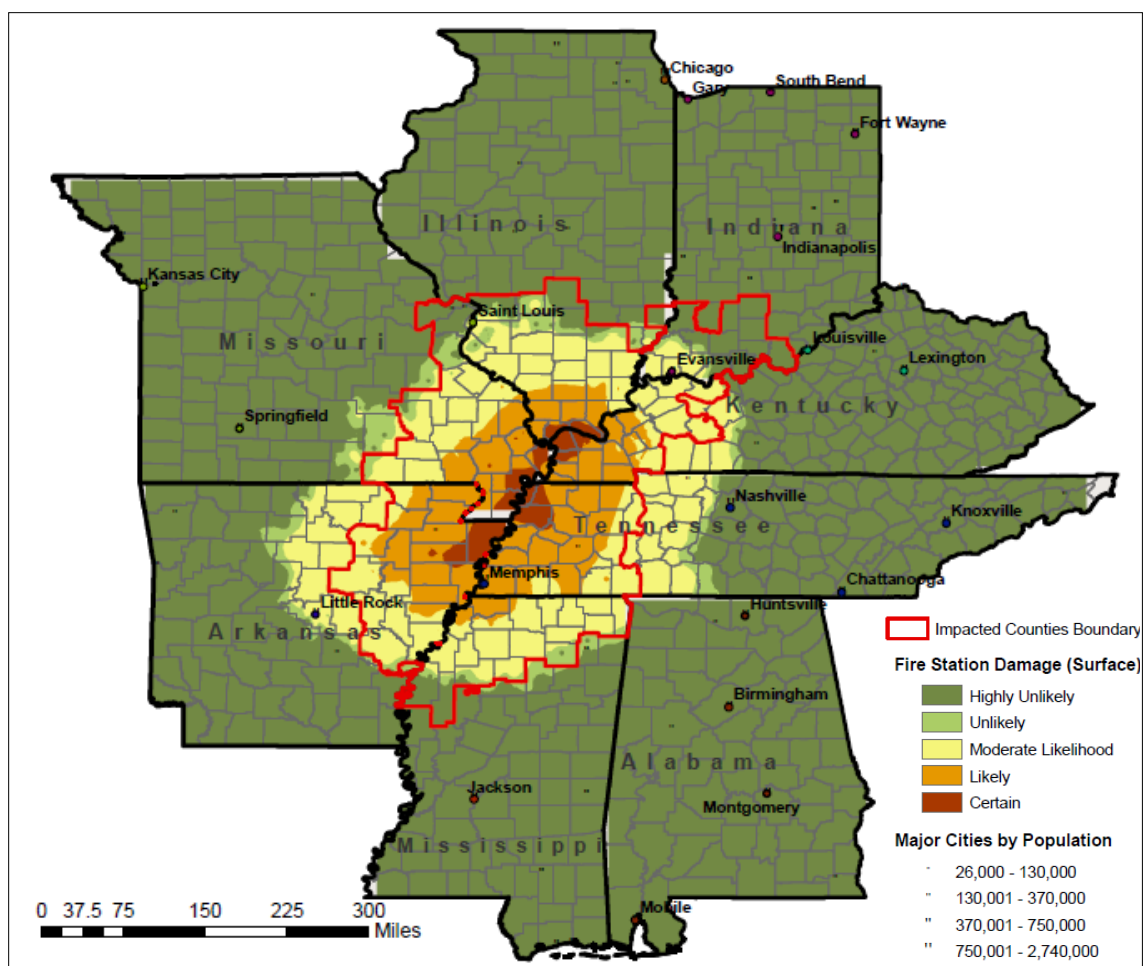
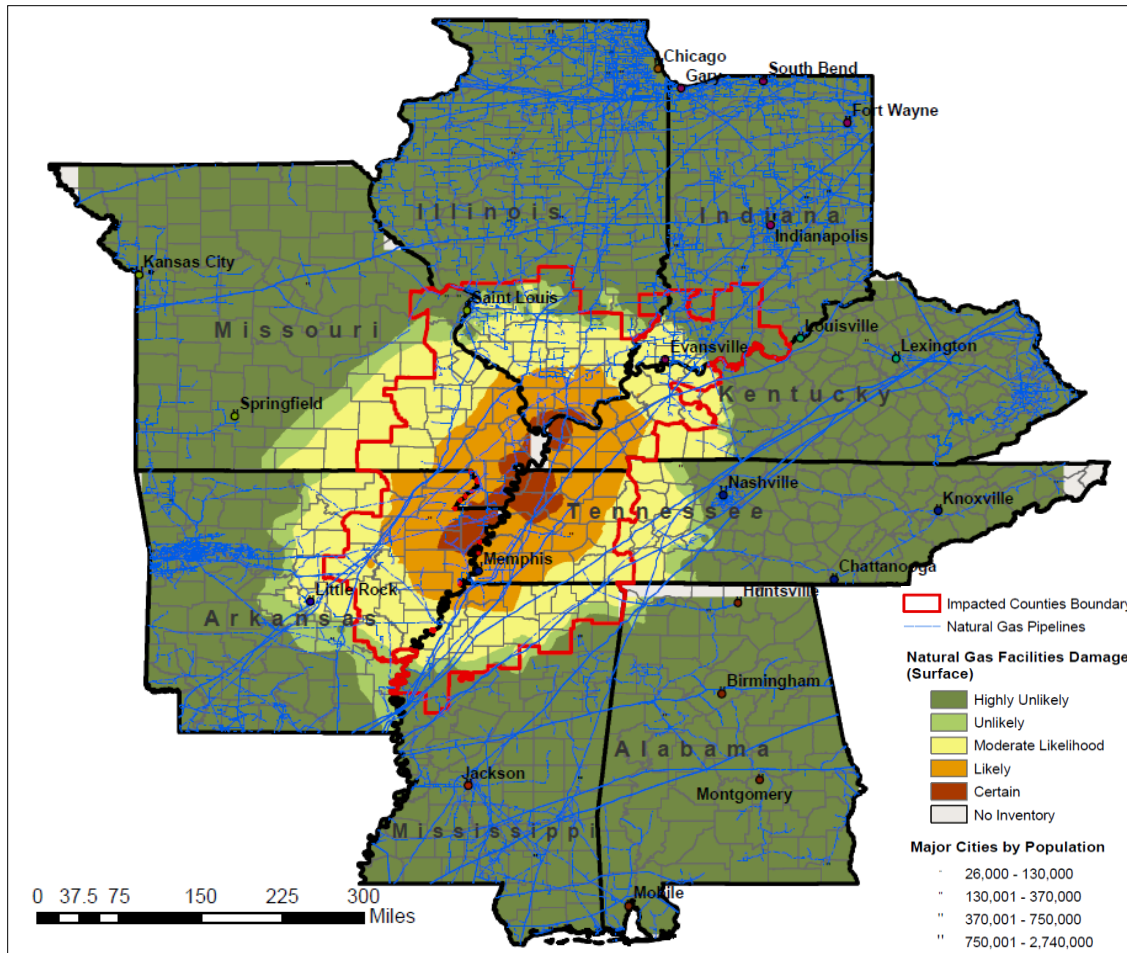
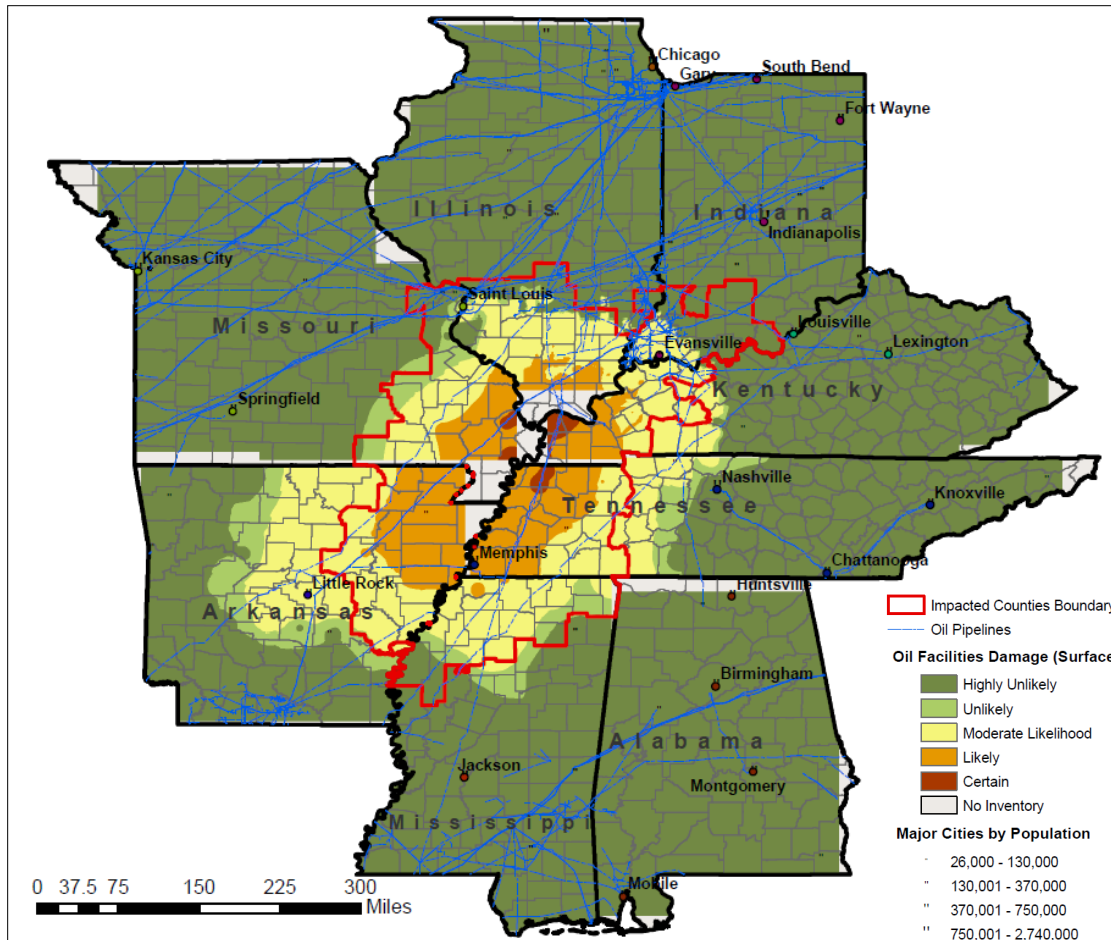


Figure 38. Electric Power Facilities Regional Impact



**Figure 39. Natural Gas Facilities Regional Impact**



**Figure 40. Oil Facilities Regional Impact**

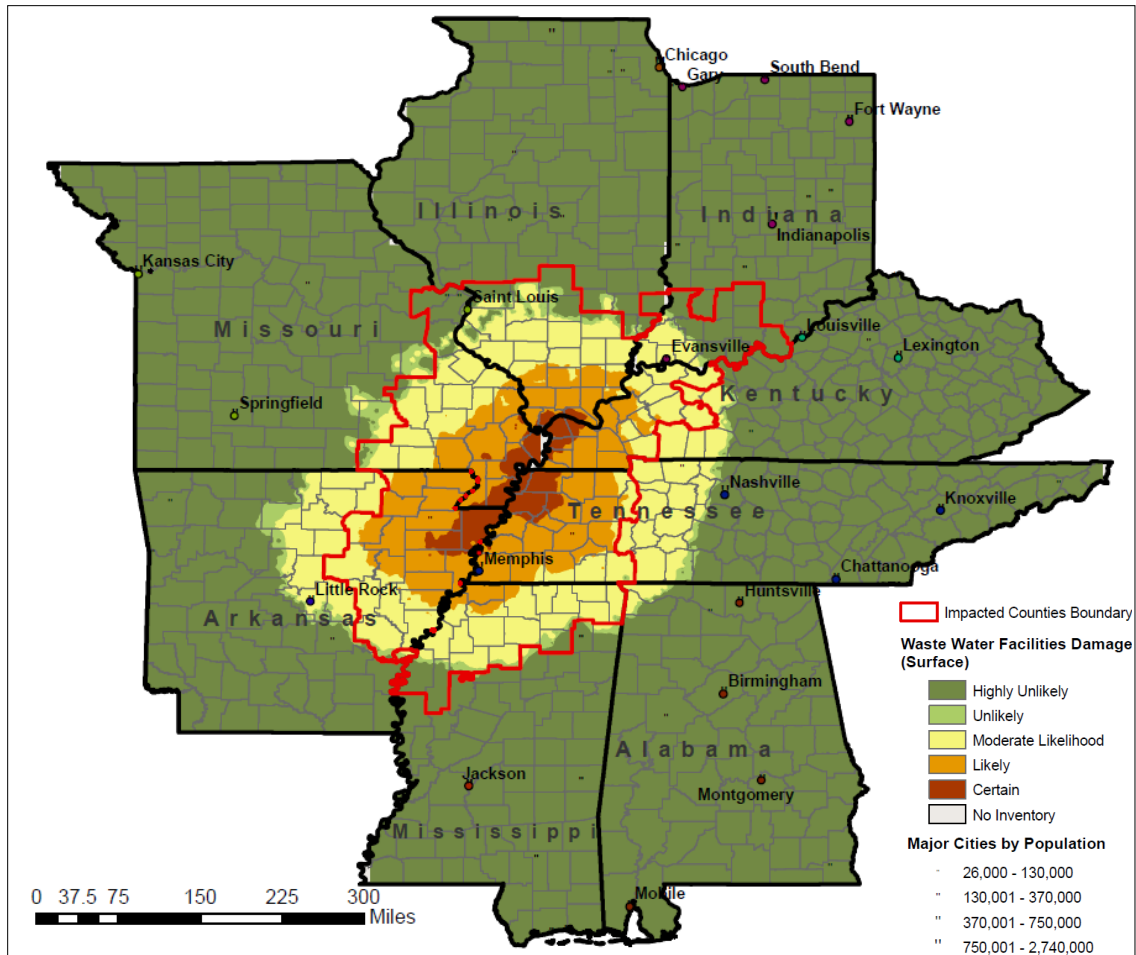


**Figure 41. Waste Water Facilities Regional Impact**

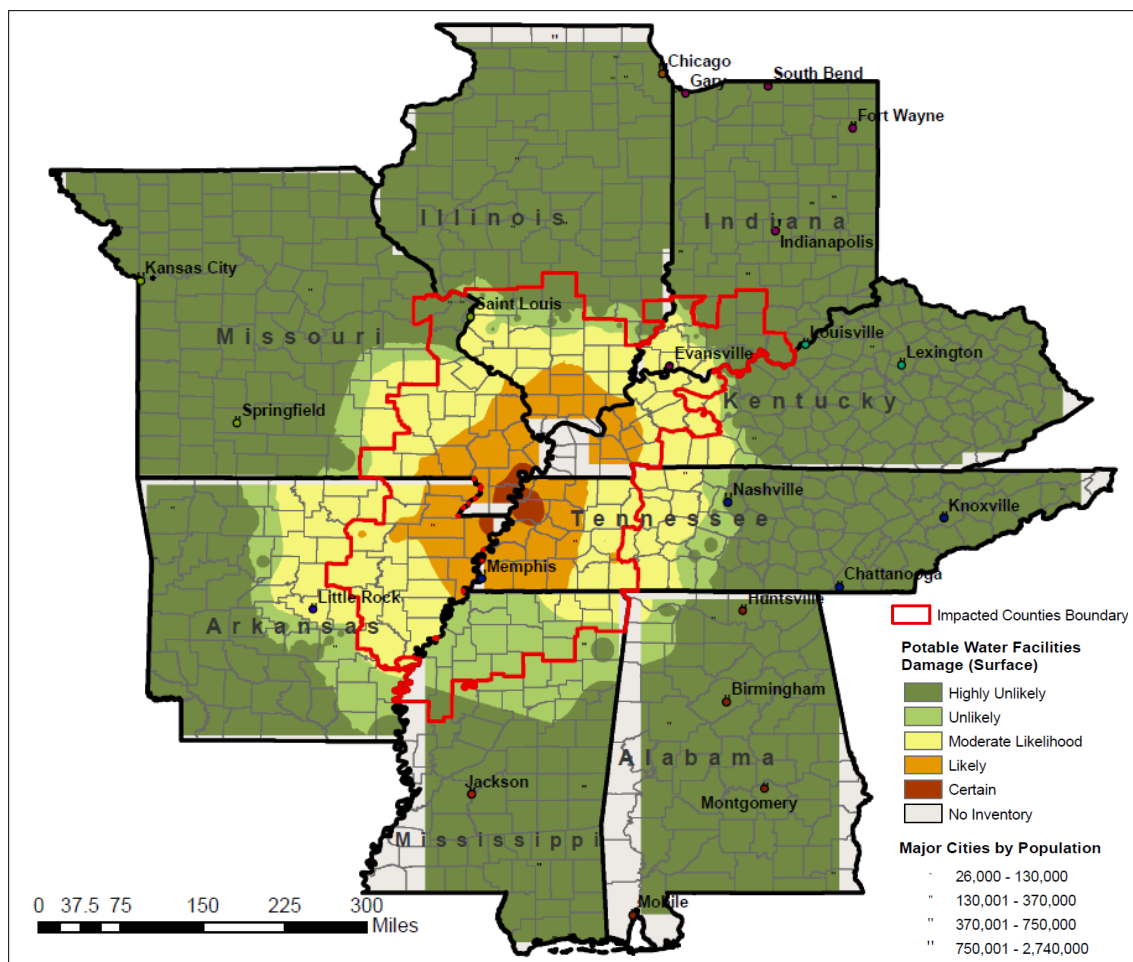


**Figure 42. Potable Water Facilities Regional Impact**



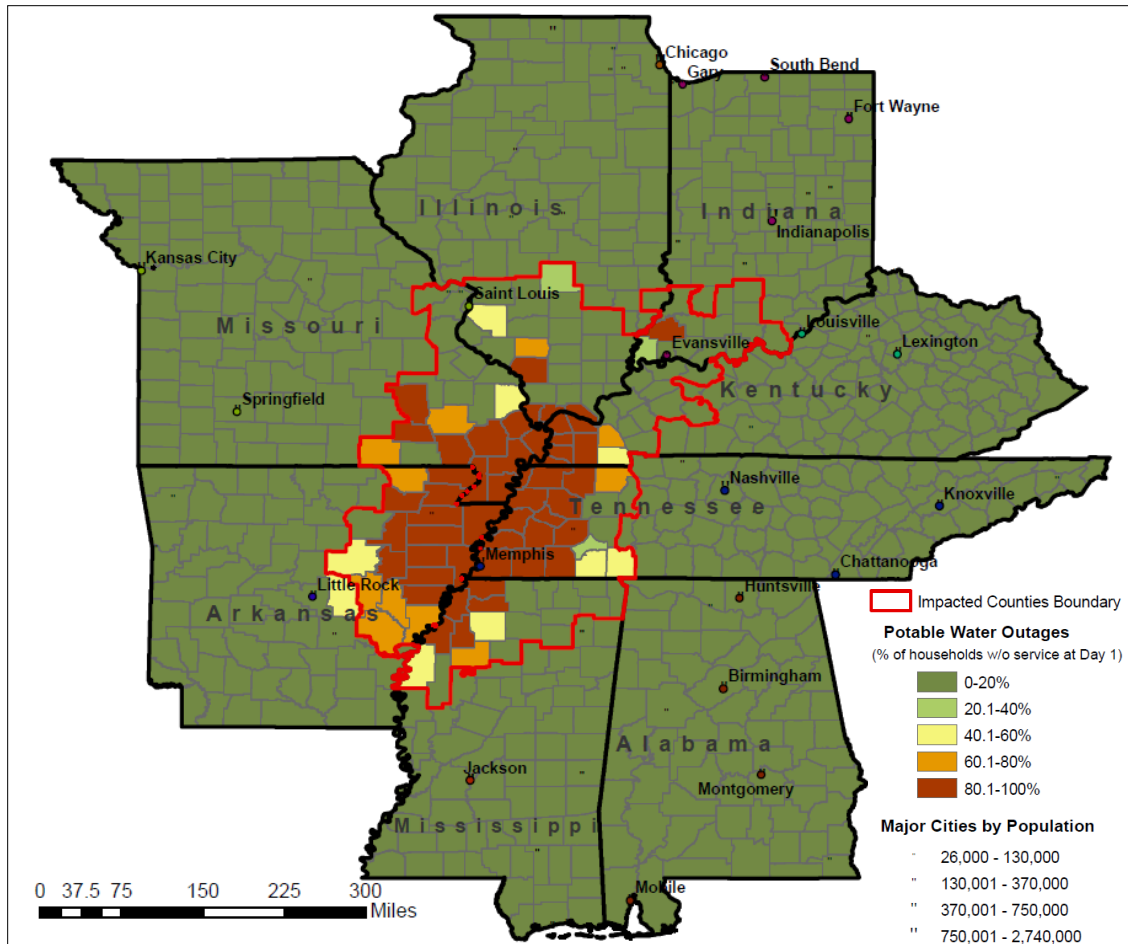


**Figure 43. Potable Water Regional Outages**



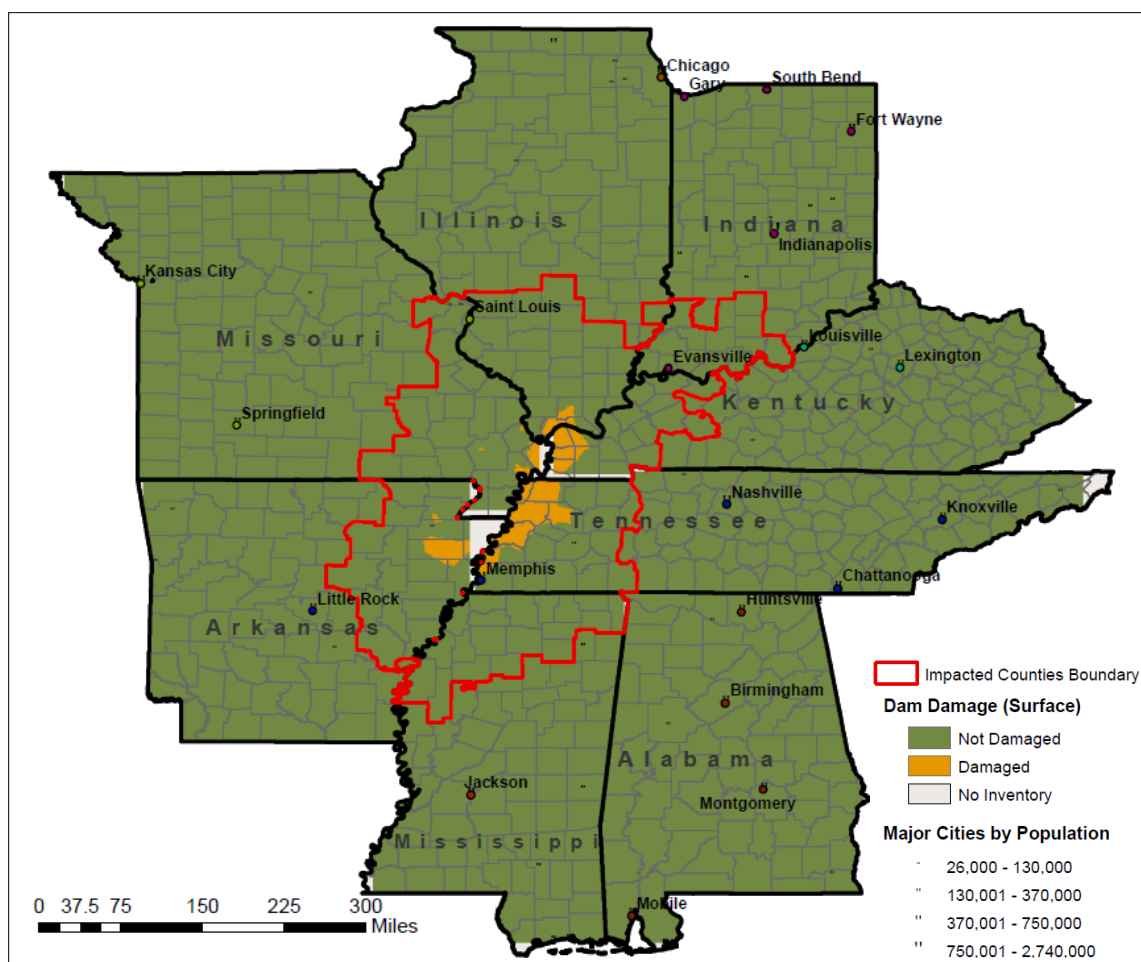


Figure 44. Dam Regional Damage

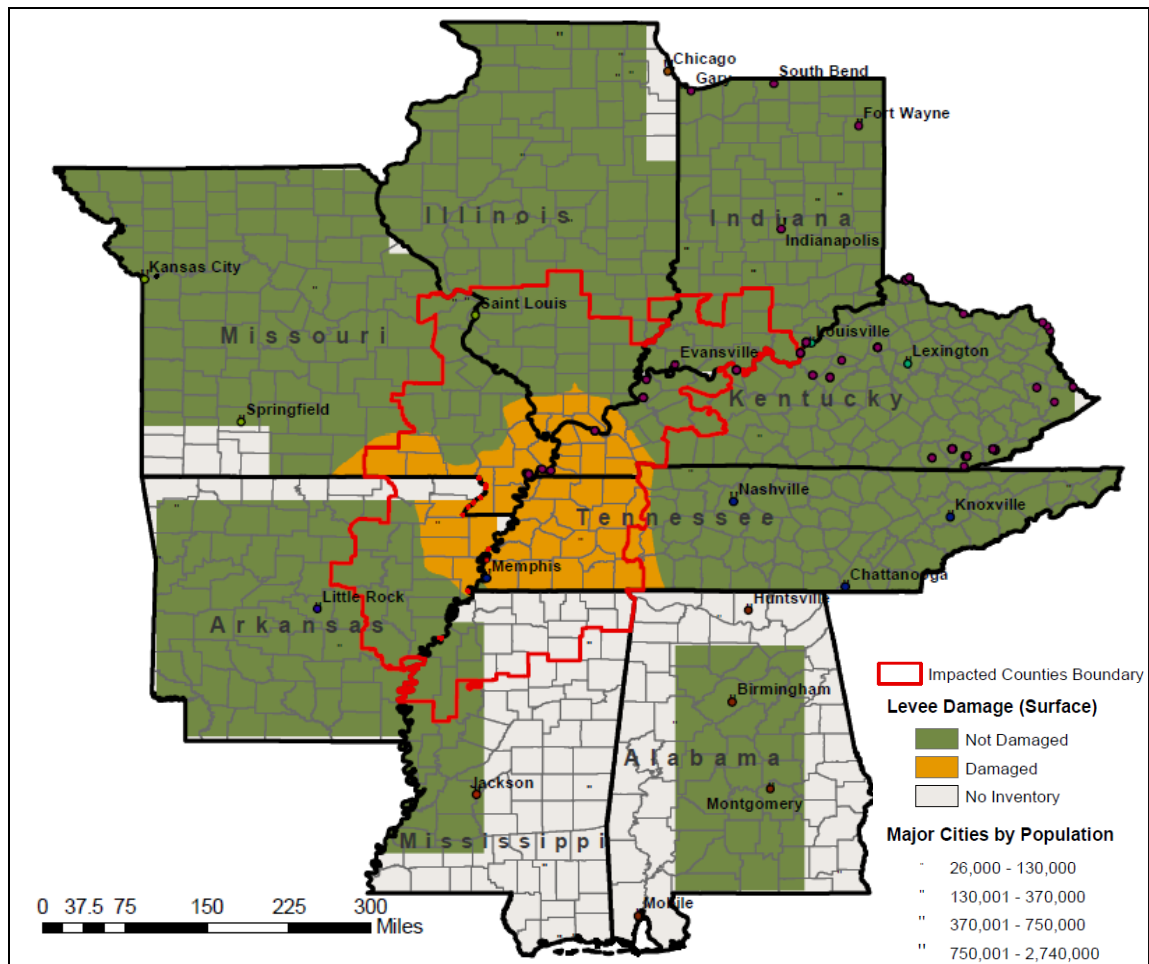


Figure 45. Levee Regional Damage

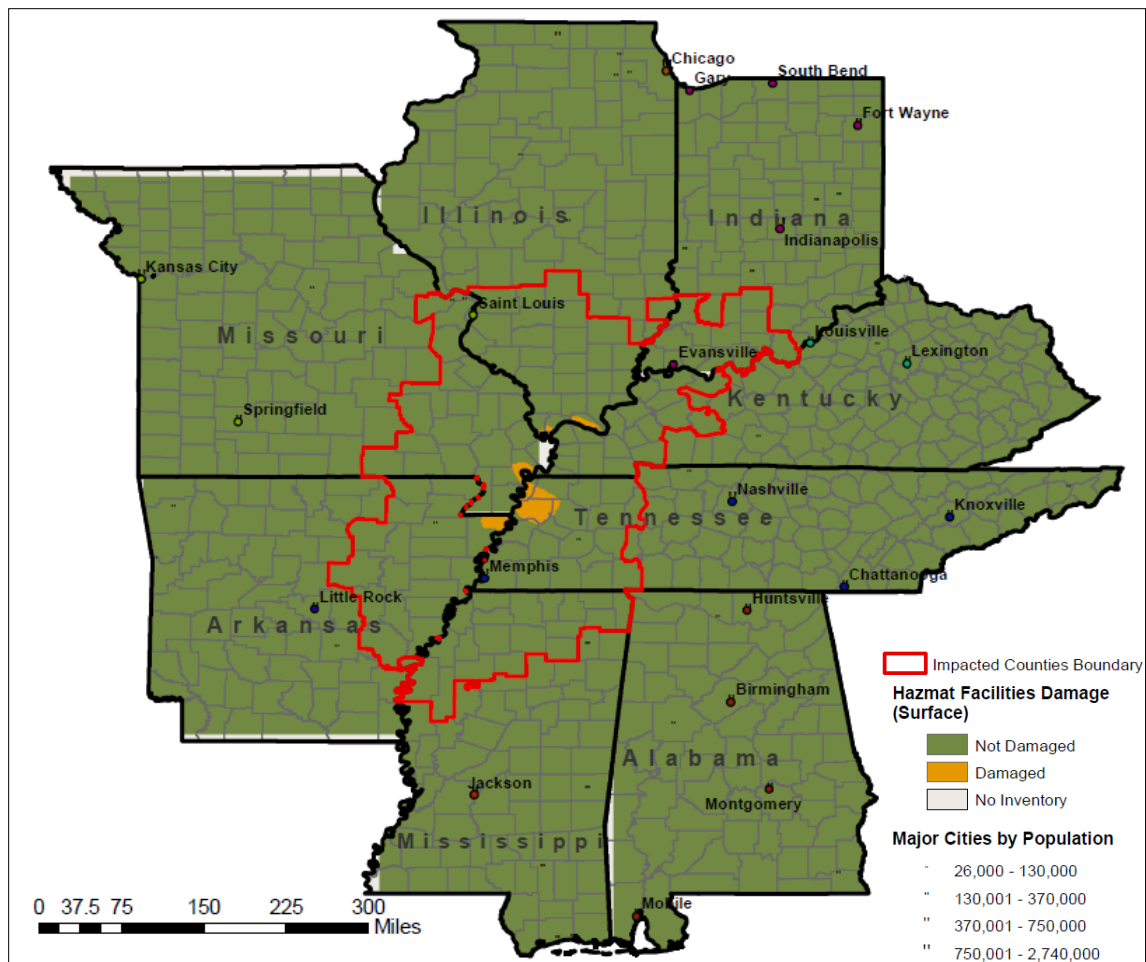


Figure 46. Hazardous Material Facilities Regional Damage

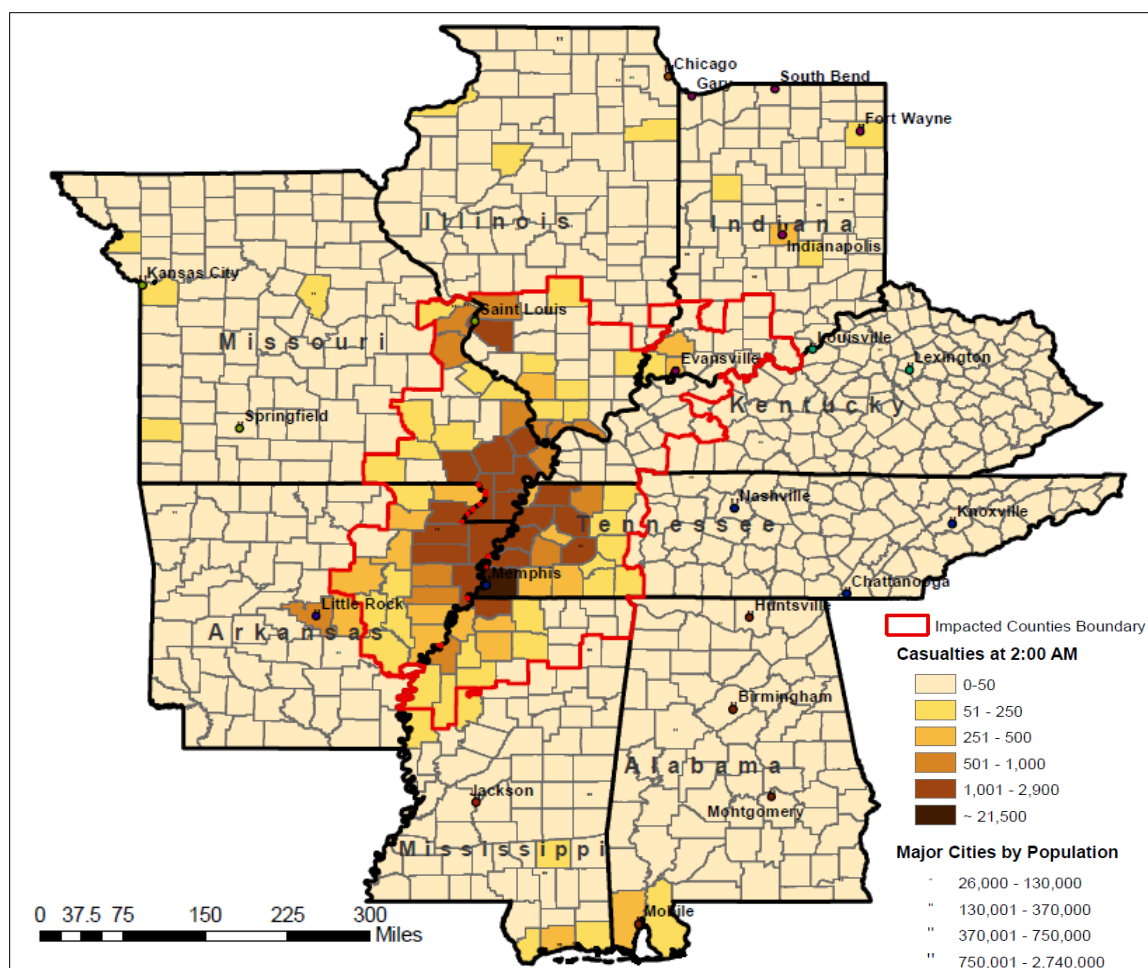
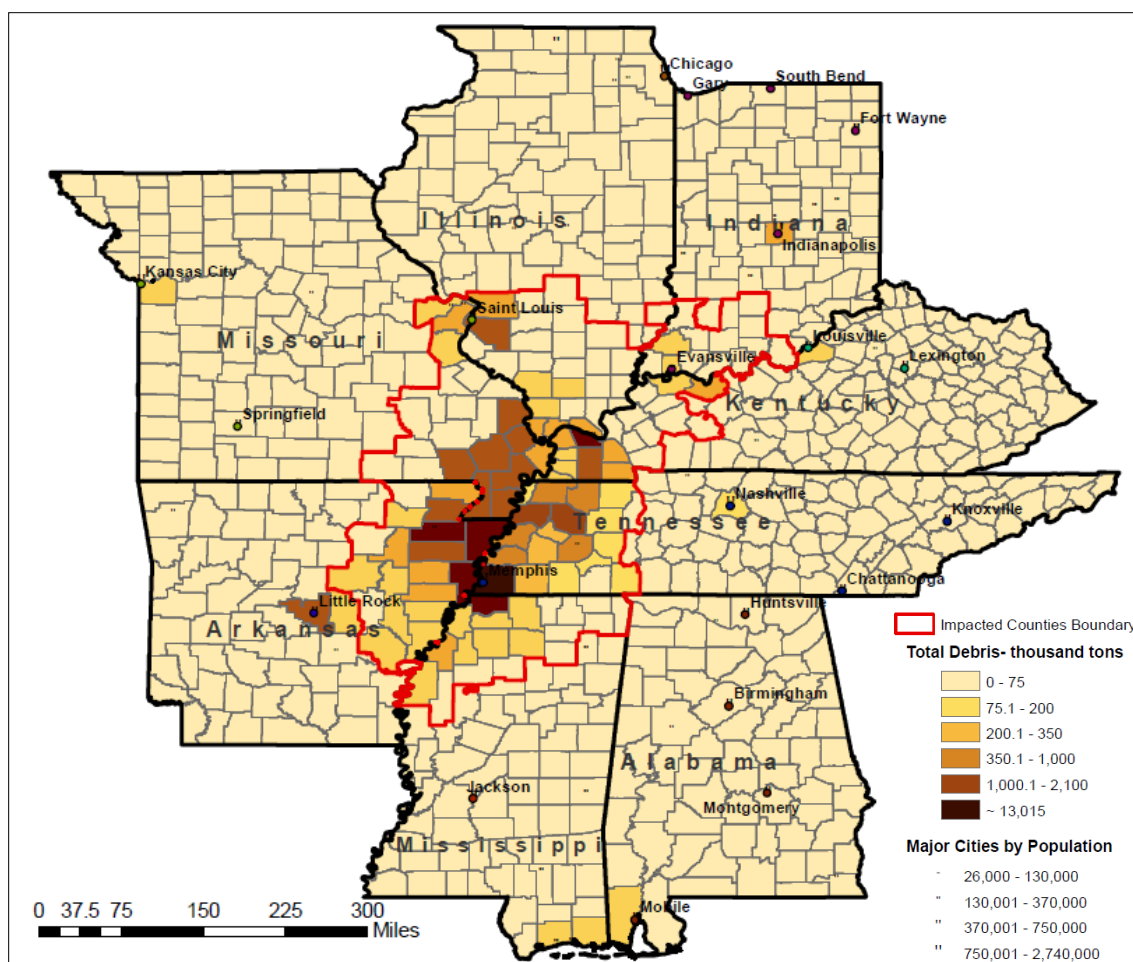


Figure 47. Regional Casualties at 2:00 AM



**Figure 48. Regional Total Debris (in thousand tons)**

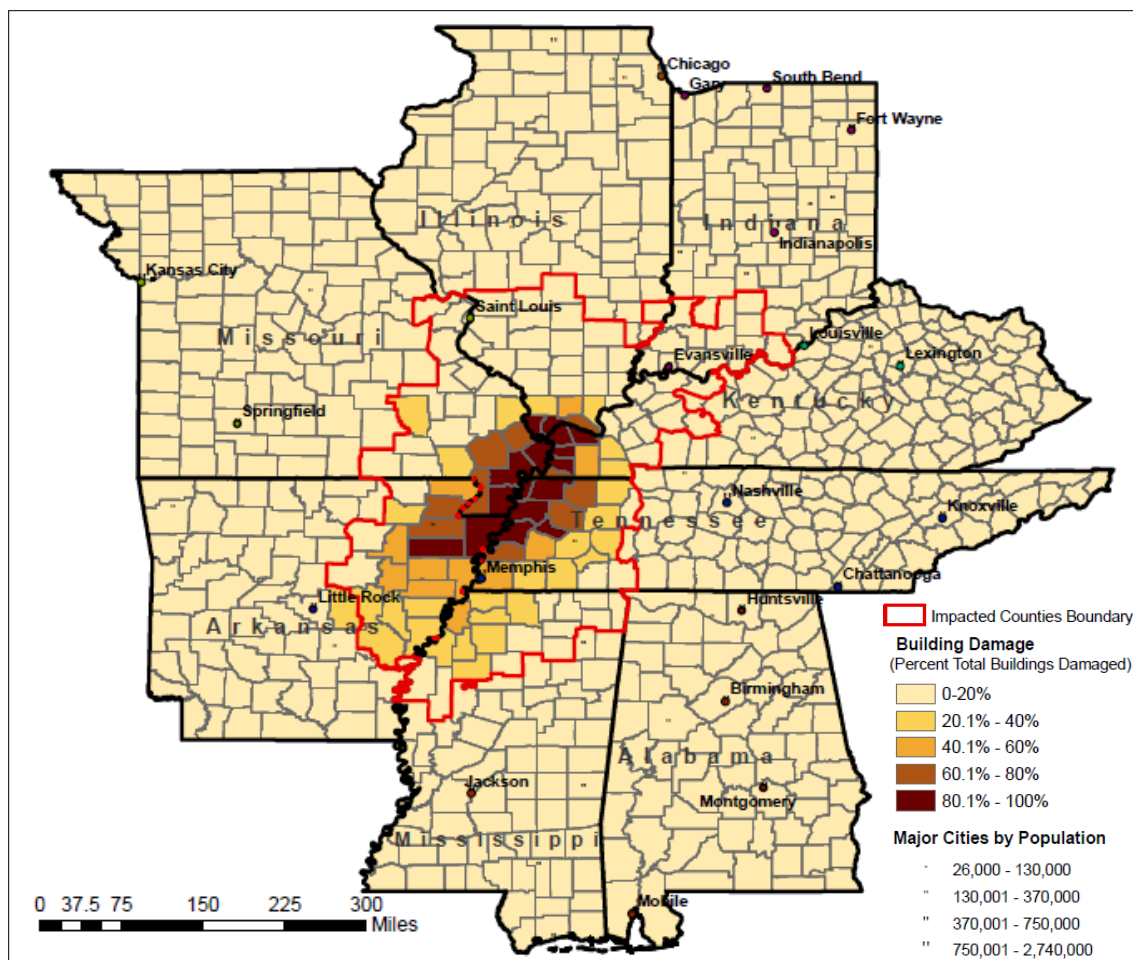


Figure 49. Building Regional Damage Percentage

## Appendix 4. Flood Risk Modeling

### Example of Danger Reach Length Calculation

Required known parameters:

- Height of dam,  $H = 10$  feet
- Volume of storage = 8 acre feet
- Average valley width (usually at the 100 year flood plain) = 400 feet

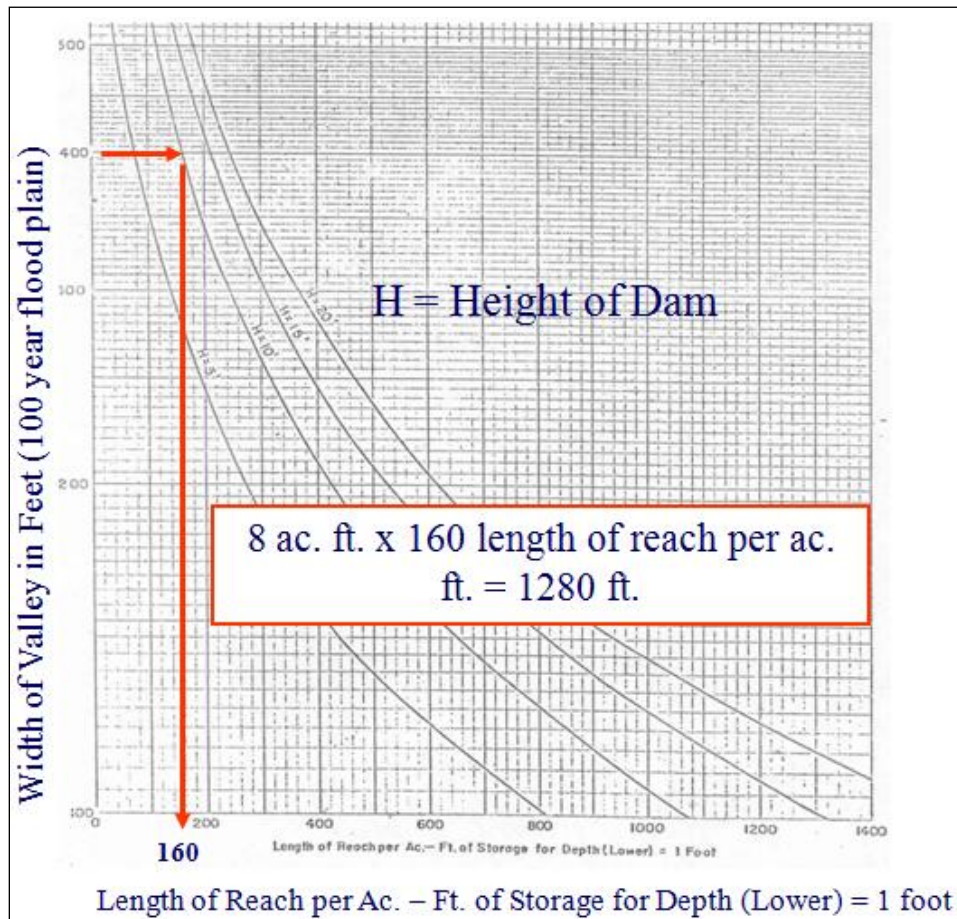


Figure 50. Danger Reach Length Determination

## Flood Risk Analysis Results by State

### Arkansas

Table 58. Arkansas Flood Risk Assessment Results

Facility Type	Number of Potentially Flooded Facilities
<b>Essential Facilities</b>	
EOC	0
Fire Stations	2
Hospitals	0
Police Stations	0
Schools	0
<b>Transportation Systems</b>	
Airports	0
Bus Facilities	0
Highway Bridges	25
Ports	0
Railway Bridges	0
Railway Facilities	0
<b>Utility Systems</b>	
Communication Facilities	0
Electric Power Facilities	0
Natural Gas Facilities	0
Oil Facilities	0
Potable Water Facilities	0
Waste Water Facilities	0
<b>Total Facilities at Risk</b>	<b>27</b>



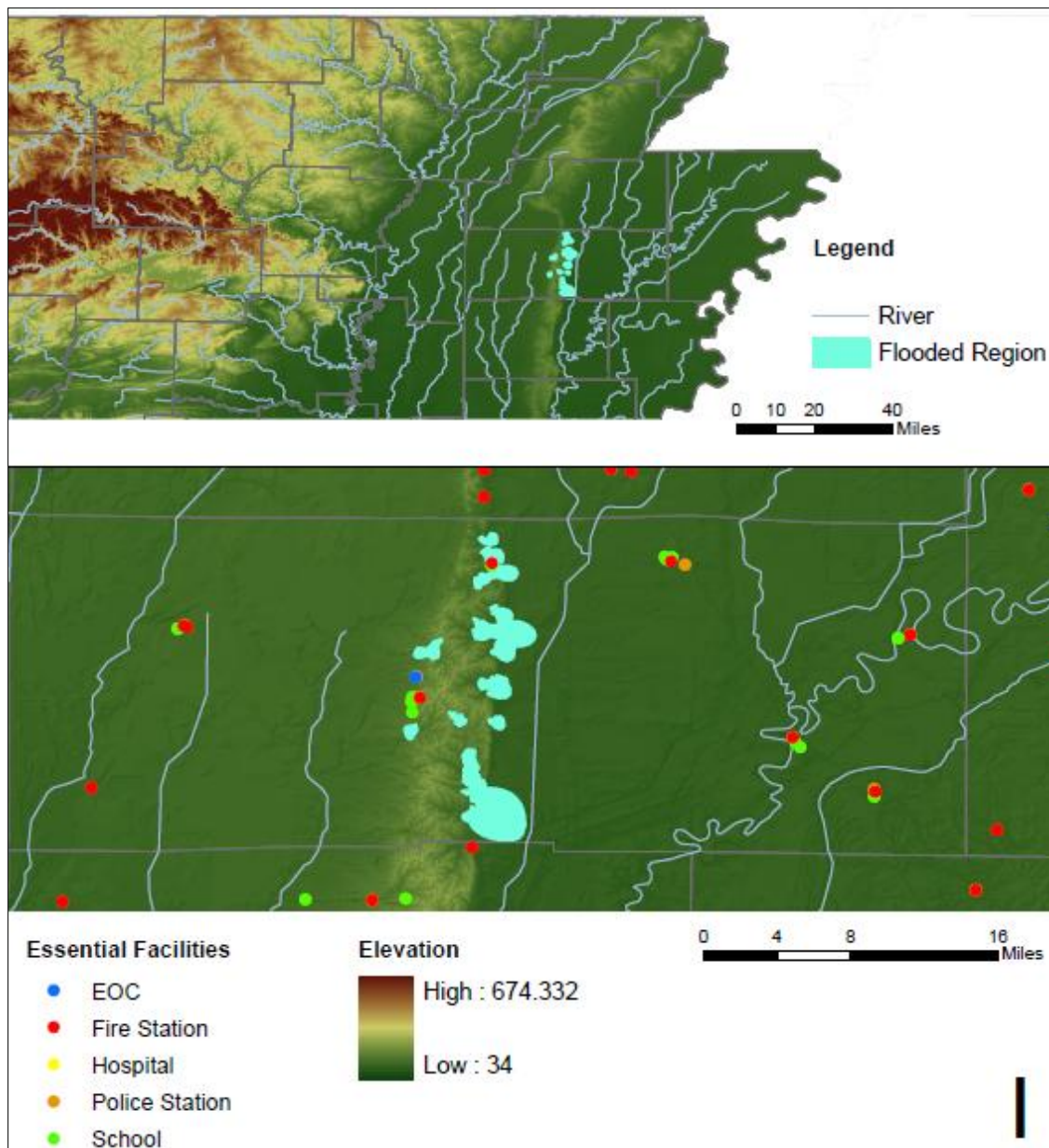


Figure 51. Flood Risk of Arkansas Essential Facilities

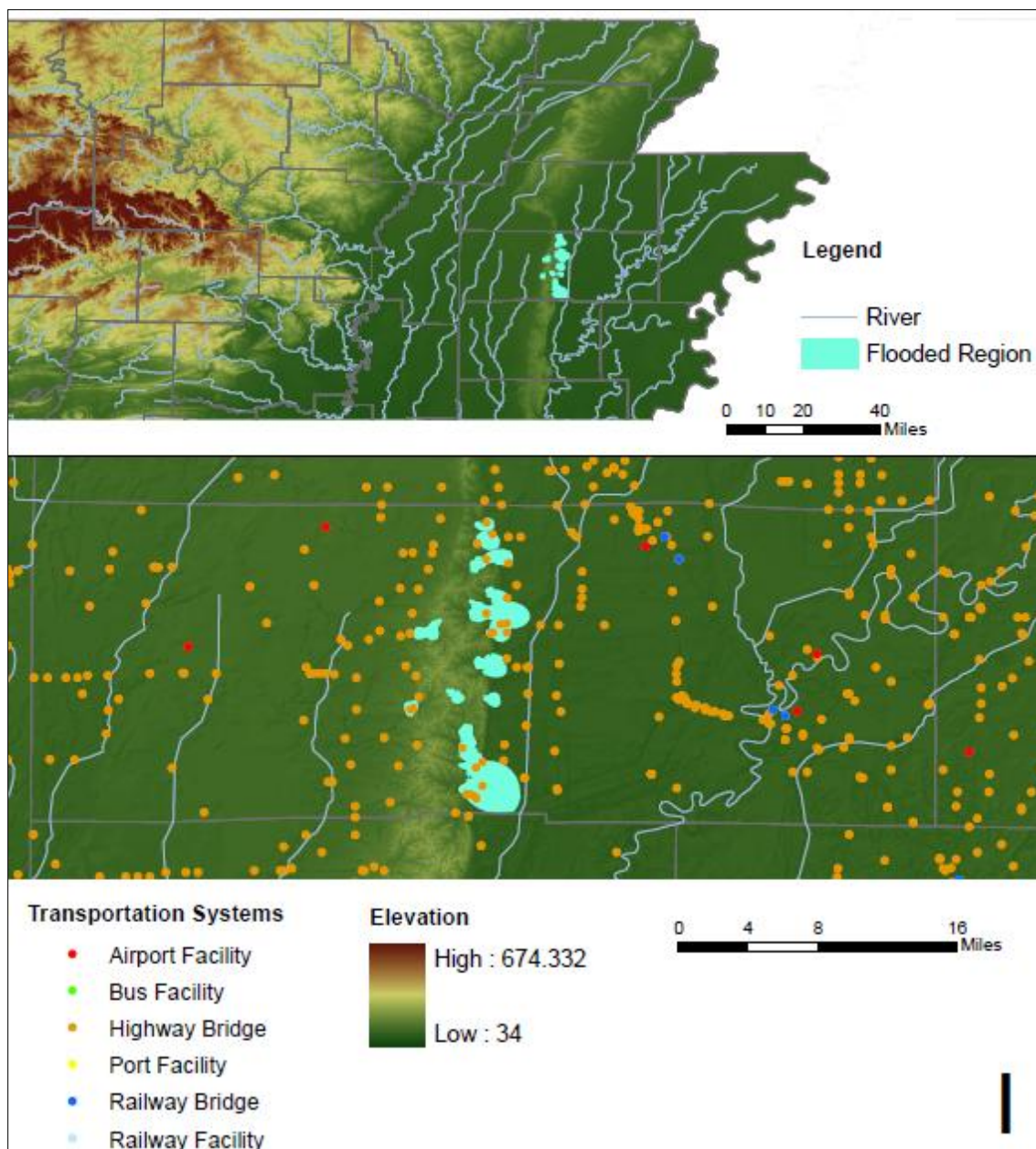
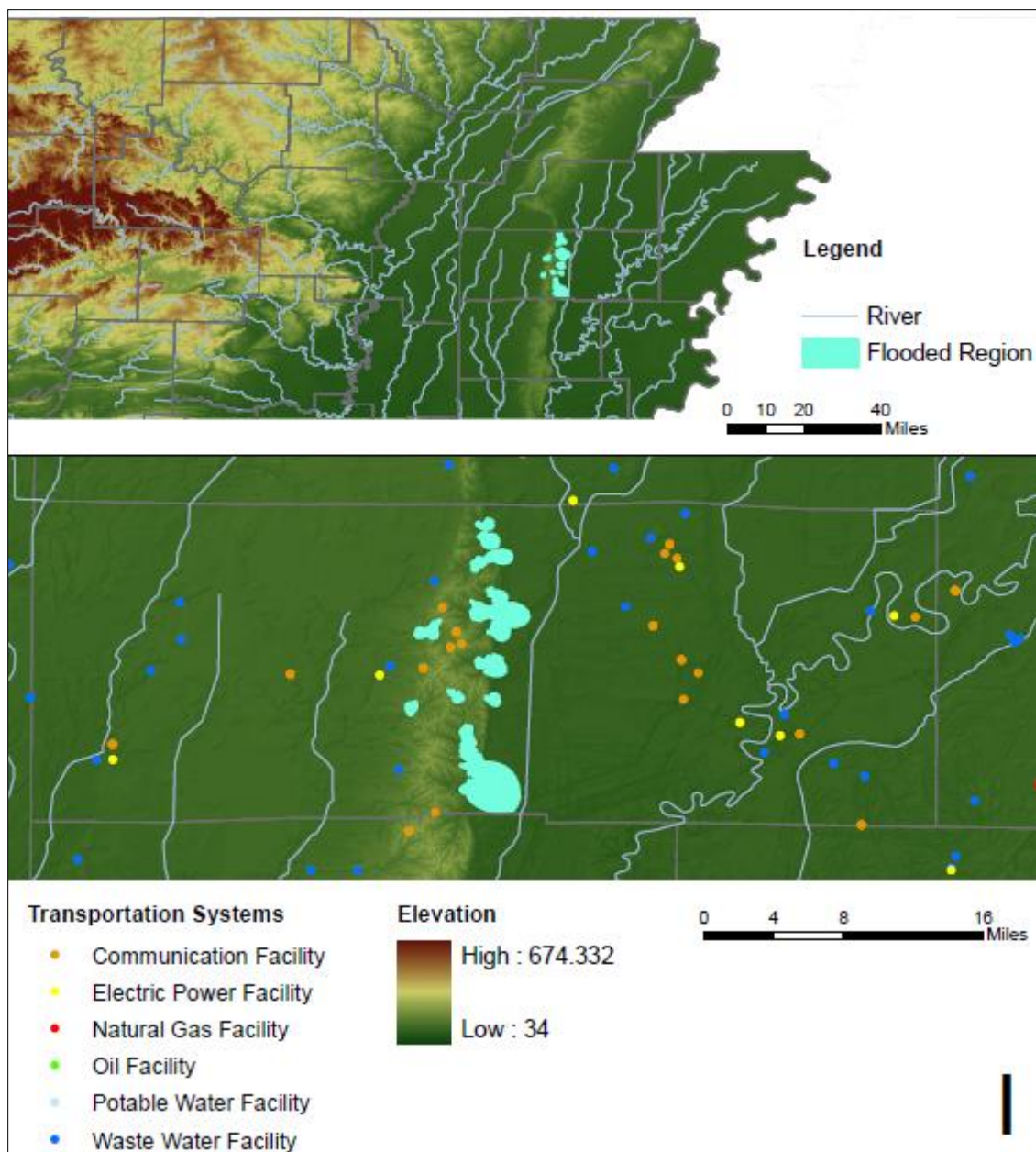


Figure 52. Flood Risk of Arkansas Transportation Systems



**Figure 53. Flood Risk of Arkansas Utility Systems**

## Illinois

**Table 59. Illinois Flood Risk Assessment Results**

<b>Facility Type</b>	<b>Number of Potentially Flooded Facilities</b>
<b>Essential Facilities</b>	
EOC	0
Fire Stations	1
Hospitals	0
Police Stations	0
Schools	1
<b>Transportation Systems</b>	
Airports	0
Bus Facilities	0
Highway Bridges	2
Ports	0
Railway Bridges	0
Railway Facilities	0
<b>Utility Systems</b>	
Communication Facilities	0
Electric Power Facilities	0
Natural Gas Facilities	0
Oil Facilities	0
Potable Water Facilities	0
Waste Water Facilities	2
<b>Total Facilities at Risk</b>	<b>6</b>



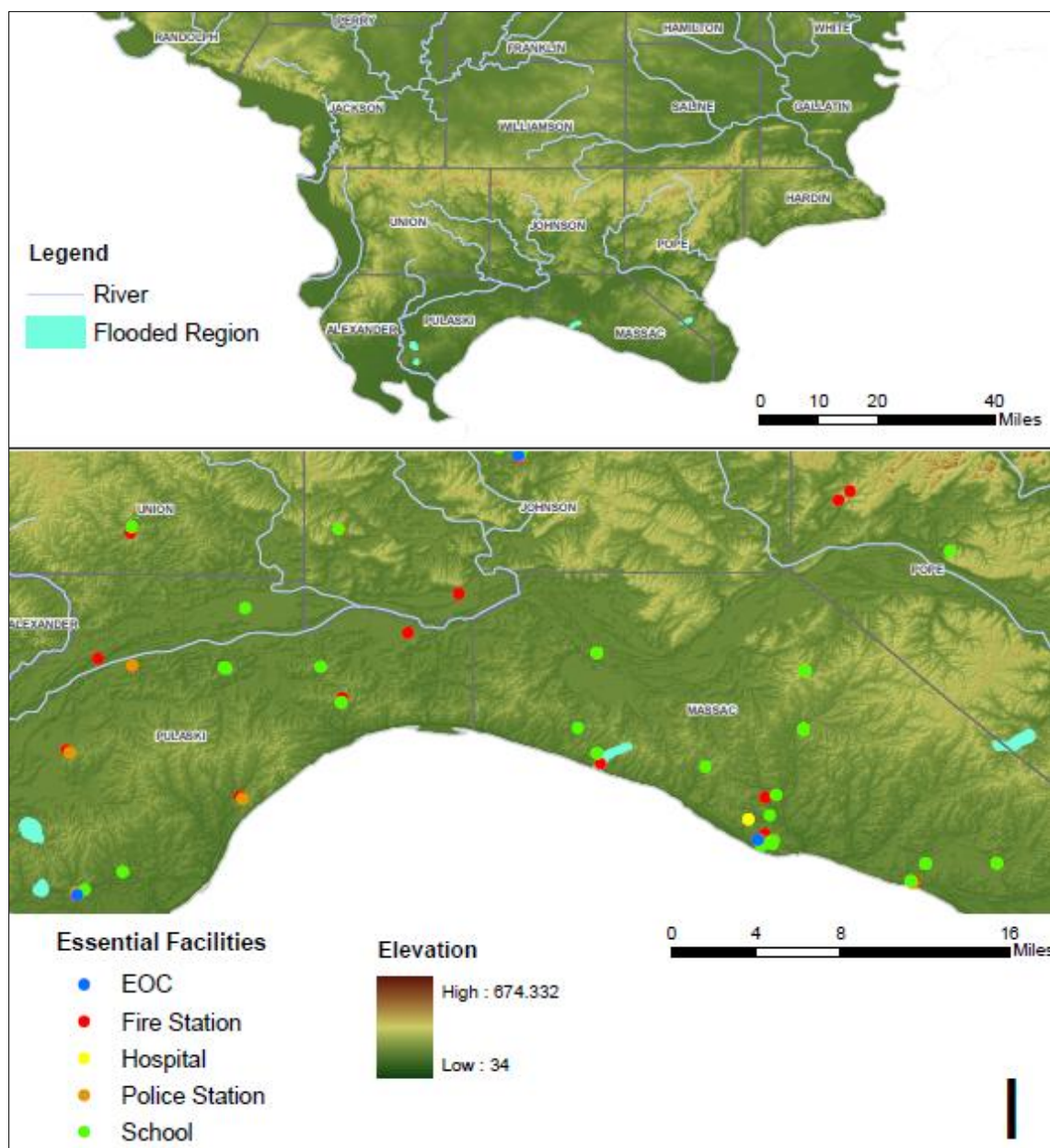


Figure 54. Flood Risk of Illinois Essential Facilities

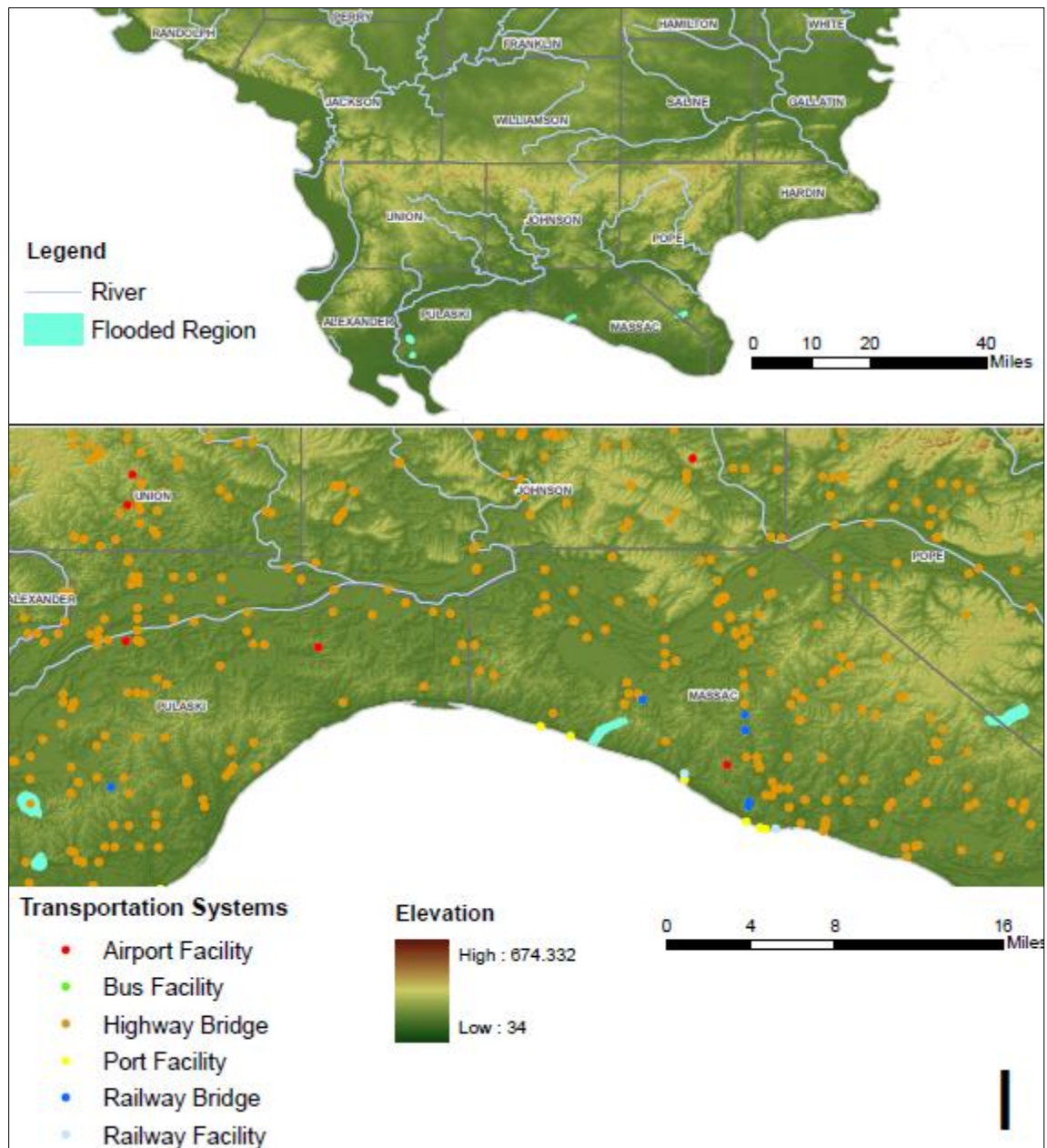


Figure 55. Flood Risk of Illinois Transportation Systems

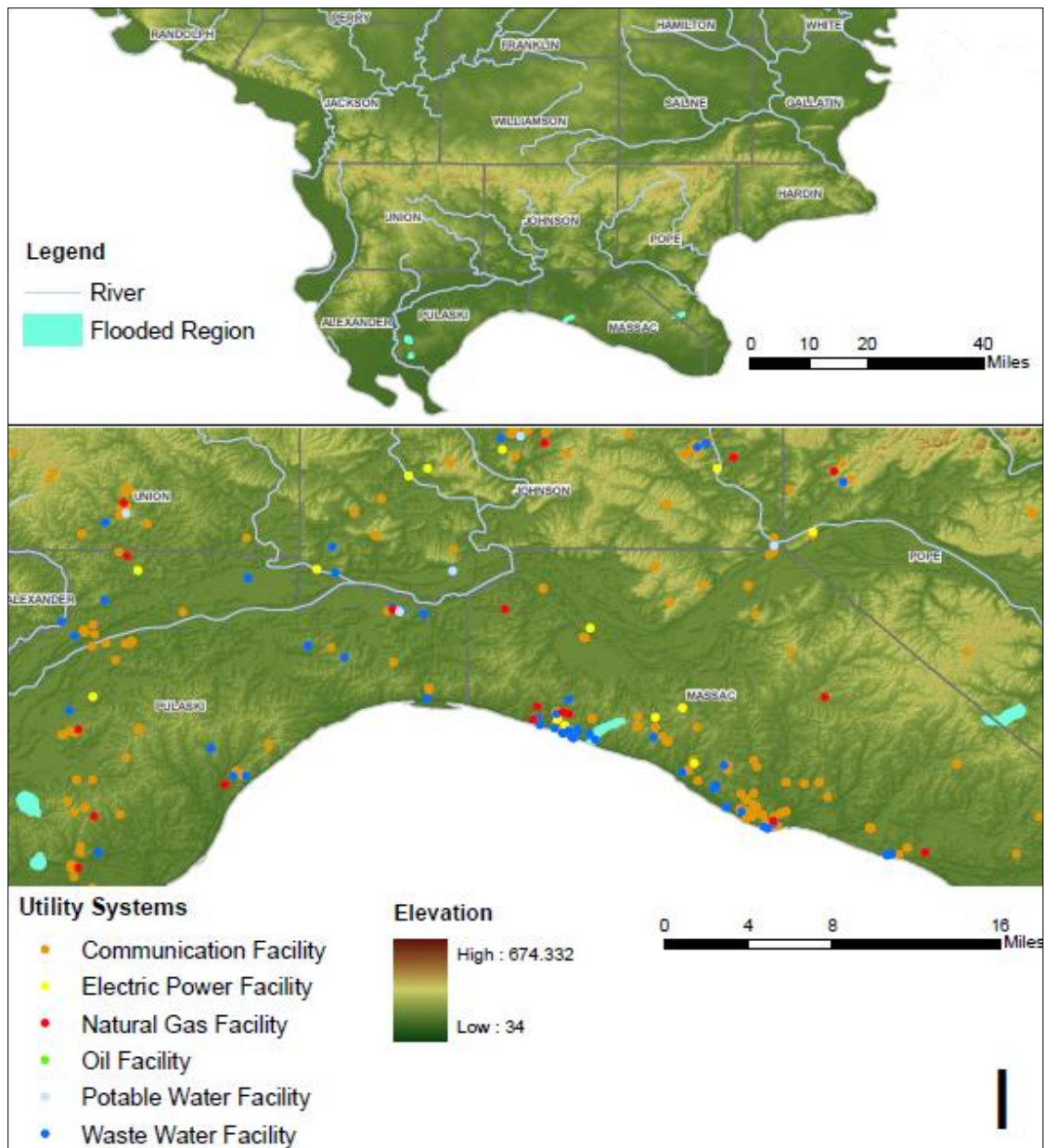


Figure 56. Flood Risk of Illinois Utility Systems

## Kentucky

**Table 60. Kentucky Flood Risk Assessment Results**

<b>Facility Type</b>	<b>Number of Potentially Flooded Facilities</b>
<b>Essential Facilities</b>	
EOC	0
Fire Stations	1
Hospitals	0
Police Stations	0
Schools	0
<b>Transportation Systems</b>	
Airports	0
Bus Facilities	0
Highway Bridges	23
Ports	0
Railway Bridges	0
Railway Facilities	0
<b>Utility Systems</b>	
Communication Facilities	4
Electric Power Facilities	0
Natural Gas Facilities	0
Oil Facilities	0
Potable Water Facilities	0
Waste Water Facilities	3
<b>Total Facilities at Risk</b>	<b>31</b>



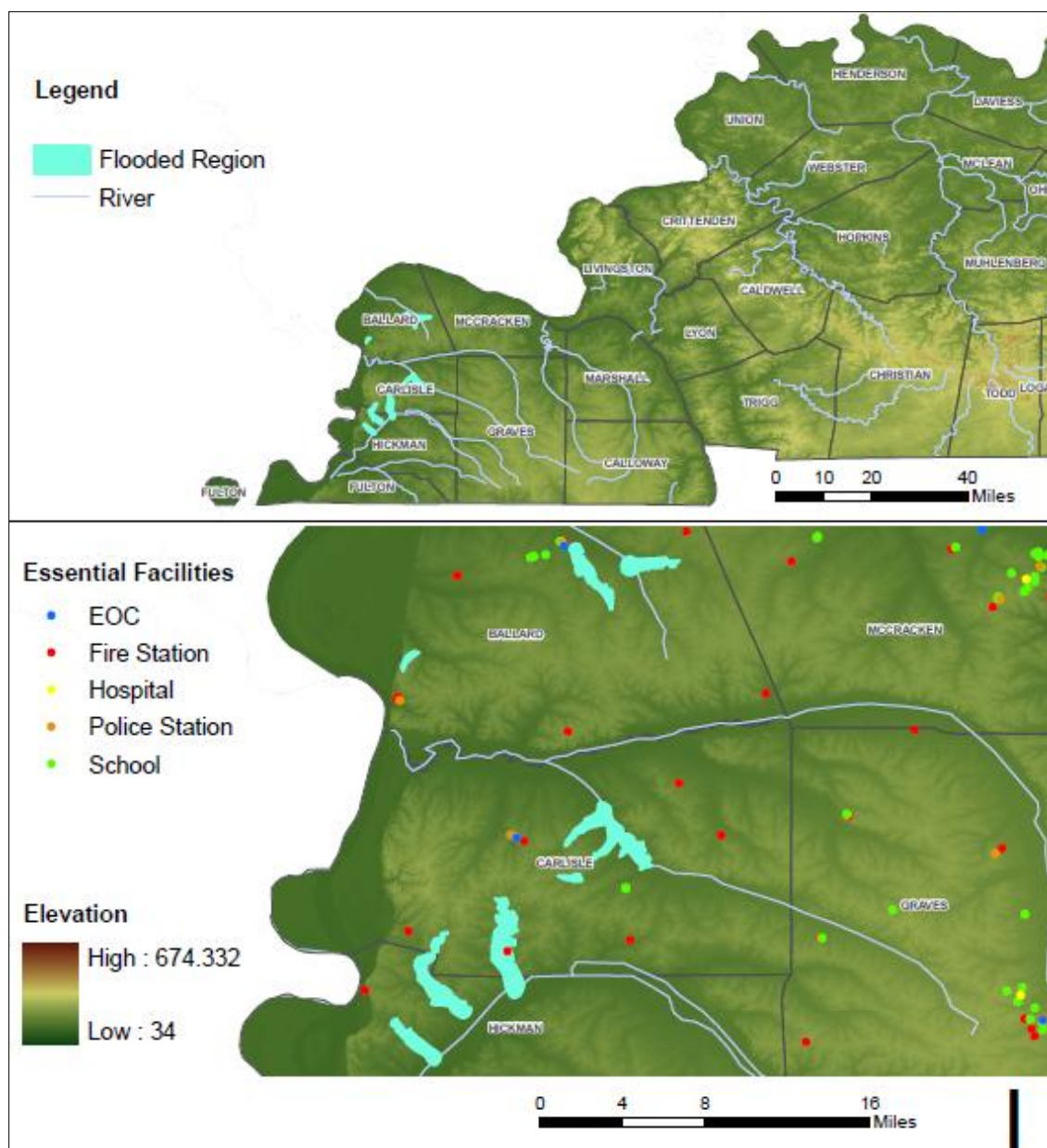


Figure 57. Flood Risk of Kentucky Essential Facilities

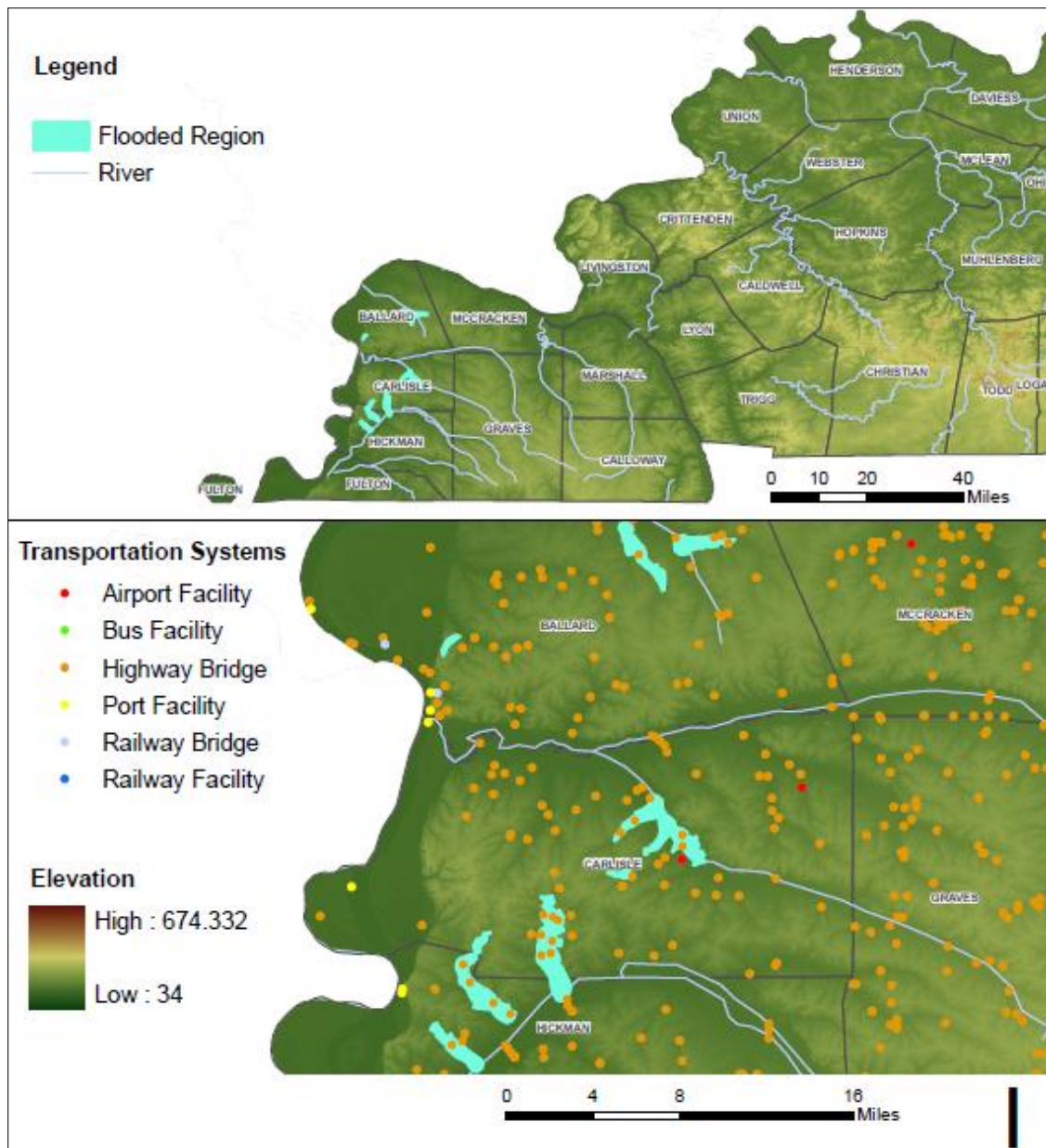


Figure 58. Flood Risk of Kentucky Transportation Systems

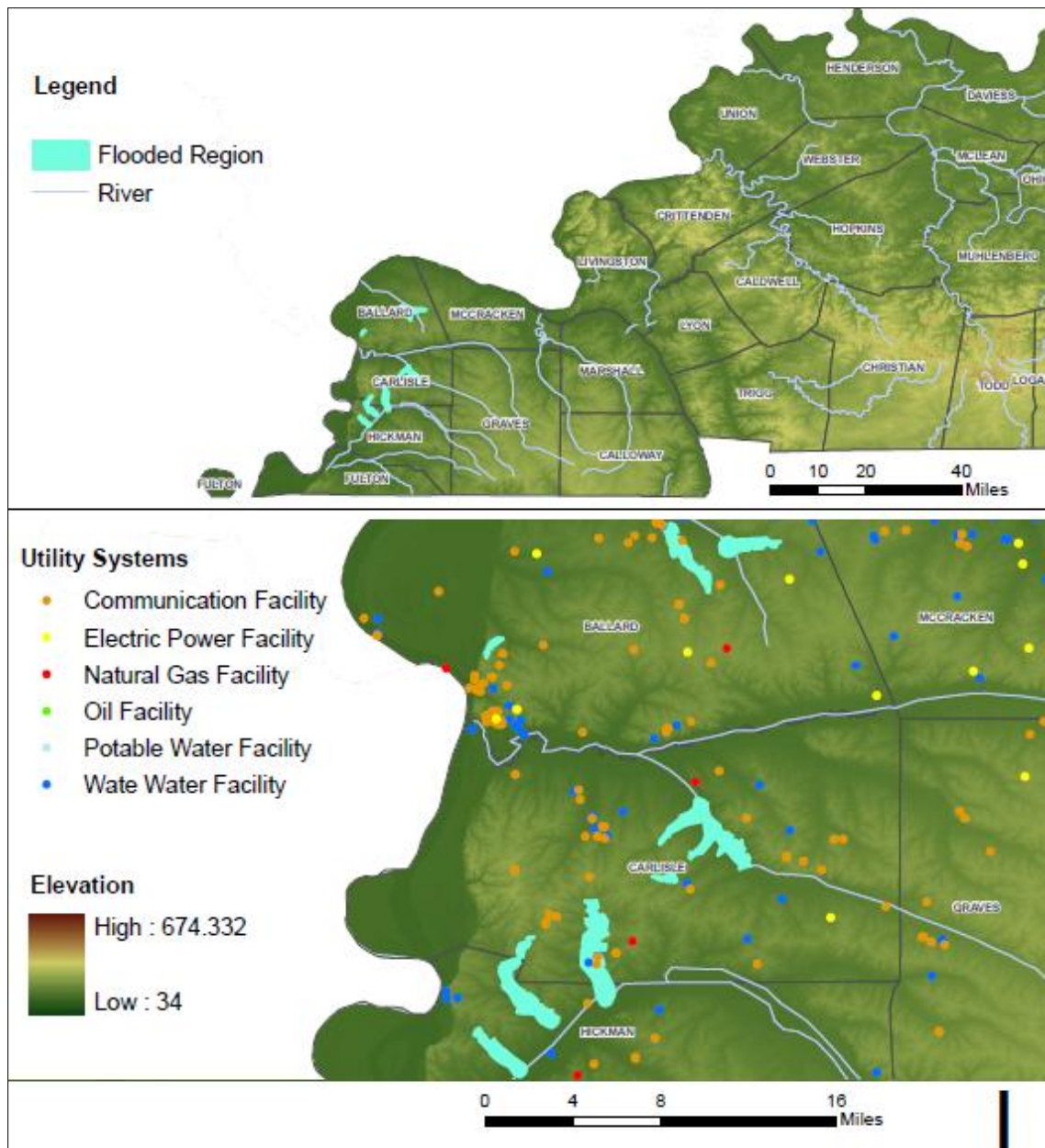


Figure 59. Flood Risk of Kentucky Utility Systems

## Missouri

**Table 61. Missouri Flood Risk Assessment Results**

<b>Facility Type</b>	<b>Number of Potentially Flooded Facilities</b>
<b>Essential Facilities</b>	
EOC	0
Fire Stations	0
Hospitals	0
Police Stations	0
Schools	1
<b>Transportation Systems</b>	
Airports	0
Bus Facilities	0
Highway Bridges	2
Ports	0
Railway Bridges	0
Railway Facilities	0
<b>Utility Systems</b>	
Communication Facilities	1
Electric Power Facilities	0
Natural Gas Facilities	2
Oil Facilities	0
Potable Water Facilities	0
Waste Water Facilities	0
<b>Total Facilities at Risk</b>	<b>6</b>



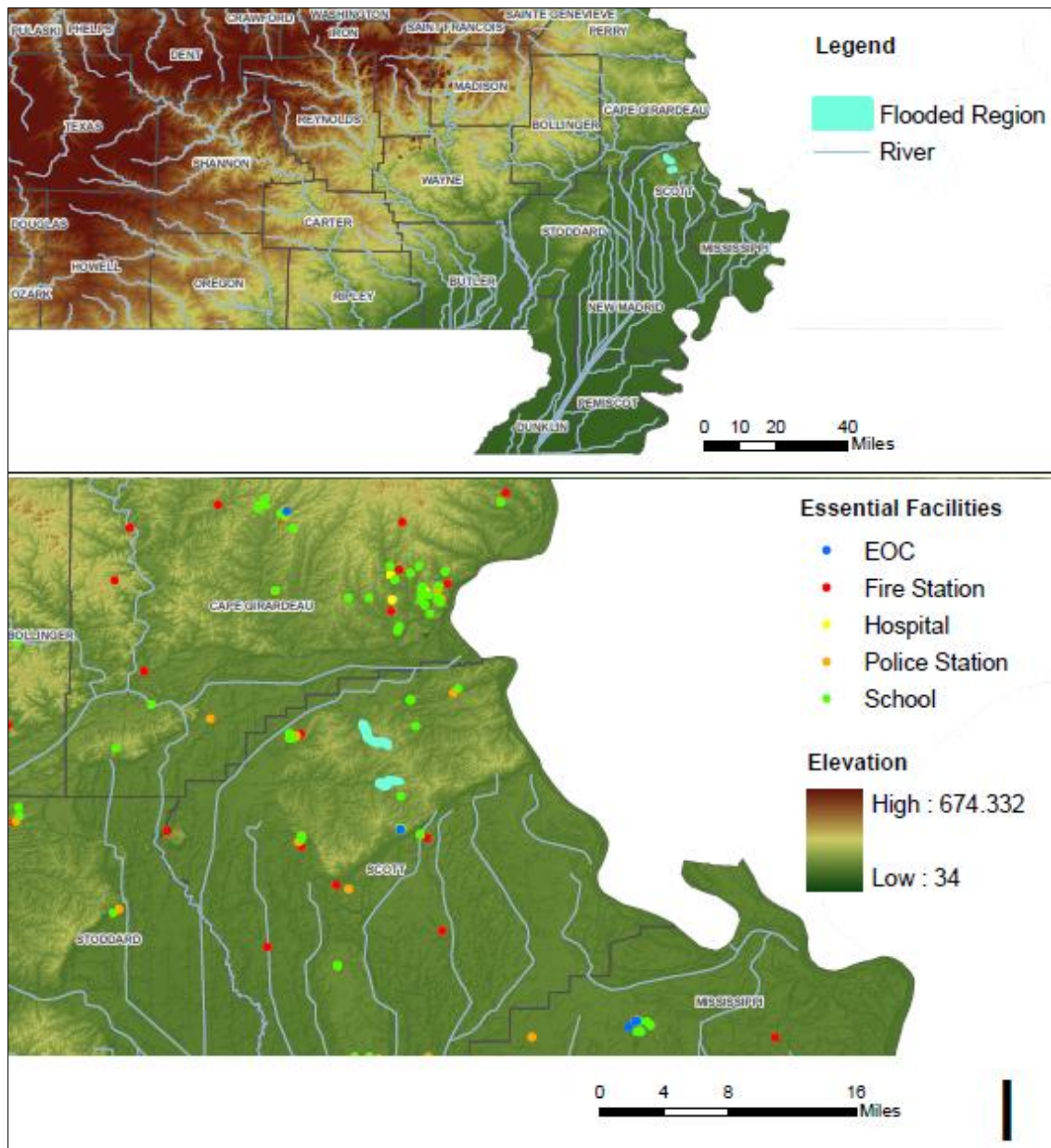


**Figure 60. Flood Risk of Missouri Essential Facilities**

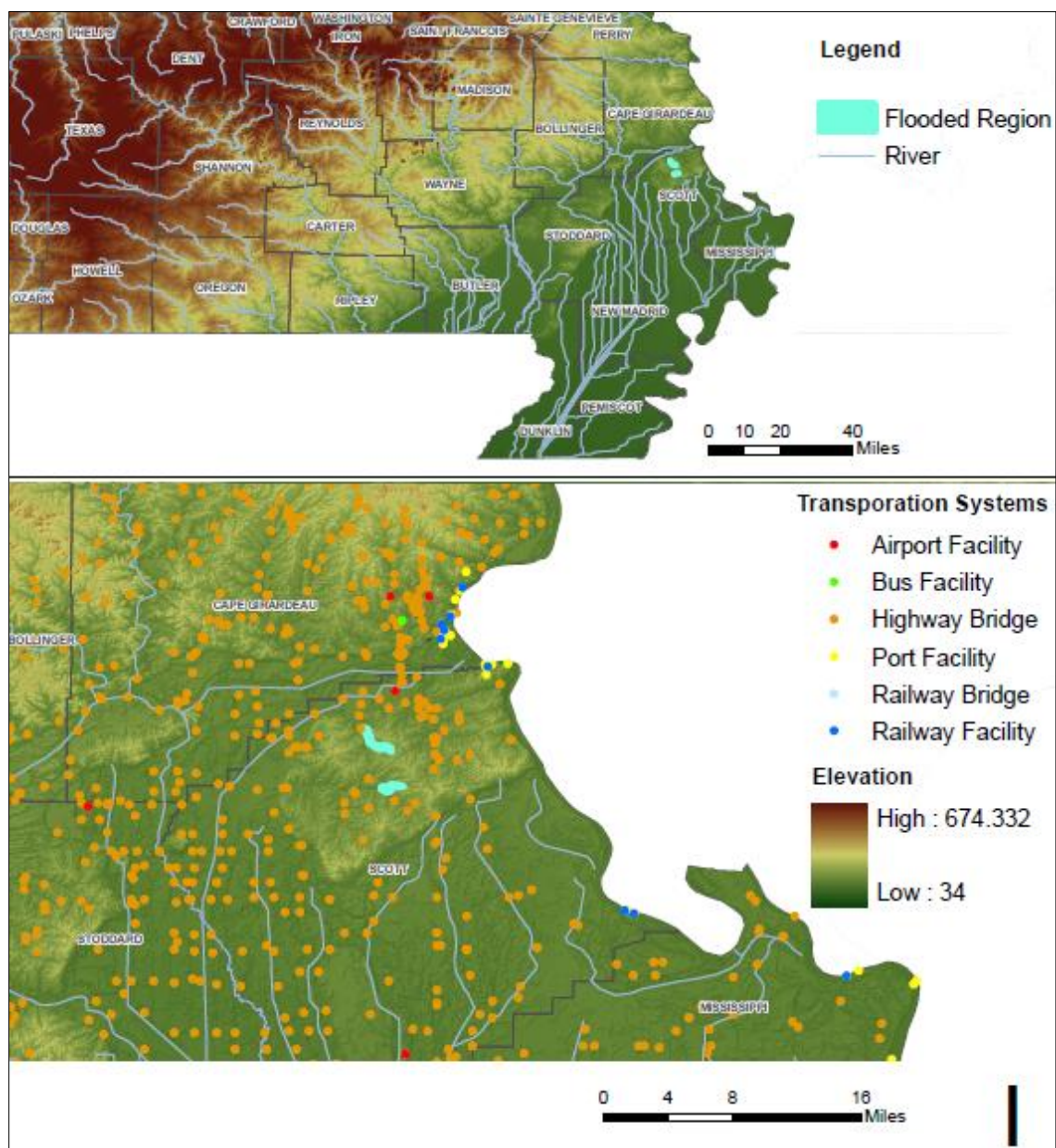


Figure 61. Flood Risk of Missouri Transportation Systems

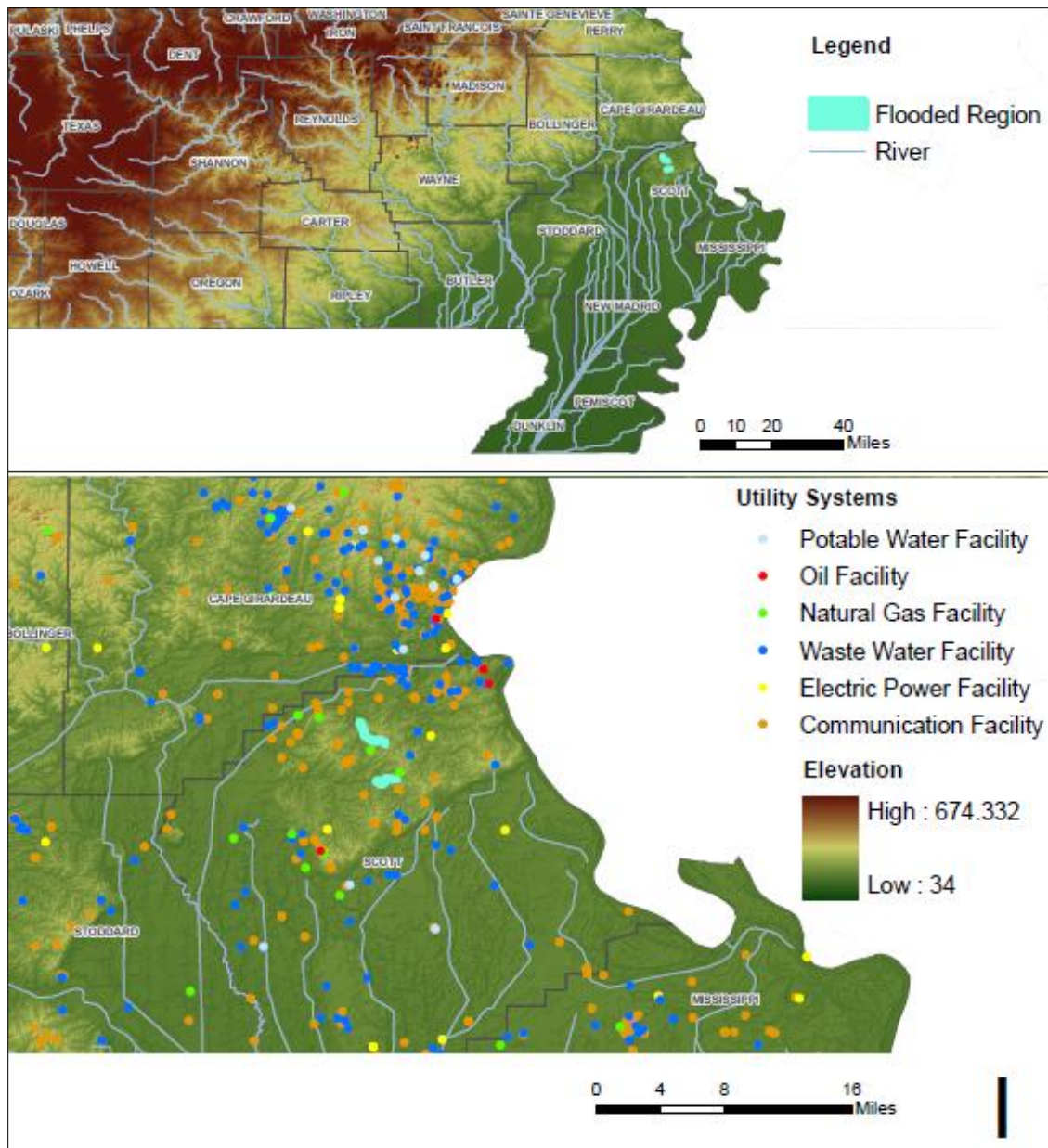


Figure 62. Flood Risk of Missouri Utility Systems

## Tennessee

**Table 62. Tennessee Flood Risk Assessment Results**

<b>Facility Type</b>	<b>Number of Potentially Flooded Facilities</b>
<b>Essential Facilities</b>	
EOC	2
Fire Stations	7
Hospitals	1
Police Stations	7
Schools	8
<b>Transportation Systems</b>	
Airports	2
Bus Facilities	1
Highway Bridges	132
Ports	0
Railway Bridges	0
Railway Facilities	0
<b>Utility Systems</b>	
Communication Facilities	59
Electric Power Facilities	1
Natural Gas Facilities	1
Oil Facilities	1
Potable Water Facilities	2
Waste Water Facilities	15
<b>Total Facilities at Risk</b>	<b>239</b>



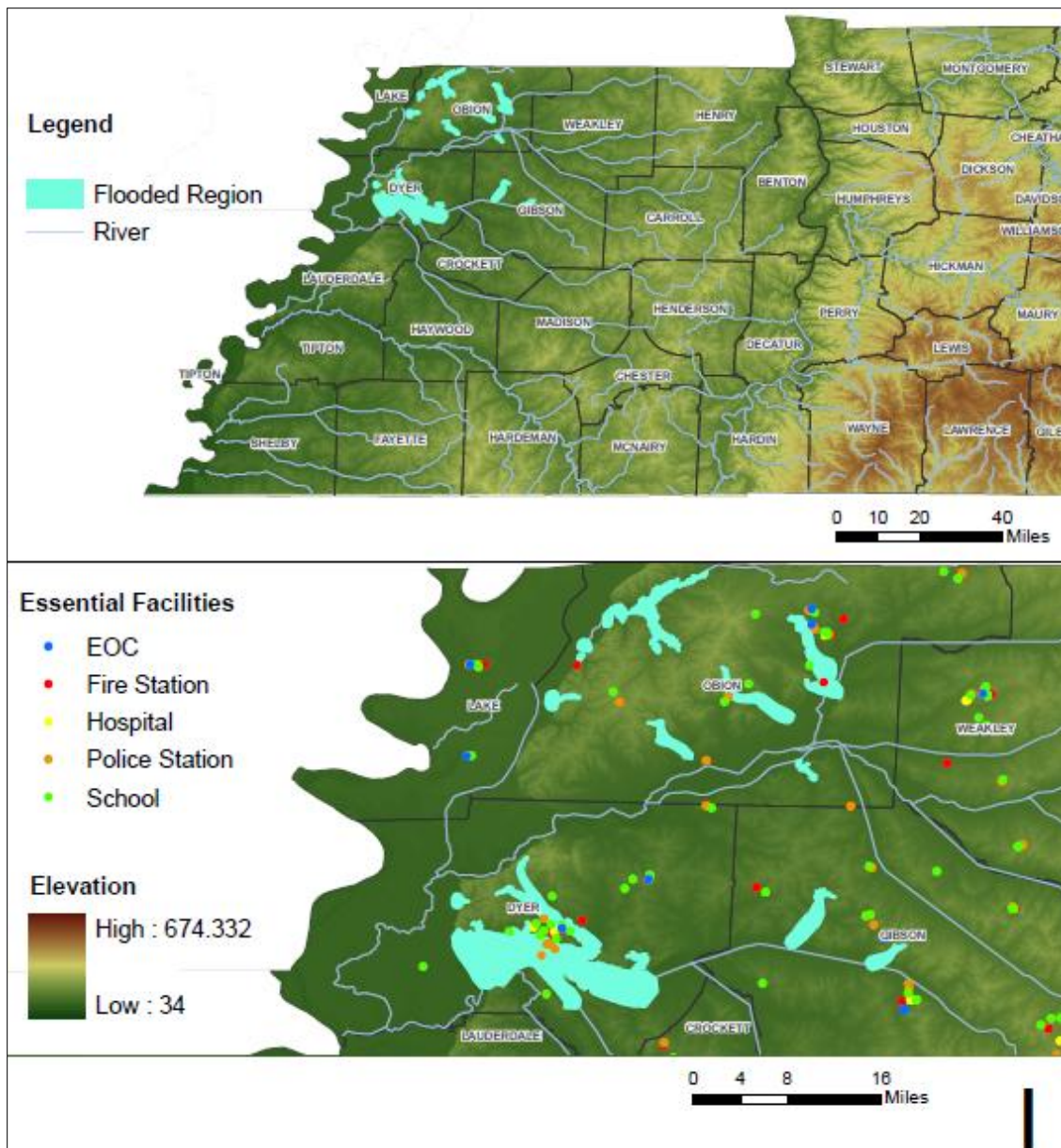


Figure 63. Flood Risk of Tennessee Essential Facilities

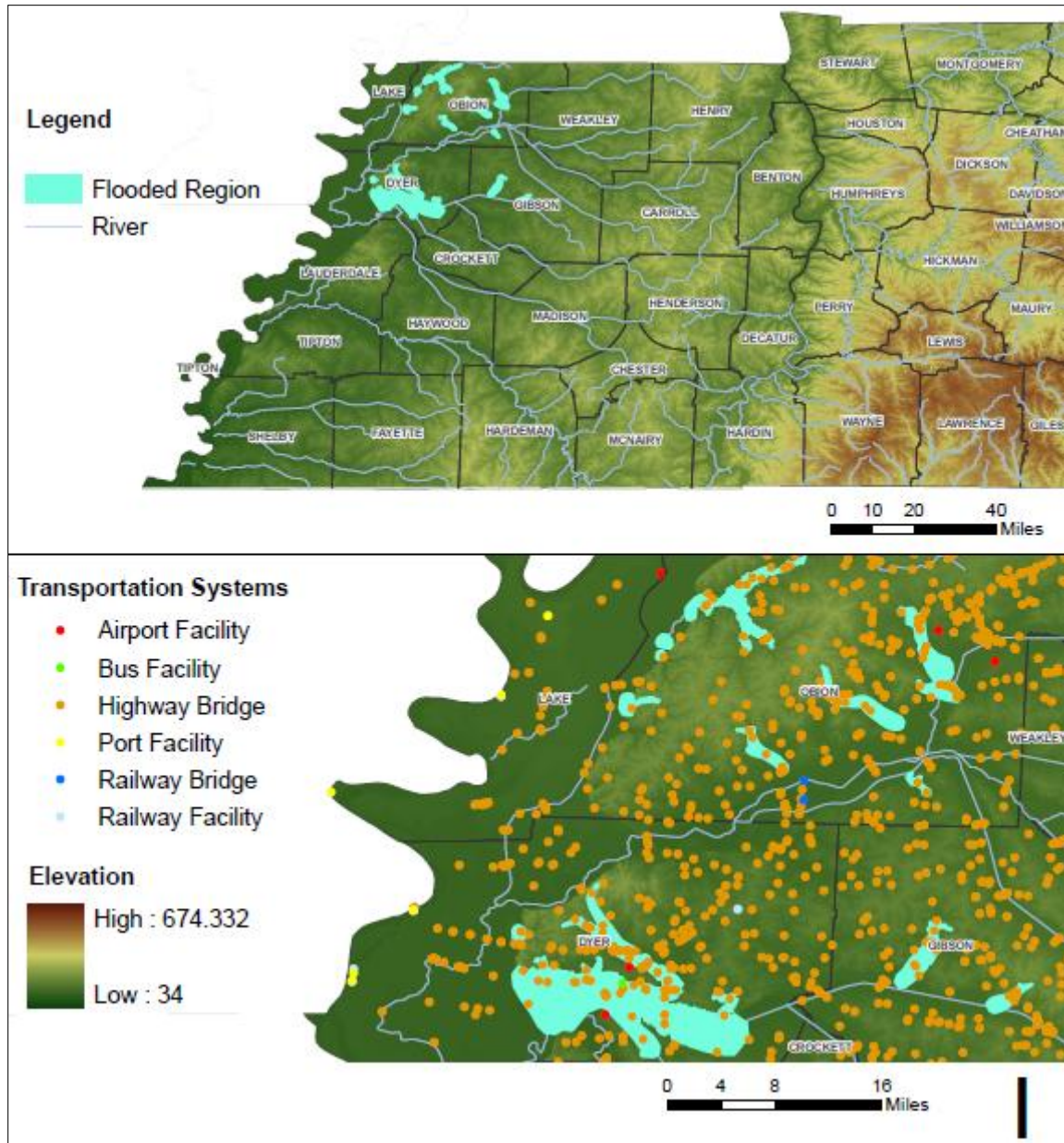


Figure 64. Flood Risk of Tennessee Transportation Systems



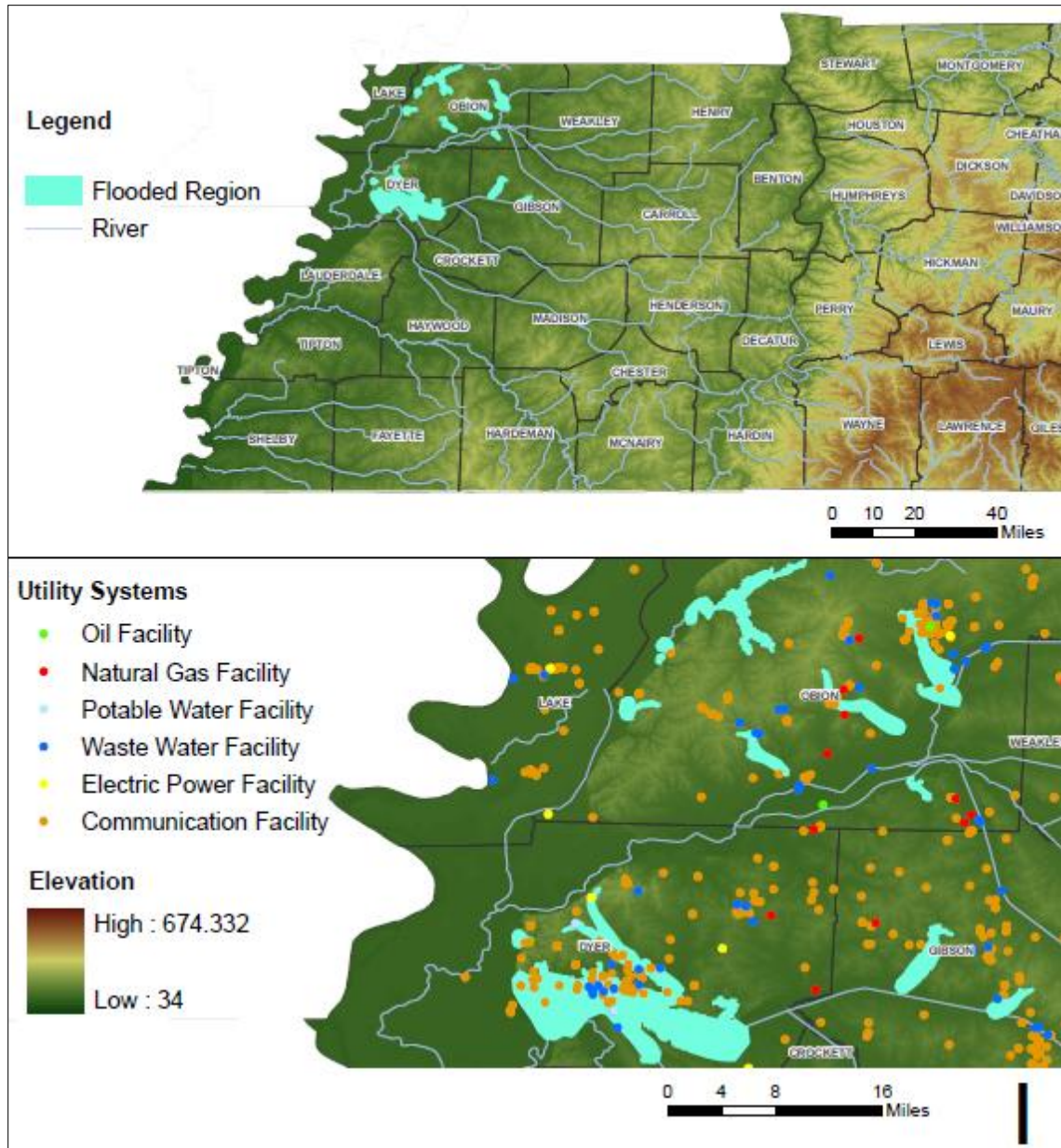


Figure 65. Flood Risk of Tennessee Utility Systems